EXPERIMENTAL AND NUMERICAL INVESTIGATION OF A HIGHLY MEANDERING CHANNEL

A Thesis Submitted in Partial Fulfilment of the Requirement for the Degree of

Master of Technology

In

Civil Engineering

SUMIT KUMAR JENA

(213CE4101)

DEPARTMENT OF CIVIL ENGINEERING

NATIONAL INSTITUTE OF TECHNOLOGY, ROURKELA

MAY 2015

EXPERIMENTAL AND NUMERICAL INVESTIGATION OF A HIGHLY MEANDERING CHANNEL

A Thesis

Submitted by

Sumit Kumar Jena

(213CE4101)

In partial fulfillment of the requirements

for the award of the degree of

Master of Technology

In

Civil Engineering

(Water Resources Engineering)

Under The Guidance of

Dr. K. K. Khatua

DEPARTMENT OF CIVIL ENGINEERING

NATIONAL INSTITUTE OF TECHNOLOGY, ROURKELA

ORISSA -769008, INDIA

DEPARTMENT OF CIVIL ENGINEERING
NATIONAL INSTITUTE OFTECHNOLOGY, ROURKELA

DECLARATION

I hereby state that this submission is my own work and that, to the best of my knowledge and belief, it contains no material previously published or written by any other person nor substance which to a substantial extent has been accepted for the award of any other degree or diploma of the university or other institute of higher learning, except where due acknowledgement has been made in the text.

SUMIT KUMAR JENA

DEPARTMENT OF CIVIL ENGINEERING
NATIONAL INSTITUTE OFTECHNOLOGY, ROURKELA

CERTIFICATE

This is to certify that the thesis entitled **"Experimental and Numerical Investigation of a Highly Meandering Channel"** is a bonafide record of authentic work carried out by **Sumit Kumar Jena** under my supervision and guidance for the partial fulfilment of the requirement for the award of the degree of Master of Technology in hydraulic and Water Resources Engineering in the department of Civil Engineering at the National Institute of Technology, Rourkela.

The results embodied in this thesis have not been submitted to any other University or Institute for the award of any degree or diploma.

Date:

Place: Rourkela

Prof. K.K. Khatua
Associate Professor
Department of Civil Engineering
National Institute of Technology, Rourkela

ACKNOWLEDGEMENT

A complete research work can never be the work of anybody alone. The contribution of various individuals, in their distinctive ways, has made this conceivable. One page can never ample to express the feeling of appreciation to those whose direction and support was basic for the fruition of this venture. I want to express my unique thankfulness to my guide Dr. Kishanjit Kumar Khatua. Sir, thank you for teaching me that every mistake is just a learning experience, you are always being cordial to me. I have learnt so much from you and ever since I have been working with you I found myself evolving more and more with respect to my research work. Your invaluable counsel, warm fillip and continuous support have made this research easier.

I would also like to show my heartfelt esteem and reverence to the professors of our department, Dr.K.C Patra, Dr.Ramakar Jha and Professor A.Kumar and Dr.S.K Sahu, head of the department Civil engineering for the kind co-operation and requisite advice they have provided whenever required. . I wish to express my earnest appreciation to Dr. S K Sarangi, Director, NIT Rourkela for issuing me the opportunities to complete my research work.

I want to extend my gratitude to Arpan Pradhan PhD. Scholar of Civil engineering for the kind co-operation and vital guidance he has given me always. You helped me a great deal regarding me as your younger brother. I additionally need to say thanks to Abinash Mohanta PhD. Scholar of Civil engineering for his eagerness to help and guide me always.

My research work won't have been completed if I had not got a chance to share such a friendly atmosphere with my two close friends Mamata rani Mohapatra and Rashmi rekha Das. I want to extend my thanks to Sovan Sankalp, Balram bhai and those who are directly and indirectly associated with my work. I would like to thank my Parents for their support and assurance which made me self-confident to complete this big task. At last but not the least thank God who shows me the right path always.

SUMIT KUMAR JENA

ABSTRACT

Research on various aspects of velocity distribution, boundary shear stress etc. has been carried out on curved and meandering channels. But no systematic effort has been made to investigate the experimental and numerical simulation on a highly sinuous meandering channel along its meandering path. In this research work, detailed investigation of velocity distribution and boundary shear distribution along the depth and width of a highly sinuous channel (Sr 4.11) has been carried out.

The analysis is performed at thirteen different sections along a meander path, i.e. from one bend apex to another. The study includes longitudinal velocity distribution, depth-averaged velocity and boundary shear stress analysis at each section. The results iterate that the higher longitudinal velocity always remains towards the inner bank and as the channel changes its curvature, so does the movement of higher velocity which moves from one bank towards the other.

The experimental results are then validated through numerical modelling by using Ansys-Fluent which takes large eddy simulation model to solve the turbulence equations. The numerical results are found to be well complimenting with the experimental results. The experimental results are also analysed with another researcher's work having the same geometrical parameters, having a different aspect ratio.

Keywords: bend apex, meander path, cross-over, longitudinal velocity distributions, boundary shear stress, numerical modeling, turbulence, Ansys-Fluent

TABLE OF CONTENTS

CHAPTER	DESCRIPTION	PAGE NO.
Declaration		**i**
Certificate		**ii**
Acknowledgement		**iii**
Abstract		**iv**
Table of Contents		**v-vii**
List of Tables		**viii**
List of Photos		**viii**
List of Figures		**ix**
List of Symbols		**x-xi**
1	**INTRODUCTION**	**1-12**
1.1	Channel	1
1.2	Types of Channel	1
1.3	Meandering river	4
1.4	Meander Path	6
1.5	Velocity Distribution	6-7
1.6	Boundary Shear Distribution	8-9
1.7	Numerical Modelling	9-10
1.8	Objectives of Research	11
1.9	Thesis Structure	12
2	**LITERATURE REVIEW**	**14-32**
2.1	Overview	14
2.2	Previous Research on Velocity Distribution	15
2.3	Previous Research on Boundary Shear	21

	2.4	Previous Research on Numerical Modelling	27
3		**METHODOLOGY**	**33-59**
	3.1	Overview	33
	3.2	Design and Construction of Channel	33-35
	3.3	Apparatus and Equipment Used	35-36
	3.4	Experimental Procedure	36
		3.4.1 Experimental Channel	36-38
		3.4.2 Position of Measurement	38-39
		3.4.3 Measurement of Bed Slope	39-40
		3.4.4 Notch Calibration	40-41
		3.4.5 Measurement of Longitudinal Velocity	41
		3.4.6 Measurement of Boundary Shear Stress	41-43
	3.5	Numerical Modelling	43
		3.5.1 Description of Numerical Model Parameter	43-44
		3.5.2 Turbulence Modelling	44-46
		3.5.3 Turbulence Models	46-47
		3.5.4 Governing Equations	47-48
		3.5.5 Numerical Methodology	48
		3.5.6 Preprocessing	49
		3.5.7 Creation of Geometry	49-50
		3.5.8 Mesh generation	50-52
		3.5.9 Courant number	52-53
		3.5.10 Solver settings	53
		3.5.11 Two Phase Modelling	53-54
		3.5.12 Volume of Fluid Model	54
		3.5.13 Solving For Turbulence	55-56

3.5.13.1 Used LES Turbulence Models 56

3.5.14 Set Up Physics 57-58

3.5.14.1 Inlet and Outlet Boundary Condition 58-59

4 RESULT AND DISCUSSIONS 60-93

4.1 Overview 60

4.2 Longitudinal Velocity Distribution 60-63

4.3 Longitudinal Velocity Contours at different sections along the meander path 64-68

4.4 Velocity Distribution along the channel width through the meander path 68-73

4.5 Boundary Shear stress Distribution at different sections along the meander path 73-79

4.6 Comparison With Other Researcher's work 79-83

4.7 Numerical Results 83

4.7.1 Velocity Contours along the Meander path 84-88

4.7.2 Velocity Contour For total Channel 88

4.7.3 Boundary Shear Contours 89

5 CONCLUSIONS AND SCOPE FOR FUTURE WORK 91-93

5.1 Conclusions 91-92

5.2 Scope for Future Work 93

REFERENCES

LIST OF TABLES

TABLE NO.	DESCRIPTION	PAGE NO.
Table 2.1	Degree of Meandering	14
Table 3.1	Details of Geometric Parameters of the Channel	37

LIST OF PHOTOS

PHOTO NO.	DESCRIPTION	PAGE NO.
Photo1.1	Straight Channel	2
Photo1.2	Meandering Channel	3
Photo1.3	Braided Channel	3
Photo 3.1	Meandering channel in lab	36
Photo 3.2	Meander Path	36
Photo 3.3	Pitot tube arrangement	36
Photo 3.4	Manometers	36
Photo 3.5	Point Gauge	37
Photo 3.6	Volumetric Tank	37
Photo 3.7	Stilling Chamber	37
Photo.3.8	Tail Gate	37
Photo 3.9	Moving Bridge Arrangement	38
Photo 3.10	Flow Straightener	38

LIST OF FIGURES

FIGURE NO.	DESCRIPTION	PAGE NO.
Fig.1.1	Different points of Meandering River	6
Fig.1.2	Contours of Constant Velocity in Open Channel Sections	7
Fig.1.3	Schematic influence of Secondary Flow Cells on Boundary Shear Distribution in a Trapezoidal Section	9
Fig.3.1	Schematic diagram of Experimental Meandering Channel with Setup	35
Fig.3.2	Plan geometry of The Meandering Path	38
Fig.3.3	Grid arrangement of points for velocity measurement across the Channel Section	39
Fig.3.4	Channel geometry in Ansys Design Moduler	49
Fig.3.5	Channel Cross section	50
Fig.3.6	Meshing of the channel Top view	52
Fig.3.7	Meshing View By zooming	52
Fig.3.8	Boundary Conditions	58
Fig.4.1.1-4.1.13	Vertical Velocity Profile Plots for all 13 sections Along the Meander path	60-63
Fig.4.2.1-4.2.13	Longitudinal Velocity contours for all 13 sections along the meander path	69-72
Fig.4.3.1-4.3.13	Lateral Velocity Profile at 0.4H depth from bed of the Channel section along the meander Path	70-73
Fig.4.4.1-4.4.13	Boundary Shear stress Plots across all 13 sections along the Meander Path	74-78
Fig.4.5.1-4.5.13	Comparison of Velocity Profiles at different Aspect Ratios	79-82
Fig.4.6.1-4.6.13	Velocity Contours along the Meander path of all the 13 sections by Ansys fluent	84-88
Fig.4.7	Velocity Contour of the Channel as a whole	89
Fig.4.8	Boundary Shear Stress Contours for total Channel	89

LIST OF SYMBOLS

SYMBOL	DESCRIPTION
A	Cross-sectional Area of Channel
C	Chezy's channel coefficient
C_d	Coefficient of Discharge
d	Diameter of Preston tube
f	Darcy-Weisbach Friction factor
g	Acceleration due to Gravity
h	Pressure Difference
H	Average flow Depth of water at a Section
h_w	Height of Water
H_n	Height of water above the Notch
L	Length of Channel for one Wavelength
L_n	Length of Rectangular Notch
n	Manning's Roughness Coefficient
ΔP	Differential Pressure
Q_a	Actual Discharge
Q_{th}	Theoretical Discharge
r_c	Radius of Curvature of a Sinuous Channel
ρ	Density of the Flow
S	Bed Slope of the Channel
S_r	Sinuosity
SF_{Bed}	Shear Force at the Bed of the Channel
SF_{Inner}	Shear Force at the Inner Wall of the Channel Section
SF_{Outer}	Shear Force at the Outer Wall of the Channel Section

τ	Boundary Shear Stress
υ	Kinematic Viscosity
V_w	Volume of Water
v	Point Velocity
W	Width of Channel
x^*, y^*	Non-Dimensional Parameters
λ	Wavelength of a Sinuous Channel
μ_m	Viscosity of the mixture;

CHAPTER 1
INTRODUCTION

1.1 CHANNEL

A channel is a wide strait or waterway between two land masses that lie close to each other. It can also be the deepest part of a waterway or a narrow body of water that connects two larger bodies of water.

Channel analysis is necessary in order to assess

- Potential flooding caused by changes in water surface profile
- Disturbance of river system upstream or downstream of the highway right of way
- Changes in lateral flow distribution
- Changes in velocity or direction of flow
- Need for conveyance and disposal of excess runoff
- Need for channel lining to prevent erosion

1.2 TYPES OF CHANNEL

Channels are of two types

- **Natural channel**

  Natural channels are not regular, non - prismatic and their material of construction can vary widely. The surface roughness will often change with distance time and even with elevation, consequently it becomes more difficult to accurately analyze and obtain satisfactory results for natural channel than does for man-made ones. The structure may be further complicated if the boundary is not fixed i.e. erosion and deposition of sediment

- **Artificial channel**

  These are channels made by man. They include irrigation canals, navigation canals, spillways sewers, culverts and drainage ditches. They are usually constructed in a regular cross section shape throughout and are thus prismatic channels. In the field they are commonly constructed of concrete, steel or earth

and have the surface roughness reasonably well defined. Analysis of flow in such well-defined channels will give reasonably accurate results.

Also channels can be divided into three types considering their geometry

- **STRAIGHT CHANNEL**

  If in a channel no variation occurs in its passage along its flow path then it is called straight channel. The channel is usually controlled by a linear zone of weakness in the underlying rock, like a fault or joint system.

Photo1.1: Straight Channel

- **MEANDERING CHANNEL**

  If a channel deviates from its axial path and a curvature of reverse order developed with short straight reaches, it is known as meandering channel. Because of the velocity structure of a stream and especially in streams flowing over low gradients which easily eroded banks, straight channels will eventually erode in to meandering channel.

Photo 1.2: Meandering Channel

- **BRAIDED CHANNEL**

  These are the channels consist of network of small channels. In streams having highly variable discharge and easily eroded banks, sediment gets deposited to form bars and islands that are exposed during periods of low discharge. In such a stream the water flows in a braided pattern around the islands and bars, dividing and reuniting as it flows downstream. Such a channel is termed a braided channel.

Photo 1.3: Braided Channel

1.3 MEANDERING RIVER

Rivers flowing over gently sloping ground begin to curve back and forth across the landscape. These are called meandering rivers. A meander in general is a bend in a sinuous water course or river. A meander forms when moving water in a stream erodes the outer banks and widens its valley, and the inner part of the river has less energy and deposits silt. We can consider a river as Straight River, if its length is straight for around 10 to 12 times its channel width, which is not generally possible in natural conditions .Sinuosity is defined as the ratio of the curvilinear length and the distance between the end points of the curve. For rivers Sinuosity is the ratio of channel lengths to that of its down valley length. A river is regarded as meandering if it is having a sinuosity greater than equal to 1.5.

Stream characterizes its own way. Meandering of a river is an exceptionally muddled procedure including flow interaction during bends, erosion and sediment transport. Meandering rivers erode sediment from the outer curve of each meander bend and deposit it on an inner curve further downstream. This causes individual meanders to grow larger and larger over time.

Meandering river channels are asymmetrical. The deepest part of the channel is on the outside of each bend. The water flows faster in these deeper sections and erodes material from the river bank. The water flows more slowly in the shallow areas near the inside of each bend. The slower water can't carry as much sediment and deposits its load on a series of point bars. Oxbow lakes form when a meander grows so big and loopy that two bends of the river join together. Once the meander bends join, the flow of water reduces and sediment begins to build up. Over time oxbow lakes will fill with sediment and can even disappear. The point where the two bends intersect is called a meander cut-off. The low-lying area on either side of a river is called a floodplain. The floodplain is covered with water when the river

overflows it banks during spring floods or periods of heavy rain. Sediment is deposited on the floodplain each time the river floods. Mud deposited on the floodplain can make the soil really good for agriculture.

Inglis (1947) showed that river bend erode at the time of flood because of the excess turbulent energy and as a result it broadens and ridges. There is an inclination for sediment to store at one bend and move towards the other due to the fluctuating discharges and silt formation**. Levliasky (1955)** proposed the centrifugal force to be the reason for winding of a river, due to the helicoidal cross-current formation. **Chang (1984)** prescribed, that "as a general rule, the channel slope can't exceed the valley slope under the condition of equilibrium. If the discharge and loads are such that the channel slope so created exceeds the valley slope, the dynamic changes as aggradations will happen, achieving steepening of the valley slope. As the channel slope can't exceed the valley slope under the state of equilibrium, it should either be equal or less than as valley slope. The meandering channel example talks a level of channel adjustment so that a river with a flatter slope can exist in a steeper valley slope.

River persistently modifies itself concerning its capacity to balance the water discharge and sediment load supplied from the watershed. These changes, likely changes in the channel geometry, side slope, meandering pattern, roughness etc. are made such that the stream experiences least energy expenditure in transportation of its load.

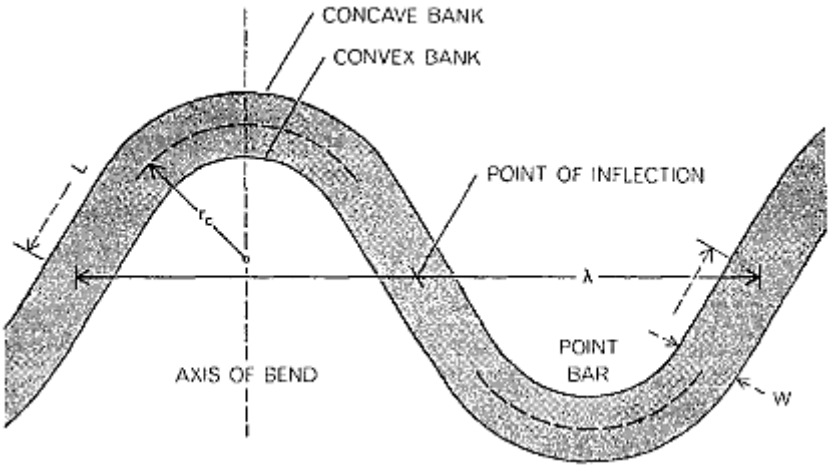

Figure 1.1: Different points of meandering river (Leopold and Langbein, 1966)

1.4 MEANDER PATH

Meander path is a flow route grasped by a conduit like meandering channel or a river. The meander path under this experimentation is starting with one bend apex to the next bend apex. Bend apex of a channel is the segment having greatest curvature. Water in a channel while moving from one bend apex to the next other it goes through the cross-over. Cross-over is a segment at the point of inflection where the meander path changes its course .The concave bank or the external bank transforms into the convex bank or the internal bank after the cross-over and the convex bank or the internal bank transforms into the concave bank or the external bank. In the Fig.1.4 above W means the width of the channel, **λ** signifies the wavelength, **L** indicates the length of channel for one wavelength and $\mathbf{r_c}$ identifies with the range of the channel

1.5 VELOCITY DISTRIBUTION

The knowledge of velocity distribution helps to know the velocity magnitude at each point across the flow cross-section. It is also essential in many hydraulic engineering studies involving bank protection, sediment transport, conveyance, water intakes and geomorphologic investigation The measured velocity in an open channel flow will always

across the channel section because of friction along the boundary. This velocity distribution is usually asymmetric due to existence of free surface. It might be expected to find the maximum velocity at the free surface where the shear force is zero but this is not the case. The maximum velocity is usually found just below the surface. The explanation of this is the presence of secondary currents which are circulating from the boundaries towards the section centre and resistance at the air/water interface. These have been found in both laboratory measurements and 3-d numerical simulation of turbulence. . In straight channel velocity distribution varies with different width-depth ratio, whereas in meandering channel velocity distribution varies with aspect ratio, sinuosity, meandering making the flow more complex to analyse. In laminar flow max stream wise velocity occurs at water level; for turbulent flows, it occurs at about 5-25% of water depth below the water surface**.** In longitudinal velocity variations along the width, it is considered that the maximum velocity occurs somewhere in the middle of the channel as shown in the figures. But it has been observed that in a bend, the maximum velocity occurs at the inner curve of the bend.

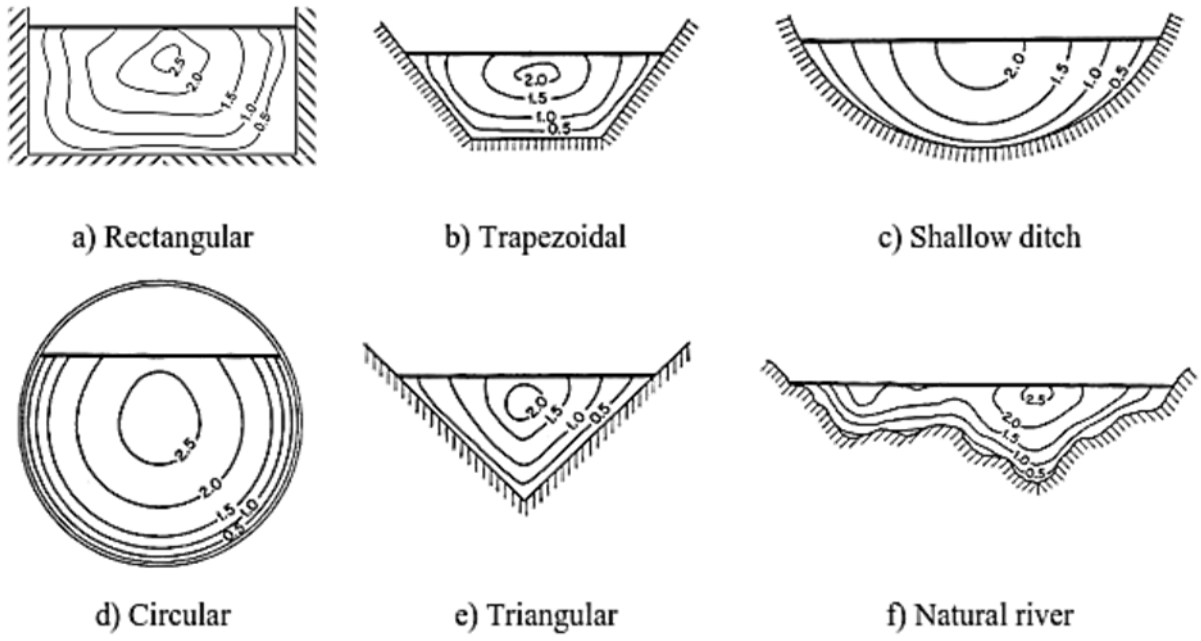

Figure1.2: Contours of constant velocity in various open channel sections (Chow, 1959)

In this experiment the meandering channel under study changes its course, and both the clockwise and anticlockwise curves of the channel are analysed. Hence the movement of velocities can be studied from one bank of the channel to that of the other. The detailed investigation of velocity distribution along the depth and width of a channel is also useful.

1.6 BOUNDARY SHEAR

Water streaming in an open channel is restricted by resistance from the beds as well as the side slopes of the channel. This force of resistance is called the boundary shear force. Boundary shear stress is the tangential component of the hydrodynamic forces acting along the channel bed. Flow qualities of an open channel flow are specifically depending on the boundary shear force distribution along the wetted perimeter of the channel.

Calculation of bed resistance, channel relocation, side wall correction, sediment transport, dispersion, cavitation, conveyance estimation and so on can be considered and dissected by the boundary shear stress distribution.

The shear force, for steady uniform flow is identified with the bed slope, hydraulic radius and unit weight of the liquid. However in a viable perspective, these forces are non-uniform even for straight prismatic channels. The non-consistency of shear stress is predominantly due to the secondary currents composed by the anisotropy of vertical and transverse turbulent intensities, given by **Gessner (1973). Tominaga et al. (1989) and Knight and Demetriou (1983)** explained that boundary shear stress generally increases at the time when the secondary currents flow towards the wall and diminishes when it flows far from the wall. The presence of secondary flow cells in main channel affects the distribution of shear stress along the channel's wetted perimeter which is illustrated in Fig. 1.3. . Other factors affecting the shear stress distribution are the shape of channel cross-section, depth of flow, later-longitudinal distribution of wall roughness and sediment concentration. For the case of

meandering channels, the factors increase even more due to the nature of flow of water in such channels. Different components influencing the shear stress distribution are the shape of channel cross-area, depth of flow, lateral-longitudinal distribution of wall roughness and silt concentration. For the instance of meandering channels, the components build more significantly because of the nature of flow of water in such channels. Sinuosity on account of meandering channel is regarded to be a critical parameter in the shear stress distribution along the channel bed and walls.

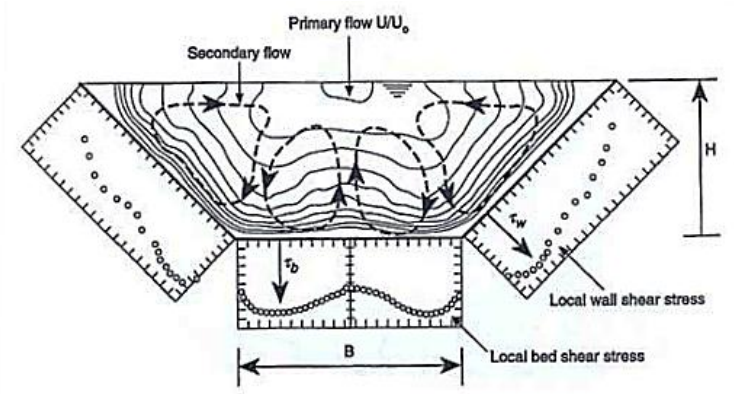

Figure1.3: Schematic influence of secondary flow cells on boundary shear distribution in a trapezoidal section (Knight *et al.*, 1944)

1.7 NUMERICAL MODELLING

Computational fluid dynamics, usually abbreviated as CFD, is a branch of fluid mechanics that uses numerical methods and algorithms to solve and analyze problems that involve fluid flows thus worked as a computer based numerical analysis tool. The growing interest on the use of CFD based simulation by researchers have been identified in various fields of engineering as numerical hydraulic models can significantly reduce costs associated with the experimental models. The basic principle in the application of CFD is to analyze fluid flow in-detail by solving a system of non-linear governing equations over the region of interest, after applying specified boundary conditions. A stride has been taken to do

numerical investigation on a highly sinuous meandering channel. The work will help to simulate the distinctive flow variables in such type of complex flow geometry. The utilization of computational fluid flow was essential for the fulfillment of this undertaking project since it was the main tool of simulation. In general, CFD is a means to precisely foresee phenomena in applications such as fluid flow, heat transfer, mass transfer, and chemical reactions. There are assortments of CFD projects accessible that have abilities for modeling multiphase flow. Some basic projects incorporate ANSYS and COMSOL, which are both multipackage. CFD is a prevalent tool for solving of transport problems due to its capacity to give results for issues where no correlations or experimental data exist furthermore to create results not conceivable in laboratory situations. CFD is additionally valuable for design since it can be specifically meant to a physical setup and is cost effective **(Bakker et al., 2001).** In the present work, an effort has been made to research the velocity profiles for 13 distinctive sections of a simple meandering channel by utilizing a computational liquid motion (CFD) modeling tool, named as FLUENT. The CFD model created for an open-channel was validated by looking at the velocity profile acquired by the numerical simulation with the actual measurement did by experimentation in the same channel utilizing Preston tube. The CFD model has been used to investigate the impacts of flow meandering of the channel, and to study the varieties in velocity profiles along the meander path from one bend apex to the other. The reproduced the simulated flow field in each case is compared with corresponding laboratory measurements of velocity distribution. . Distinctive models are utilized to unravel Navier-Stokes mathematical equations which are the governing equations for any fluid flow. Finite volume method is applied to discretize the governing equations. The precision of computational results essentially relay upon the mesh quality and the model used to simulate the flow.

1.8 OBJECTIVES OF THE RESEARCH

The current work is proposed for examining various flow characteristics of a meandering path of a 120°cross-over angle meandering channel. Although considerable research has been carried out on flow characteristics of open channel curves with different angles, but not much research has been carried out along a path of meandering channel which is preceded and followed by the meandering channel of same sinuosity. The path being a part of a longer meandering channel helps to get more precise informations about its own characteristics which can be applied to real field conditions.

The objectives of the present work are summarized as:

- To Study the longitudinal velocity profiles and contours of a highly meandering channel along the meander path conducted experimentally. The vertical profiles are to be studied systematically across 4cm intervals along the width of the channel at every section of the same meander path. The study helps to understand the detailed characteristic of velocity distribution throughout the channel section and also along the meander path.
- The depth-averaged velocity distribution is to be analysed at different sections of the meandering channel i.e. from one bend apex to the next bend apex.
- Analysis of the boundary shear stress along the bed and side slopes of every section along the meander path. The study helps to observe the variation of shear stress at a section and how it changes with the progression of meander path.
- The velocity distribution obtained experimentally is to be compared with the work of Pradhan (2014) having the same geometrical parameters.
- Application of Numerical software to analyse the flow parameters of the above channel.

1.9 THESIS STRUCTURE

The thesis consists of five chapters. General introduction is provided in Chapter 1, Chapter 2 contains literature survey, methodology is described in Chapter 3 which contains experimental setup along with numerical modelling and numerical simulation, experimental results are demonstrated and analysis of results as well as numerical modelling are explained in Chapter 4, Chapter 5 contains the conclusions drawn from the analysis and at last the references are presented.

Chapter 1 represents briefly about channel, types of channel, meandering river and meander path. General concept of velocity distribution, boundary shear stress distribution along with numerical modelling is also described.

Chapter 2 provides detailed literature survey on the researches done by other researchers on velocity distribution, boundary shear distribution and numerical modelling.The previous research works are arranged according to the year of publication with the latest work at the later.

Chapter 3 gives details about the construction of the channel, the apparatus and equipments used. The methodology adopted for obtaining velocity distribution, boundary shear stress, channel geometry, meshing, governing equations, turbulence models and boundary condition for Numerical modelling are also discussed.

Chapter 4 illustrates the experimental results and its analysis. The results discussed are the horizontal velocity distribution, the vertical velocity distribution, and the boundary shear stress distribution at thirteen different sections along the meander path of the highly sinuous channel. Along with these things numerical modelling is also presented there.

Finally Chapter 5 outlines the conclusions accomplished through the research and the suggestions for further scope are provided. References made in the subsequent chapters are also given.

CHAPTER 2
LITERATURE REVIEW

2.1 OVERVIEW

In this chapter former research in hydraulic engineering related to the behavior of rivers and channels has been composed to obtain an outline of the various features and characteristics of meandering rivers. For better knowledge about river systems, analysis of its velocity distribution along its width, depth and also along the meander path with maximum accuracy is crucial. The flow characteristics of a river is imperative for flood control, channel design, channel stabilization and restoration projects and it influences the transport of pollutants and sediments. Flow in meandering channels is of increasing importance as this type of channel is common in the case of natural rivers, and research work regarding flood control, discharge estimation and stream restoration need to be conducted for this type of channel. It has exposed from investigators that the flow structure of meandering channels is unpredictably more complex than straight channels due to its velocity distribution. There are boundaries studies available in literature concerning the flow in meandering channels. Meandering effectively lengthens the channel path, within the existing valley or flood plain. The degree of meandering may be measured by the term sinuosity, which is defined as the ratio of channel length to valley length. Chow (1959) described the degree of meandering as follows:

Table 2.1:-Degree of meandering

Sinuosity ratio	Degree of meandering
1.0 - 1.2	Minor
1.2 - 1.5	Appreciable
1.5 and greater	Severe

The analysis of flow along a meander path is not only confined to its velocity distribution but also the shear force variations along the bed and inner and outer walls is also studied to get an outline of the shear force sharing between them. This would help in the design of bank

protection and channel designs. This chapter is therefore divided into sections related to the previous research carried out on velocity distributions and boundary shear force distribution of meandering channels.

2.2 PREVIOUS RESEARCH ON LONGITUDINAL VELOCITY DISTRIBUTION

The longitudinal velocity signifies the speed at which the water is moving in the stream wise direction. If a number of velocity measurements are taken throughout the depth across the channel, it is possible to produce a distribution of the isovels which represents contour lines.. Each of these lines stands for the same velocity magnitude over the channel. The isovels achieve values as low as zero in the region of the channel perimeter and increment to a maximum value underneath the water surface in the area encompassing the centre of the channel. These isovels are influenced by the secondary currents that results in a bulge in their distribution in their dispersion.

Thomson (1876) studied that flow motion in a channel bend is spiral. It was observed that centrifugal force was the main cause for such a phenomenon, which is generated because of the curved flow path, and resulting spiral motions, i.e. secondary flows, have a substantial effect on engineering matters such as flow resistance, sediment transport, erosion and deposition.

Coles (1956) suggested a semi-empirical equation of velocity distribution, which can be applied to both outer and wall region of plate and open channel. He generalized the logarithmic formula of the wall with tried wake function, $w(y/8)$ which is the basic formulation towards outer layer region.

The U.S. Army Corps of Engineers (Hydraulic 1956) conducted a series of experiments on meandering channels at the Waterways Experiments Station in Vicksburg. This paper investigates the stage-discharge relationship and the effect of geometric parameters like

radius of curvature of the bends, sinuosity of the channel, depth of flow, channel roughness etc. on the conveyance capacity of meandering channels.

Chow (1959) demonstrates the tables determining roughness coefficients for characteristic channels with consistent roughness characteristics along a full river reach. However in any one reach these attributes may fluctuate significantly.

The original Soil Conservation Service (SCS) (1963) method is useful in selecting roughness coefficient values for meandering channels. It consists of an empirically-based model which integrates the extra flow resistance resulting from the influence of a channel sinuosity by adjusting the roughness coefficients which has been used in the standard resistance formulae.

Sellin (1964) discourses about the existence of vertical vortices at the junction adopting a flow visualization technique. He also explained that through these vortices momentum is exchanged between the main channel and the flood plain.

Toebes and Sooky (1967) carried an experiment from which the roughness, slope and channel depth on the discharge capacity of a meandering channel was investigated. A sinuosity of 1.09 was set for all the models which meant that the key parameters of these models were not similar with the key parameters in natural river channels. They observed the insight into general flow behavior and the dependency of meandering channels on longitudinal slope as well as channel aspect ratio.

Donald W. Knight, *et. al.* (1983) carried out experiments on flood plain and main channel flow interactions. The discharge characteristics, boundary shear stress and boundary shear force distributions in a compound section comprising of one rectangular main channel and two symmetrically disposed flood plains which are obtained from experimental results.

Equations are formed taking the shear force on the flood plains as a percentage of the total shear force in terms of two dimensionless parameters. The resulting shear force from experiments is used to derive auxiliary equations for the lateral and vertical transfer of momentum within the cross section. The apparent shear force which is acting on the vertical interface between one flood plain and the main channel is indicated to increase rapidly for low relative depths and high flood plain widths. Equations are modeled also to give the proportion of the total flow which occurs in the various sub areas. The division of flow based on linear proportion of the areas is shown to be inadequate on account of the interaction between the flood plain and main channel flows.

Chang (1984) conducted experiment on the meander curvature and other geometric features of the channel using the energy approach. It directly accounts for variations in bend radius along the length of a channel. The modified Chang (1984) method is generally on the assumption that the channel is wide as compared to its depth. This paper shows that it is difficult to apply this method to natural channels because of their variability in configuration. In some of the illustrations the modified Chang method will give results which are physically correct; however in most of the circumstances the simple LSCS method will be more appropriate than this method.

Booij (1985) presented his experimental work and measure of the various shear stress components in a mildly curved flume. He considered a 2-component LOA in his analysis which set up a unique configuration of the laser beams to obtain lateral and vertical components. His paper calculated the eddy viscosity coefficients in three directions: 1'yx -'-I (*a.---uv -8yx -J+ b-Tl) -8yax.Jp* 0/ & 0/ and so on. It is shown that the assumption of isotropic eddy viscosities was not justified in the curved channel.

James and Wark (1992) studied the step function defined above with a linear function to avoid the discontinuity at the certain boundaries of the defined sinuosity ranges with consequent ambiguity. To overcome from this difficulty the existing equation was further liberalized known as the Linearized SCS (LSCS) Method [1992] and this method was easy to apply and yields a significant result.

Willets and Hardwick (1993) led an experiment to study flow in a small laboratory flume where meandering channels of different sinusitis and geometry were used. It was observed that the conveyance of channel vary with sinuosity. As such, the flow resistance increments generously with an increment in channel sinuosity. The flow interaction in charge of the stream resistance was additionally discovered to be reliant on channel cross section geometries cross section geometries.

Shiono, et. al. (1999) contemplated the impact of bed slope and sinuosity on discharge estimation of a meandering channel. Conveyance capacity of a meandering channel was inferred utilizing dimensional analysis and therefore helped in discovering the stage-discharge relationship for meandering channels. The study demonstrated that the discharge increases with an increment in bed slope and decreases with increase in sinuosity for the same channel.

Sarma et al. (2000) attempted to formulate the velocity distribution law in open channel flows by taking generalized binary version of velocity distribution, which consolidates the logarithmic law of the inner region and parabolic law of the outer region. The law grew by taking velocity-dip into account.

Patra, Kar and Bhattacharya (2004) demonstrated that the flow and velocity distribution in meandering channels are firmly administered by flow collaboration. By taking sufficient

consideration of the collaboration influence, they proposed equations that are found to be in great concurrence with natural rivers furthermore the experimental meandering channel data acquired from a progression of symmetrical and unsymmetrical test channels with smooth and rough sections.

Wilkerson et al. (2005) utilizing information from three past studies, developed two models for foreseeing depth-average velocity distribution in straight trapezoidal channels that are not wide, where the banks apply form drag on the fluid and in this manner control the depth average velocity distribution. The data they utilized for building up the model are free from the impact of secondary current. The 1st model required measured velocity data for calibrating the model coefficients, whereas the 2nd model utilized prescribed coefficients. The 1st model is prescribed when depth-averaged velocity data are available. At the point when the 2nd model is utilized, the predicted depth average velocities are required to be inside 20% of actual velocities.

Afzal et al. (2007) investigated power law velocity profile in completely developed turbulent pipe and channel flows in terms of the envelope of the friction factor. This model gives good close estimation for low Reynolds number in planned process of actual system compared to log law.

Khatua (2008) studied the distribution of energy in a meandering channel. It is come about because of the variety of the resistance variables like Manning's n, Chezy's C, and Darcy-Weisbach's f with flow depths. Stage-discharge relationship from in-bank to the over-bank flow, channel resistance coefficients were found for meandering channel.

Pinaki (2010) analysed a series of laboratory tests for smooth and rigid meandering channels and created mathematical equation utilizing dimension analysis to calculate roughness coefficients of smooth meandering channels of less width ratio and sinuosity.

Seo and Park (2010) conducted laboratory and numerical studies to discover the impacts of secondary flow structures and distribution of pollutants in curved channels. Primary flow is discovered to be skewed towards the inward bank at the bend while flow gets to be symmetric at the cross-over.

Khatua and Patra (2012) performed a series of laboratory tests for smooth and rigid meandering channels and created mathematical models utilizing dimensional analysis to assess roughness coefficients. The vital variables considered in influencing the stage-discharge relationship were velocity, hydraulic radius, and viscosity, acceleration due to gravity, bed slope, sinuosity, and aspect ratio.

Moharana (2012) contemplated the impact of geometry and sinuosity on the roughness of a meandering channel. ANFIS was used to foresee the roughness of a meandering channel utilizing a large data set.

Dash (2013) dissected the vital parameters influencing the flow behaviour and flow resistance in term of Manning' n in a meandering channel. Elements influencing roughness coefficient are non-dimensional zed to foresee and discover their reliance with different parameters. A scientific model was formulated to anticipate the roughness coefficient which was connected to foresee the stage-release relationship.

Mohanty (2013) anticipated lateral depth averaged velocity distribution in a trapezoidal meandering channel. A nonlinear manifestation of equation including overbank flow depth, main channel flow depth, incoming discharge of the main channel and floodplains were

formulated. A quasi1D model Conveyance Estimation System (CES) was connected to the same experimental compound meandering channel to validate with the experimental depth averaged velocity.

Pradhan (2014) analysed the flow along the meander path of a highly sinuous rigid channel. He has done the study thoroughly to find the changes in the water surface profile throughout the meander path and also longitudinal velocity distributions along the width and depth of the channel i.e. the horizontal and vertical velocity profiles were investigated.

2.3 PREVIOUS RESEARCH ON BOUNDARY SHEAR

In straight channels, the longitudinal velocity in the channel is generally faster. This results a shear layer at the interface of straight channel. Due to the presence of this shear layer, the flow in the straight channel decreases because of the effect of faster flows. This result shows that the flow decreases the whole discharge of the cross section.

Leighly (1932) contemplated the boundary shear stress distribution in open-channel flow by utilizing conformal mapping. He pointed out that, without secondary currents, the boundary shear stress acting on the bed must be adjusted by the downstream component of the weight of water contained inside the bounding orthogonal.

Cruff (1965) contemplated the utilization of the Preston tube technique and additionally the Karman - Prandtl logarithmic velocity law to estimate the boundary shear stress resulting because of uniform flow in a rectangular channel. A Preston tube is navigated around the boundary of a rectangular channel and an estimation of the boundary shear stress distribution obtained. From contemplations of the longitudinal force equilibrium Equation, an apparent shear force, which is basically an "out of balance" force, could be figured to act on any vertical plane in the flow. In spite of the fact that he didn't quantify boundary shear stress in a channel with overbank flow, his work perceived a technique to empower agents to ascertain

the apparent shear stress and henceforth momentum transfer between a channel and its flood plain. Additionally Wright and Carstens utilized the Preston tube procedure to quantify boundary shear stresses in a Closed conduit aerodynamic model 6 meters long.

Ghosh and Jena (1972) demonstrates the distribution of boundary shear stress for rough and smooth walls in a compound channel. The test is directed in an 8*5 meter long flume with a main channel width of 0.203 meters flanked by two flood plains, each of width 76 mm. additionally they got the boundary shear appropriation along the wetted perimeter of the total channel for different depths of stream utilizing the Preston tube technique consolidated with the Patel calibration. It is watched that the greatest shear weight on the channel bed happens roughly halfway between the inside line and corner, and the most extreme shear in the flood plain dependably happens at the channel/flood plain intersection. Likewise they arranged no immediate reference to the cooperation between the main channel and its flood plain; however results acquired can be utilized to compute the degree of any connection which was occurring amid their tests. From the test consequences of the shear circulation it is conceivable to compute Tc' the normal shear push in the- channel amid association. It is watched that by roughening the aggregate fringe of the channel and flood plain the boundary shear in the channel could be redistributed with the most extreme shear in the channel bed now happening at the channel Centre line.

Knight and Macdonald (1979) contemplated that the resistance of the channel bed differed by artificial strip roughness components, and estimations made of the divider and bed shear stresses. The distribution of velocity and boundary shear stress in a rectangular flume was analysed tentatively, and the impact of fluctuating the bed roughness and aspect ratio were accessed. Dimensionless plots of both shear stress and shear force parameters were presented for different bed roughness and aspect ratio, and those represented the intricate way in which

such parameters are varied. The definition of a wide channel was also examined, and a graph giving the blundering aspect ratio for distinctive roughness conditions was exhibited. The boundary shear stress disseminations and isovel examples were used to look at one of the standard side-wall correction procedures.

Rajaratnam and Ahmadi (1979) directed an experimental work in a channel 18.29 meters in length, 1.22 meters wide and 0.9 meters deep. A main channel 0.2032 meters wide, flanked by two flood fields, every 0.508 meters wide is utilized to show the Interaction mechanism in a symmetrical compound channel. Velocity navigates and boundary shear stress was recorded. Analysis of velocity profiles uncovered that the lateral velocity profiles at different depths in the main channel showed similarity.

Bathurst et al. (1979) displayed the field measurements for the bed shear stress in a curved river and it is reported that the distribution of bed shear stress is influenced by both the position of the center of the main velocity and the structure of secondary flow.

Knight (1981) gave an empirically determined equation that presented the percentage of the shear force carried by the walls as a component of the breadth/depth proportion and the proportion between the Nikuradse identical roughness sizes for the bed and the walls. The outcomes were contrasted and other accessible information for the smooth channel case and a few differences noted. The systematic reduction in the shear force conveyed by the walls with expanding breadth/depth proportion and bed roughness was shown. Further equations were exhibited giving the mean wall and bed shear stress variety with aspect ratio and roughness parameters.

Knight and Patel (1985) reported a part of laboratory examination results concerning the distribution of boundary shear stress in smooth close conduits of a rectangular cross section for an aspect ratio around 1 and 10. The distributions were shown to be influenced by the number and state of the secondary flow cells, which, therefore, depended essentially upon the aspect ratio. For a square cross section with 8 symmetrically arranged secondary flow cells, a twofold top in the distribution of the boundary shear stress along every wall was shown to dislodge the maximum shear stress far from the centre position towards every corner. For square cross portions, For a square cross segment with 8 symmetrically arranged optional stream cells, a twofold top in the appropriation of the limit shear push along every divider was demonstrated to uproot the most extreme shear stretch far from the inside position towards every corner. For rectangular cross sections, the quantity of secondary flow cells increased from 8 by augmentations of 4 as the aspect ratio increased, bringing on alternate perturbations in the boundary shear stress distribution at positions where there were adjacent contra-rotating flow cells. Equations were presented for the most extreme, centreline and mean boundary shear stress on the duct walls in terms of aspect ratio**.**

Knight and Sterling (2000) studied the appropriation of boundary shear stress in circular conduits flowing mostly full with and without a smooth level bed for an information extending from 0.375<F<1.96 and 6.5*104<R<3.42*105, utilizing Preston-tube technique. The distribution of boundary shear stress is demonstrated to rely on upon geometry and Froude no. The outcomes have been examined as far as variety of local shear stress with edge separation and the rate of aggregate shear force following up on wall or bed of the course. The %SFW results have been indicated to concur well with Knight's (1981) exact equation for prismatic channels. The interdependency of secondary flow and boundary shear stress has been made and its implications for sediment transport have been analysed.

Ervine, Alan, Koopaei, and Sellin (2000) displayed a practical strategy to anticipate depth averaged velocity and shear stress for straight and meandering over bank flows. They additionally displayed an analytical solution to the depth coordinated turbulent form of Navier-Stokes equation that incorporates lateral shear and secondary flows in addition to bed friction. They connected this analytical solution for various channels, at model, and field scales, and compared with other accessible systems, for example, that of Shiono and Knight and the lateral distribution method (LDM).

Patra and Kar (2000) have taken into account the flow collaboration of meandering channel with floodplains. A series of lab test results are led about the limit shear stress, shear force, and discharge qualities of compound meandering channel areas made out of a rectangular main channel and possibly a few floodplains discarded to its sides. Five dimensionless parameters are used to shape equations representing the aggregate shear force rate passed on by floodplains. An arrangement of smooth and rough sections is examined over with an aspect ratio extending from 2 to 5. Apparent shear forces on the assumed vertical, horizontal and diagonal Interfacial plains are found to be non-zero at low depths of flow and change sign with an increment in the depth over the floodplain. Here a variable-inclined interface is proposed for which evident shear force is determined as zero. This paper shows comparisons related with the degree of discharge passed on by the main channel and floodplain. The equations agree well with experimental river discharge data. Using the variable-inclined interface, the lapse between the computed and measured discharges for the meandering compound section is found to be minimum when compared with distinctive interfaces.

Patra and Kar (2004) described the test results concerning the flow and velocity distribution in meandering compound river sections. Utilizing power law they showed mathematical equations concerning the three-dimensional mixture of longitudinal, transverse, and vertical

velocity in the main channel and floodplain of a meandering compound segment in terms of channel parameters. The consequences of plans contrasted well and their individual experimental channel datas got from a progression of symmetrical and unsymmetrical test channels with smooth and rough surfaces. They moreover affirmed the points of interest against the natural river and other meandering compound channel data.

Khatua (2008) propelled the work of Patra and Kar (2000) towards meandering compound channels. Utilizing five parameters (sinuosity *Sr*, amplitude, relative depth, width ratio and aspect ratio) general mathematical equations representing the aggregate shear force percentage conveyed by floodplain was shown. The proposed equations are simple, quite reliable and gave awesome results with the observed data for straight compound channel of Knight and Demetriou (1983) and furthermore for the meandering compound channel.

Khatua (2010) showed the distribution of boundary shear force for staggeringly meandering channels having noticeably different sinuosity and geometry. He also indicated the interrelationship between the boundary shear, sinuosity and geometrical parameters taking into account the experimental results. The given models are also accepted utilizing the well published data of other investigators.

Patnaik (2013) Calculated boundary shear stress at the bend apex of a meandering channel for both in bank and overbank flow conditions. Test reports were accumulated under different discharge and relative depths having same geometry, slope and sinuosity of the channel. Effect of aspect ratio and sinuosity on wall (internal and outer) and bed shear forces were surveyed and equation was delivered to focus the rate of wall and bed shear forces in smooth trapezoidal channel only for in bank flows. The given equations were compared with the past studies and the model was reached out to wide channels.

2.4 PREVIOUS RESEARCH ON NUMERICAL MODELLING

The features characterized in open channel flow result from the complex interaction between the fluid and a number of mechanism including shear stress along the channel bed and walls, friction, gravity and turbulence. As numerical hydraulic models can significantly reduce costs associated with the experimental models, therefore in recent decades the use of numerical modelling has been rapidly expanded. With widely spread in computer application, interest has risen in applying more techniques providing more accurate results. In other fluid flow fields such as aeronautics and thermodynamics the implementation of more complex models has represented the advances in computer technology and 3D models are now commonly used. However in open channel flow this conversion has not occurred as rapidly than other sector of engineering and most hydraulics models are either 1D or 2D with very few application of 3D models. In this work the application of Computational Fluid Dynamics (CFD) package to open channel flow has been considered. The software includes various models to solve general fluid flow problems. Across the globe various numerical models such as standard k-ε model, non-linear k-ε model, k-ω model, algebraic Reynolds stress model (ASM), Reynolds stress model (RSM) and large eddy simulation (LES) have been implemented to simulate the complex secondary structure in open channel flow. The standard k- ε model is an isotropic turbulence closure but fails to reproduce the secondary flows. Although nonlinear k- ε model can simulate secondary currents successfully in a compound channel, it cannot accurately capture some of the turbulence structures. Reynolds stress model (RSM) is very effective in computing the time-averaged quantities and requires much less computing cost. RSM computes Reynolds stresses by directly solving Reynolds stress transport equation but its application to open channel is still limited due to the complexity of the model. Large eddy simulation (LES) solves spatially-averaged Navier-Stokes equation. Large eddies are directly resolved, but eddies smaller than mesh are modelled. Though LES

is computationally expensive to be used for industrial application but can efficiently model nearly all eddy sizes. The work of previous researchers regarding the advancements in numerical modelling of open channel flow has been listed below.

Giuseppe and Pezzinga(1994) used the k-ε model to analyze the problem of prediction of uniform turbulent flow in compound channel. This model is useful to predict the secondary currents, caused anisotropy of normal turbulent stresses which are important features of the flow in compound channel as we can determine transverse momentum transfer. He made a comparison which shows that the model predicts with accuracy the distribution of primary of the velocity component, the secondary circulation and the discharge distribution.

Cokljat and Younis,Basara and Cokljat(1995) gave the RSM for numerical simulation of free surface flows in a rectangular main channel and a compound channel. They found good agreement between predicted and measured data.

Thomas and Williams (1995) gave description of a LES of steady uniform flow in a symmetric compound channel of trapezoidal cross section with flood plains at Reynolds's number of 430000.This simulation helps to predict the bed stress distribution, velocity distribution and secondary circulation across the flood plain by interacting with main channel and flood plain.

Salvetti et.al(1997) has done LES simulation at a relatively large Reynolds number which in turn gives the result of bed shear, secondary motion and vortices well comparable to experimental results.

Ahmed Kassem, Jasim Imran and Jamil A. Khan (2003) examined from the three dimensional modeling of negatively buoyant flow in a diverging channel with a slanting

bottom. They modified the k- turbulence model for the lightness impact and Boussinesq close estimation for the Reynolds- averaged equations in diverging channels.

Lu et al. (2004) connected a three-dimensional numerical model to reenact secondary flows the distribution of bed shear stress, the longitudinal and transversal changes of water depth and the distribution of velocity components at a 180° bend utilizing the standard k- turbulence model.

Sugiyama H,Hitomi D.saito T.(2006) developed turbulence model which includes transport equation of turbulent energy and dissipation along with an algebraic stress model based on the Reynold's stress transport equation. They have demonstrated that the fluctuating vertical Velocity approaches zero close to the free surface. Furthermore, the compound meandering open channel was elucidated to some degree based on computed results. As an aftereffect of the investigation, the present algebraic Reynolds stress model is shown to be able to reasonably predict the turbulent flow in a compound meandering open channel.

Bodnar and Prihoda (2006) exhibited a numerical recreation of the turbulent free surface flow by utilizing the k- turbulence model and analyzed the way of non-linearity of water surface slant at a sharp bend.

Booij (2003) and VanBalen et al. (2008) displayed the flow design at a mildly bended 180º twist and evaluated the secondary flow structure utilizing Large Eddy Simulation (LES) model.

Cater and Williams (2008) reported an unequivocal Large Eddy Simulation of turbulent flow In a long compound open channel with one floodplain. The Reynolds number is pretty about 42,000 and the free surface was managed as totally deformable. The results are in simultaneousness with test estimations and support the use of high spatial determination and

a vast box length interestingly with a past reenactment of the same geometry. A discretionary flow is perceived at the internal corner that endures and grows the bed weight on the floodplain.

Jing, Guo and Zhang (2009) reenacted a three-dimensional (3D) Reynolds stress model (RSM) for compound meandering channel flows. The velocity fields, wall shear stresses, and Reynolds stress are ascertained for a range of input conditions. Great assertion between the simulated results and measurements shows that RSM can effectively anticipate the confounded flow phenomenon.

B. K. Gandhi, H.K. Verma and Boby Abraham (2010) determined the velocity profiles In both the directions under distinctive real flow conditions, as ideal flow conditions seldom exists in the field. 'Fluent', a commercial computational fluid dynamics (CFD) code, has been utilized to numerically model different situations. They examined the impacts of bed slope, upstream bend.

Balen et.al. (2010) performed LES for a bended open-channel flow over topography. It was observed that, despite the coarse technique for representing the ridge shapes, the Qualitative assertion of the test results and the LES results is fairly great. Also, it is observed that in the bend the structure of the Reynolds stress tensor demonstrates an inclination toward isotropy which upgrades the execution of isotropic eddy viscosity closure models of turbulence.

Esteve et.al. (2010) reenacted the turbulent flow structures in a compound meanderingChannel by Large Eddy Simulations (LES) utilizing the experimental arrangement of Muto and Shiono (1998). The Large Eddy Simulation is performed with the in-house code LESOCC2. The anticipated flow wise velocities and secondary current vectors and in addition turbulent intensity are in great concurrence with the LDA measurements.

Ansari et.al. (2011) decided the distribution of the bend and side wall shear stresses in trapezoidal channels and examined the effect of the variety of the slant angles of the side walls, aspect ratio and composite roughness on the shear stress distribution. The outcomes demonstrate a noteworthy contribution on secondary currents and overall shear stress at the boundaries

Rasool Ghobadian and Kamran Mohammodi (2011) recreated the subcritical flow Pattern in 180° uniform and convergent open-channel curves utilizing SSIIM 3-D model with Maximum bed shear stress. They noticed toward the end of the convergent bend, bed shear stress show higher values than those in the same locale in the channel with a uniform twist.

Khazaee & M. Mohammadiun (2012) explored three-dimensional and two phase CFD model for flow distribution in an open channel. He completed the Finite volume method (FVM) with a dynamic Sub grid scale for seven instances of distinctive aspect ratios, different inclination angles or slopes and converging diverging condition.

Omid Seyedashraf, Ali Akbar Akhtari& Milad Khatib Shahidi (2012) reached in a conclusion that the standard k-ε model has the ability of catching particular flow features in open channel curves more precisely. Looking at the location of the minimum velocity occurrences in a customary sharp open channel bend, the minimum velocity occurs close to the inward bank and inside the separation zone along the meandering.

Larocque, Imran, Chaudhry (2013) displayed 3D numerical recreation of a dam-break Flow utilizing LES and k- ε turbulence model with following of free surface by volume-of-fluid model. Results are compared with published experimental data on dam break flow through incomplete break and additionally with results acquired by others utilizing a shallow water model. The outcomes demonstrate that both the LES and the k –ε displaying palatably

imitate the fleeting variety of the measured bottom pressure. Nonetheless, the LES model catches better the free surface and velocity variety with time.

Ramamurthy et al. (2013) reenacted three-dimensional flow design in a sharp bend by utilizing two numerical codes alongside different turbulent models, and by comparing the numerical results with results approved the models, and guaranteed that RSM turbulence model has a better agreement with experimental results.

Mohanta (2014) gave the Flow Modelling of a Non Prismatic compound channel By Using CFD. He used the large eddy simulation model to accurately predict the flow features, specifically the distribution of secondary circulations both for in-bank channels as well as over-bank channels at varying depth and width ratios in symmetrically converging flood plain compound sections

CHAPTER 3
METHODOLOGY

3.1 OVERVIEW

Experimentation on natural rivers is very intricate; therefore the flow characteristics of a river can be analysed generally by studying them on a model designed similar to that of natural rivers. Rivers are usually meandering by nature, having different sinuosity throughout their path. Flow patterns are to be studied on experimental models for different sinuosites and can then be used to model them on natural channels.

For study of the flow patterns and characteristics of meandering rivers, a highly meandering channel is constructed and the different velocities and shear changes are measured for the total meander path. The study helps to analyze the movement of rivers in natural meanders.

3.2 DESIGN AND CONSTRUCTION OF CHANNEL

The required experimental channel was manufactured in a large tilting flume having a width of 4m and length of 15m. The flume has a course of action of pressure driven jacks for creating different bed slopes on tilting. This aggregate plan is made available at the Fluid Mechanics and Hydraulics Laboratory of NIT, Rourkela. A meandering channel has been constructed inside of the tilting flume through Perspex sheets to complete the experimentations. The Perspex sheets are about 6mm to 10mm thick.

The meandering channel made, has straight flood plains, beneath which the main channel is established having a bank full depth of 0.065m with a base width of 0.33m and 1:1 side slope. Fig. 3.1 illustrates the schematic diagram of the channel setup. The main channel is a meandering channel, similar to a sine curve of one and half wave length. The aggregate wavelength being λ=2.162m preceded and followed by a bell mouth section for proper flow field development at the experimental setup which is from the second bend apex to the following bend apex of the central curve.

Water into the channel is flowed from an underground sump to an overhead tank with the help of radial pumps. Overhead tank is useful in keeping up a steady head of water, where the

excess water is allowed to drift back into the sump. Water comes into the flume from the overhead tank through customizable pipes which can be utilized to keep up a desired amount of discharge. This water falling into the flume is first detained in a stilling tank. Then it is directed through an adjustable vertical gate into a series of baffle wall suitable ahead of the rectangular notch. These are provided for decreasing the turbulence of the approaching water. Water from the notch falls over a wire mesh placed just underneath the notch, to further steady the flow. Water then flows into the main channel through smooth bell mouth transition section to achieve steady flow in the channel. The stream accomplishes a Quasi-Uniform flow. Water flows in the channel due to gravity, achieved by giving a small slope to the tilting flume. The flow of water is going through the main channel subsequently directed into a volumetric tank through a regulating tailgate. The volumetric tank is joined with the underground sump. The volumetric tank is utilized for measuring the actual discharge of flow; otherwise the water is permitted to move into the underground sump .Hence forth a complete distribution of water is achieved. All the measurements are observed from the second bend apex to the next following bend apex of the experimental channel from the upstream site. Observations are recorded under steady and uniform flow conditions. A moving bridge arrangement is provided along the width of the channel of around 1.2m width by 4m length across the channel. The measuring instruments, for example, point gauges and pitot tubes are arranged on the bridge such that every section of the meandering path is accessible for measurements.

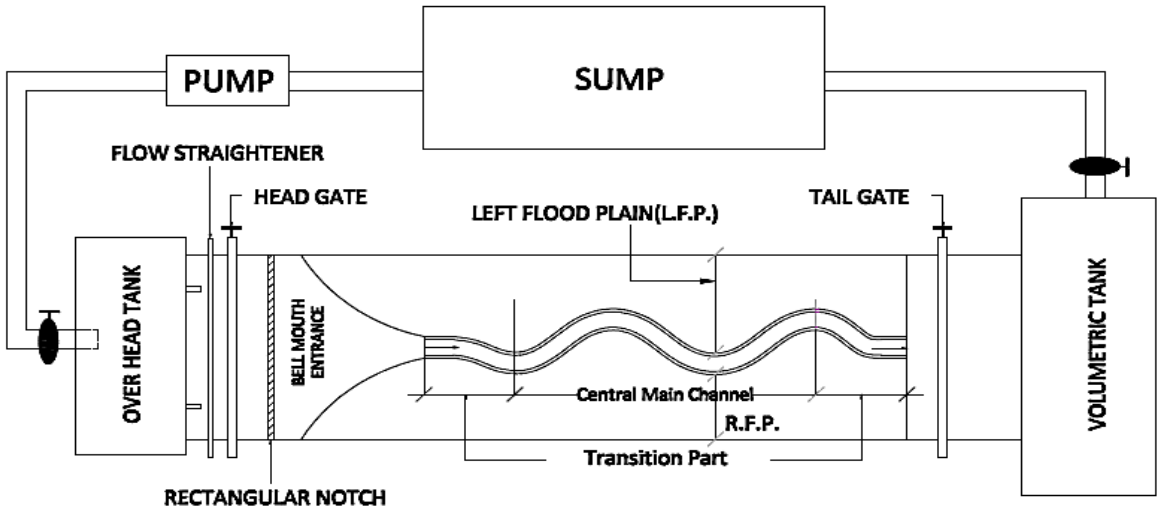

Fig 3.1: Schematic Diagram of Experimental Meandering Channel with Setup

3.3 APPARATUS AND EQUIPMENTS USED:-

Five pitot tubes are fitted with the moving bridge and are unequally spaced with an external diameter of 4.7mm along with a point gauge having a least count 0.1mm. The moving bridge is traversed along the meander path to reach at required sections so that respective readings can be taken. The pilot tubes show the pressure difference at every predefined grid across every section of the meander path. Velocities at those points are then computed from the pressure differences. All the five pitot tubes are associated with five unique manometers which are connected on a vertical board having a spirt level. The spirit level helps to keep up the verticality of the manometers. A rectangular notch arrangement is provided at the upstream section for maintaining and calculating the discharge of water into the meandering channel. The following photographs display the measuring devices used for experimentation.

Photo 3.1: Meandering Channel

Photo 3.2: Meander path

Photo 3.3: Pitot tube arrangement

Photo 3.4: Manometers

Photo 3.1 – 3.4: Photographs of Channel and some of the equipments

3.4 EXPERIMENTAL PROCEDURE

3.4.1 EXPERIMENTAL CHANNEL

The meandering main channel constructed has a sinuosity of 4.11 with a wavelength of 2.162m. The main channel is a trapezoidal section of 1:1 side slopes and having a bottom width of 0.33m and top width of 0.46m with the bank full depth of 0.065m. The detailed geometric parameters of the meandering channel are illustrated in the following tabulation.

Table 3.1: Details of Geometrical Parameters of the Channel

Sl No	Parameter	Description
1	Channel type	Meandering
2	Dimension of flume	4.0 m × 0.5 m × 15 m Long
3	Geometry of main channel	Trapezoidal with side slopes 1:1
4	Bed Surface type	Smooth Bed
5	Cross Section of Channel	0.33 m at Bottom and 0.46 m at Top
6	Bank Full Depth	0.065 m
7	Bed Slope of the Main Channel	0.00040146
8	Sinuosity of the Main Channel	4.11
9	Amplitude of the Meandering Channel	1.555 m
10	Wave length of the Meandering Channel	2.162 m

Photo 3.5: Point Gauge

Photo.3.6: Volumetric Tank

Photo.3.7: Stilling Chamber

Photo.3.8: Tail gate

Photo3.9: Moving Bridge

Photo3.10: Flow Straightener

Photo 3.5-3.10: Meandering Channel inside the Flume with different parts

3.4.2 POSITION OF MEASUREMENT

All observations are recorded along a meandering path from the second bend apex to the corresponding bend apex via the cross-over of the meandering channel. A section at crossover perpendicular to both the inner and outer curves of the meandering channel is drawn and extended up to the bend apex line, as shown in Fig. 3.2. An angle of 120^0 is formed for both the curves. Which is the cross-over angle or the arc angle. The curves are divided into 6 equal sections of 20^0 each to the centerline of the meandering channel. Channel sections along the width i.e. perpendicular lines drawn to both the curves from these points. Sections A and M are the bend apex while section G is the cross-over section. The sections A through M are considered for measurement of the velocity profiles.

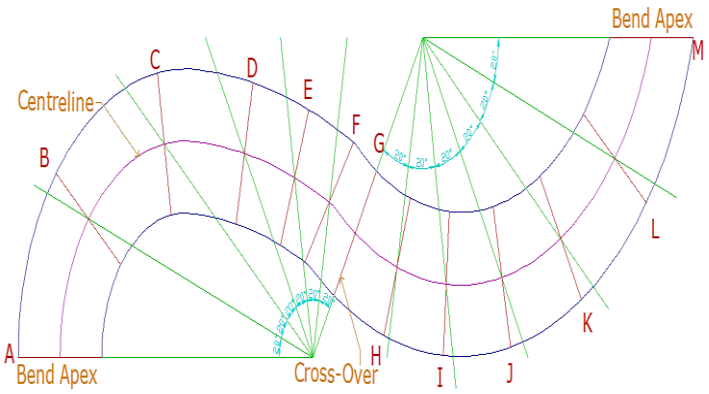

Figure 3.2: Plan Geometry of the Meandering Path.

A constant discharge is maintained during the experiment while taking the readings for the entire meandering path. Series of Pitot-tubes with moving bridge arrangement are provided to measure the velocity at different points of the flow passage of the channel. The measurements are taken at different reaches along the meander path for every section. Datas are observed from left edge to the right edge of the main channel in the direction of flow. The lateral spacing of the grid points has been taken as 4cm on either side of the centreline. The Pitot tube is navigated upwards from the bed of the channel. The bed of the channel signified here is the position of radius of the Pitot tube which is 0.2385cm from the bed. This is achieved by placing the Pitot tube at the surface of the channel. Readings are taken at the bed and then moved up by 0.2H,0.4*H*, 0.6*H*, and 0.8*H*from the bed. Where *H* is the average depth of water at the every corresponding section along the meander path. Fig.3.3 shows the grid diagram used for the experiments.

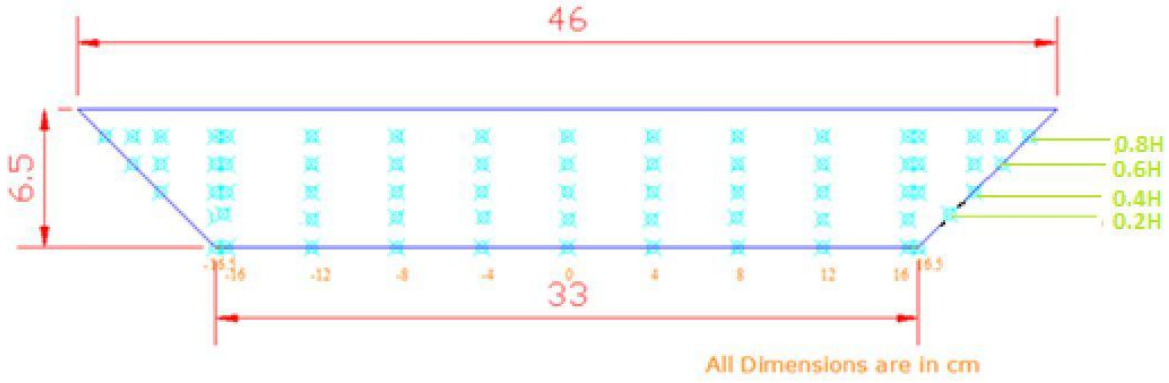

Figure 3.3: Grid Arrangement of Points for Velocity Measurement across a Channel Section.

3.4.3 MEASUREMENT OF BED SLOPE

Water level piezometric tube is utilized for estimation of bed slope. Water level about the bed of the channel at the upstream and downstream of the flume is taken which are around 15m apart. The water level calculated is from the bed of the flume without considering the thickness of the Perspex sheet. Difference in the two corresponding points was calculated. After that the required Slope is measured by dividing this level difference with the difference

between the observed points. Five such readings are taken and average value was found out for exactness. The slope calculated is 0.00165 which is the slope of the flume i.e. the valley slope. For calculating the slope of the main channel, the sinuosity of the main channel is divided by the slope of the flume which gives the channel slope. The sinuosity of the meandering channel being 4.11, the channel slope of the main channel is found to be 0.00040146.

3.4.4 NOTCH CALIBRATION

Rectangular notch is provided at the upstream section of the flume for computation of the theoretical discharge into the channel. Before computing the discharge, the rectangular notch needs to be calibrated concerning actual discharge from the volumetric tank at the downstream section. The volumetric tank has a cross-sectional area of 208666 cm^2 and a piezometer attached to it for estimation of the rate of increase in water level. Actual discharge is ascertained by recording the time taken for increase in unit increase in height of water level in the piezometer.

The volume of water collected at the volumetric tank is given by,

$V_w = Ah_w$ Eq. 3.1

Actual discharge of water collected at the volumetric tank is given by,

$Q_a = V_w/t$ Eq. 3.2

For theoretical discharge, the height of water over the rectangular notch is measured by a point gauge arrangement. Theoretical discharge is given by,

$$Q_{th} = \frac{2}{3} L_n \sqrt{2g} H_n^{3/2}$$ Eq. 3.3

The coefficient of discharge for each run is calculated as per equation given below,

$$C_d = \frac{Q_a}{Q_{th}}$$ Eq. 3.4

Where, $Q_a$is the actual discharge, $Q_{th}$is theoretical discharge, A is the area of volumetric tank, $V_w$volume of water, t time in sec, C_d is the coefficient of discharge calculated from notch calibration, $h_w$is the height of water in the volumetric tank, $L_n$is the length of the notch (3.4 m in this case), H_n is the height of water above the notch and g is the acceleration due to gravity. From the notch calibration, coefficient of discharge 'C_d' of rectangular notch was found to be 0.66. The discharge is maintained at 6.3 x 10^{-3} m^3/s throughout the experiment.

3.4.5 MEASUREMENT OF LONGITUDINAL VELOCITY

Pitot tubes are utilized for measuring velocity. Here five Pitot tubes are arranged for measurement of the pressure difference at every predefined grid on the channel cross-section throughout the meander path. The pitot tubes are having an external diameter of 4.7mm. The pitot tubes are attached to individual manometers placed on a vertical board. The vertical board is having a spirit level used for adjustment of the verticality of the manometers. The pitot tubes and the manometers are connected by long transparent PVC tubes of small diameters. Extra care is taken to ensure the absence of air bubbles in those pipes.

Pitot tubes are positioned against the direction of flow perpendicular to it. Then the pressure difference at every pre-defined grid of the channel section along the meander path is calculated. The velocity is measured by the formula $v=\sqrt{2gh}$, at that point where g signifies the acceleration due to gravity and h signifies the pressure difference. Here the tube coefficient is taken as unit and the error due to turbulence is considered negligible while measuring velocity.

3.4.6 MEASUREMENT OF BOUNDARY SHEAR STRESS

Measurement of boundary shear stress in open channel flow is crucial as it helps in determining the Shear bed load transport, momentum transfer and channel migration etc. The shear forces at the bed are important for the calculation of bed load transfer whereas shear

forces at the walls provide a general overview of channel relocation pattern. Although there are several methods f or evaluating bed and wall shear, Preston-tube method even if being an indirect estimate, is largely used for experimental observations.

Preston (1954) gave a simple technique to measure the local shear stress on smooth boundaries using a Pitot tube which is in contact with the bed surface. His method was based on the assumption on an inner law relating the boundary shear stress to the velocity distribution near the wall. Preston provided a non-dimensional correlation between the Preston tube differential pressure ΔP, and the boundary shear stress τ, of the form:

$$\left(\frac{\tau d^2}{4\rho\upsilon^2}\right) = F\left(\frac{\Delta P d^2}{4\rho\upsilon^2}\right) \qquad \text{Eq. 3.5}$$

Where d signifies the outer diameter of the Preston tube, ρ is the density of the flow, υ is the kinematic viscosity of the fluid, and F is an empirical function. **Patel (1965)** further extended this research and his calibration is given in terms of two non-dimensional parameters x^* and y^*which are used to convert pressure readings to boundary shear stress, where

$$x^* = \log_{10}\left(\frac{\Delta P d^2}{4\rho\upsilon^2}\right) \text{ and } y^* = \log_{10}\left(\frac{\tau d^2}{4\rho\upsilon^2}\right) \qquad \text{Eq. 3.6}$$

In the form

For $y^* < 1.5$ $\qquad y^* = 0.5x^* + 0.037$ $\qquad$ Eq. 3.7

For $1.5 < y^* < 3.5$ $\qquad y^* = 0.8287 - 0.1381x^* + 0.1437x^{*2} - 0.006\,x^{*3}$ $\qquad$ Eq. 3.8

and

For $3.5 < y^* < 5.3$ $\qquad x^* = y^* + 2\log_{10}(1.95y^* + 4.10)$ $\qquad$ Eq. 3.9

In the present case, all shear stress measurements are taken at thirteen sections throughout the meander path between the two bend apexes. The pressure readings were taken using pitot tubes along the predefined grids across all the sections of the channel at the bed and side slopes. The manometers attached to the Pitot tubes gave the head difference between the

dynamic and static pressures. The differential pressure is then calculated from the readings on the vertical manometer by,

$$\Delta P = \rho g \Delta h \qquad \text{Eq. 3.10}$$

Where Δh is the difference between the two readings from the dynamic and static, g is the acceleration due to gravity and ρ is the density of water. Here the tube coefficient is taken as unit and the error due to turbulence is considered negligible while measuring velocity.

Accordingly out of the Eq. 3.6-3.9, the appropriate one was chosen for computing the wall shear stress based on the range of x^* values. After that the shear stress value was integrated over the entire perimeter to calculate the total shear force per unit length normal to flow cross-section carried by the meandering section. The total shear thus computed was then compared with the resolved component of weight force of the liquid along the stream-wise direction to check the accuracy of the measurements.

3.5 NUMERICAL MODELLING

3.5.1 DESCRIPTION OF NUMERICAL MODEL PARAMETERS

In this study, Fluent, a Computational Fluid Dynamics simulation tool is utilized for model verification which is a three-dimensional form of Navier-Stokes equations. Computational Fluid Dynamics (CFD) is a branch of fluid mechanics that uses various numerical models and algorithm to analyses and solves issues that include fluid flows. Computer systems are utilized to perform the calculations needed to simulate the interaction of fluids and gases with surfaces characterized by boundary conditions. With fast supercomputers, better arrangements can be accomplished. On-going examination yields programming that enhances the precision and rate of complex simulation situations, for example, transonic or turbulent flows. It has begun around 1960 and with the procedure of change in computer processor speed, CFD simulation is currently demonstrating astonishing exactness. The CFD based

simulation depends combined numerical exactness, demonstrating accuracy and computational expense. For the most part CFD utilizes a Finite volume method (FVM). Fluent can utilize both organized and unstructured grids. In free-surface displaying e.g. VOF (Ferziger and Peric 2002) and height of Liquid (HOL) or LES, the governing equations are discretized in both space and time which generally obliges transient simulation. Here Large Eddy Simulation model is utilized for turbulence modeling. The LES equations are discretized in both space and time. In this study the calculations used to solve the coupling between the pressure and velocity field is PISO, the Pressure implicit splitting of operators used in Fluent (Issa 1986). A no iterative solution strategy PISO is utilized to ascertain the transient issue as it serves to solve the issues faster. When the residuals of the discretized transport equation reach a value of 0.001 or when the solution do not change with further iterations, the numerical solution is converged. To advance the merging of the arrangement the changing variables are controlled during the calculation. For the simulation with a unsteady solver, the distinction in the mass flow rates at the velocity inlet and pressure outlet is observed to be under 0.01% during final solution. Furthermost, various additional time steps are added to check the steadiness of the flow in the last arrangement.

3.5.2 TURBULENCE MODELLING

"Turbulence is an irregular movement which is shown in liquids and gases when they flow past solid surfaces or even when neighboring streams of the same fluid flow past over one another." **GI Taylor and von Karman, 1937** "Turbulent smooth movement is an unpredictable state of flow in which the various quantities Show an arbitrary variation with time and space coordinates, so that statically distinct average values can be perceived." **Hinze, 1959** .The stream in a meandering channel is turbulent in nature. Channel Shape or geometry and gravity force is mostly in charge of the turbulent stream. Turbulent flow is a flow regime described by turbulent and stochastic property changes. This incorporates low

momentum dissemination, high energy convection, and rapid variation of force and velocity in space and time. Turbulence occurs when the inertia forces in the fluid become significant compared to viscous forces, and is characterized by a high Reynolds Number.

Generally turbulence is a random three dimensional time-dependent eddying motion with many large scales eddies. The three dimensional nature of turbulent flows are decomposed into two different parts i.e. mean part and fluctuation part, which is well known as Reynolds decomposition. The spatial character of turbulence reveal the eddies with wide range scales. In turbulence, separated fluid particles are brought close together by eddying motion which causes the effective exchange of heat, mass and momentum. The turbulence in compound channel is quite complex and the flow structure involved in it creates uncertainty in prediction of flow variables Particularly in meandering channels, turbulent structures are generalized by large shear layers generated by difference of velocity between inner bend and outer bend . This large shear layer region creates vortices both longitudinal as well as vertical direction. The anisotropy and inhomogeneity of turbulent structure causes secondary current, which creates the velocity dip and affects the flow variables. Hence in this study an effort is made to recognize the effect of the turbulence in a meandering channel. Incorporating turbulence, CFD considers the instantaneous velocity that consisting of an average velocity component and a fluctuating velocity component given as

Instantaneous velocity = mean velocity + fluctuating is given by

$$u = \bar{u} + u' \qquad \text{Eq. 3.11}$$

The Navier-Stokes momentum equation is taken as:

$$\frac{\partial \rho u_i u_j}{\partial x_j} = -\frac{\partial p}{\partial x_i} + \frac{\partial}{\partial x_j}\left(\mu \frac{\partial u_i}{\partial x_j}\right) \qquad \text{Eq. 3.12}$$

By substituting $\bar{u} + u'$ for u in equation (3.12) and averaging the term we get:

$$\frac{\overline{\partial u}}{\partial x} = \frac{\overline{\partial(\bar{u}+u')}}{\partial x} = \frac{\partial \bar{u}}{\partial x} \qquad \text{Eq. 3.13}$$

For non-linear function the equation (3.11) becomes

$$\frac{\partial(uu)}{\partial x} = \frac{\partial(\overline{u}\overline{u})}{\partial x} + \frac{\partial \overline{u'u'}}{\partial x} \qquad \text{Eq. 3.14}$$

Now the Navier-Stokes equations become:

$$\frac{\partial \overline{u_j}}{\partial x_j} = 0 \qquad \text{Eq. 3.15}$$

$$\frac{\partial \rho \overline{u_i u_j}}{\partial x_j} = -\frac{\partial \overline{p}}{\partial x_i} + \frac{\partial}{\partial x_j}\left(\mu \frac{\partial \overline{u_i}}{\partial x_j}\right) - \frac{\partial \rho(u_i' u_j')}{\partial x_j} \qquad \text{Eq. 3.16}$$

The term $\frac{\partial \rho\left(u_i' u_j'\right)}{\partial x_j}$ is known as the "Reynolds stress". Due to closure problem of both the equations 3.15 and 3.16 we have to come up with ways of replacing the extra terms with other terms that were known or devising ways of calculating these terms. A first attempt at closing the equations is:

$$\frac{\partial}{\partial x_j}\left(\mu \frac{\partial \overline{u_i}}{\partial x_j}\right) = \frac{\partial \rho\left(u_i' u_j'\right)}{\partial x_j} \qquad \text{Eq. 3.17}$$

In equation (3.17) both terms represent a diffusion of energy. The term $\frac{\partial}{\partial x_j}\left(\mu \frac{\partial \overline{u_i}}{\partial x_j}\right)$ represents diffusion of energy through viscosity and the other term $\frac{\partial \rho\left(u_i' u_j'\right)}{\partial x_j}$ represents the diffusion through turbulence. By defining μ_t as turbulent viscosity, equation (3.16) becomes:

$$\frac{\partial \rho \overline{u_i u_j}}{\partial x_j} = -\frac{\partial \overline{p}}{\partial x_i} + \frac{\partial}{\partial x_j}\left((\mu + \mu_t)\frac{\partial \overline{u_i}}{\partial x_j}\right) \qquad \text{Eq. 3.18}$$

To enable the effects of turbulence to be predicted, a large amount of CFD research has concentrated on methods which make use of turbulence models. Turbulence models have been specifically developed to account for the effects of turbulence without recourse to a prohibitively fine mesh and direct numerical simulation. Most turbulence models are statistical turbulence model, as mentioned below.

3.5.3 TURBULENCE MODELS

- Algebraic (zero-equation) model.
- K-ε, RNG k-ε model.
- Shear stress transport model.

- K-ω model
- Reynolds stress transport model (second moment closure).
- K-ω Reynolds stress.
- Detached eddy simulation (DES) turbulence model.
- SST scale adaptive simulation (SAS) turbulence model.
- Smagorinsky large eddy simulation model (LES).
- Scalable wall functions
- Automatic near-wall treatment including integration to the wall.
- User-defined turbulent wall functions and heat transfer

3.5.4 GOVERNING EQUATIONS

The governing equation used here is based on conservation of mass, momentum and energy. The C.F.D package namely Fluent was employed to solve the governing equations, which uses Finite Volume Method (FVM) to solve the equations.FVM involves discretization and integration of the governing equations over the control volume. The numerical method FVM was based on the integral conservation which is applied for solving. The partial difference i.e. Navier-Stokes equation then calculate the values of the variables, averaged across the volume. The integration of the equations over each control volume results in a balance equation. The conservation law is enforced on small control volumes which are defined by computational mesh. The set of balance equations then discretized with respect to a set of discretization schemes and is solved by using the initial and boundary conditions. The governing Reynolds Averaged Navier-Stokes and continuity equations are stated as:

$$\frac{\partial(\rho)}{\partial t} + \frac{\partial(\rho u_i)}{\partial x_i} = S_m \qquad \text{Eq. 3.19}$$

$$\frac{\partial(\rho u_i)}{\partial t} + \frac{\partial(\rho u_i u_j)}{\partial x_j} = -\frac{\partial p}{\partial x_i} + \frac{\partial}{\partial x_j}\mu\left[\frac{\partial u_i}{\partial x_j} + \frac{\partial u_j}{\partial x_i}\right] + \frac{\partial(-\rho\overline{u_i' u_j'})}{\partial x_j} \qquad \text{Eq.3.20}$$

Where t=time, u_i=i-th component of the Reynolds-averaged velocity, x_i=i-th axis, ρ=water density, p= Reynolds averaged pressure, g=acceleration due to gravity, μ=viscosity (here it is equal to zero), S_m=mass exchange between two phase (water and air).Here for unsteady solver the time-averaged values of velocities and other solution variables are taken instead of instantaneous values. The term $\left(-\rho\overline{u_i' u_j'}\right)$ is called as Reynolds Stress. To link the mean rate of deformation with Reynolds stresses, Boussinesq hypothesis is used:

$$-\rho u_i' u_j' = \mu_t \left(\frac{\partial u_i}{\partial x_j} + \frac{\partial u_j}{\partial x_i}\right) \qquad \text{Eq. 3.21}$$

Where μ_t=the turbulent viscosity

3.5.5 NUMERICAL METHODOLOGY

The process of the numerical simulation of fluid flow using the above equation generally involves four different steps

- Problem Identification
  (1)Defining Modeling goals
  (2)Identifying the domain to model
- Pre-Processing
  (1) Creating a solid model to represent the domain (Geometry Setup)
  (2) Design and create the mesh (grid)
- Solver
  (1) Set up the physics
    a. Defining the condition of flow (e.g. turbulent, laminar etc.)
    b. Specification of appropriate boundary condition and temporal condition.
  (2) Using different numerical schemes to discretize the governing equations.
  (3) Controlling the convergence by iterating the equation till accuracy is achieved
  (4) Compute Solution by Solver Setting.
    a. Initialization
    b. Solution Control
    c. Monitoring Solution
- Post processing
  (1) Visualizing and examining the results
  (2) X-Y Plots
  (3) Contour Draw

3.5.6 PREPROCESSING

In this initial step all the necessary information which defines the problem is assigned by the user. This consists of geometry, the properties of the computational grid, various models to be used, and the number of Eulerian phases, the time step and the numerical schemes.

3.5.7 CREATION OF GEOMETRY

The first step in CFD analysis is the explanation and creation of computational geometry of the fluid flow region. A consistent frame of reference for coordinate axis was adopted for creation of geometry. Here in coordinate system, Z axis corresponded the stream wise direction of fluid flow. X axis aligned with the lateral direction which indicates the width of channel bed and Y axis represented the vertical component or aligned with depth of water in the channel. The origin was placed at the upstream boundary and coincided with the base of the center line of the channel. The water flowed along the positive direction of the Z-axis.The simulation was done on a simple meandering channel from one bend apex to the other. The geometry of the channel is shown in Figure 3.4 and the cross-section of channel geometry is shown in Figure 3.5

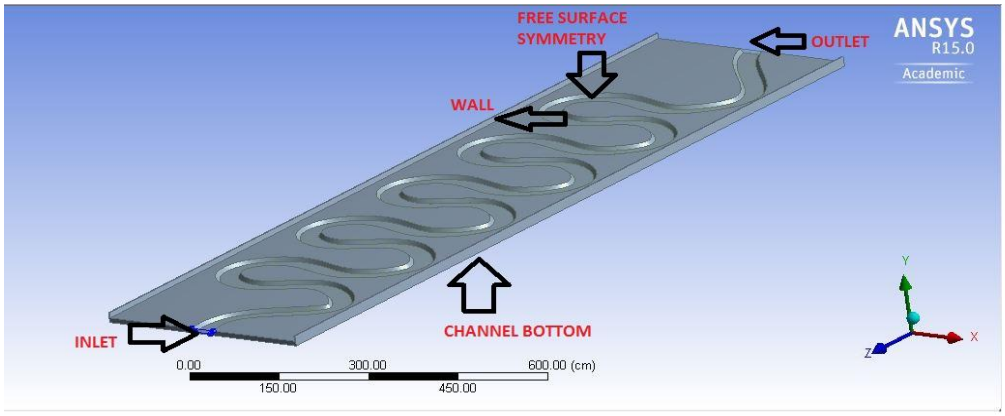

Figure 3.4: Channel Geometry in Ansys Design moduler

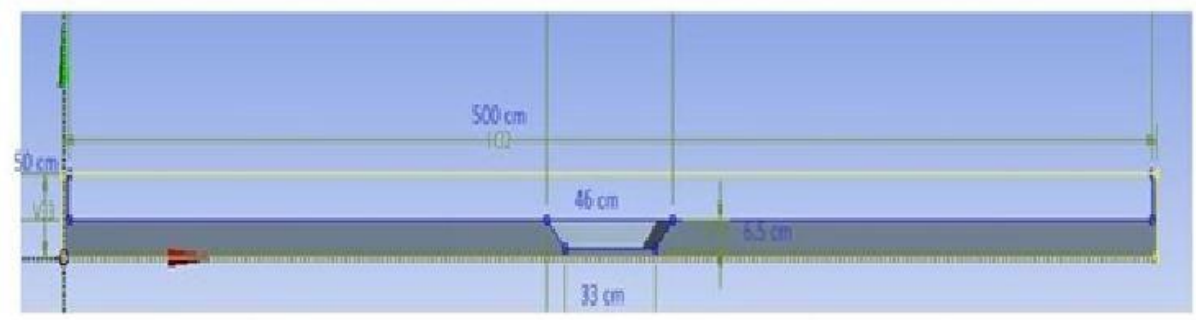

Figure 3.5 Channel cross section in Ansys Design moduler

As can be seen from the Figure 3.4 that the channel geometries were 0. 5 m height, 4 m width and 15m length. In the geometry of the channel the main channel was trapezoidal in cross section having bottom width 0.33m, top width 0.46m and bank full depth of 0.065m.

During the model construction, an additional consideration is to identify any entity of the geometry which needs to be identified for future reference as to identify a particular domain for conduct some analysis and for applying boundary condition upon a particular domain. Figure 3.4 shows the geometry of the meandering channel and Figure 3.5 shows the cross section of the channel. For identify the domain five different surfaces are generated.

- Inlet
- Outlet
- Wall
- Free surface symmetry
- Channel bottom

3.5.8 MESH GENERATION

Second and very most important step in numerical analysis is setting up the grid associated with the construction of geometry. The Navier-Stokes Equations are non-linear partial differential equations, which consider the whole fluid domain as a continuum. In order to

simplify the problem the equations are simplified as simple flows have been directly solved at very low Reynolds numbers. The simplification can be made using what is called discretization. Construction of mesh involves discretizing or subdividing the geometry into the cells or elements at which the variables will be computed numerically. By using the Cartesian co-ordinate system, the fluid flow governing equations i.e. momentum equation, continuity equation are solved based on the discretization of domain. The CFD analysis needs a spatial discretization scheme and time marching scheme. Meshing divides the continuum into finite number of nodes. Generally the domains are discretized by three different ways i.e. Finite element, Finite Volume and Finite Difference Method. Finite element method is based on dividing the domain into elements. In finite element method the numerical solutions are obtained by integrating the shape function and weighted factor in an appropriate domain. This method is suitable for both structured and unstructured mesh. But the Finite Volume method divides the domain into finite number of volumes. Finite volume method solves the discretization equation in the centre of the cell and calculates some specified variables. The values of quantities, such as pressure, density and velocity that are present in the equations to be solved are stored at the centre of each volume. The flux into a region is calculated as the sum of the fluxes at the boundaries of that region. As the values of quantities are stored at nodes but not at boundaries this method requires some interpolation at nodes. Generally finite Volume method is suitable for unstructured domain. Whereas finite Difference method is based on approximation of Taylor's series. This method is more suitable for regular domain.

For transient problems an appropriate time step needs to be specified. To capture the required features of fluid flow with in a domain, the time step should be sufficiently small but not too much small which may cause waste of computational power and time. Spatial and time discretization is linked, as evident in the Courant number.

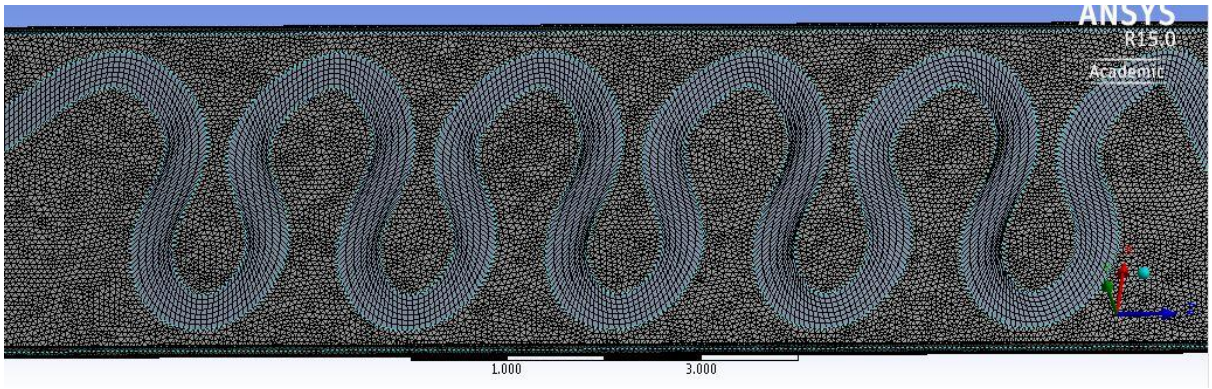

Figure 3.6: Meshing Of The Channel top view

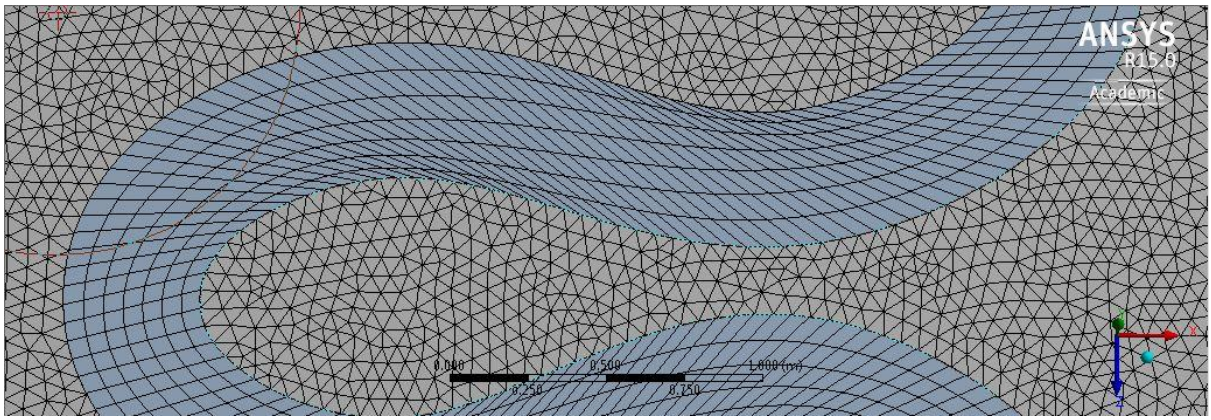

Figure 3.7: Meshing View By Zooming

3.5.9 COURANT NUMBER

A criterion often used to determine time step size is known as Courant number. The Courant number stops the time step from being large enough for information to travel entirely through one cell during one iteration. For explicit time stepping schemes Courant number should not be greater than 1. For implicit time stepping schemes this number may be higher than 1. The Courant number is defined as:

$$C_r = \frac{\bar{U}\Delta t}{\Delta l} \qquad \text{Eq.3.22}$$

Where C_r is the Courant number, $\bar{U}$ is the average velocity, Δt is the maximum time step size and Δl is the largest grid cell size along the direction of flow.

A mesh consists of too few nodes cause quick solution of simulation but not a very accurate one. However a very dense mesh of nodes causes excess computational time and memory. For CFD analysis more nodes are required in some areas of interest, such as near wall and wake regions, in order to capture the large variation of fluid properties. Thus, structure of grid lines causes further wastage of computer storage due to further refinement of mesh. In this study, the flow domain is discretized using structured grid and body-fitted coordinates. It must be noted that the running time is low and it is obtained by grid-independent results. The grid structure must be fine enough, especially near the wall boundaries (in order to consider the viscous flow), and at free surface. In this numerical simulation, various computational trials are conducted with different number of grid cells. It is concluded that the results are almost independent from the grid size and running time is optimal.

3.5.10 SOLVER SETTING

The numerical scheme that CFD codes adopt is the finite volume method. The differential transport equations are integrated over each computational cell, and the Gauss and Leibnitz theorems are applied in this method. This consists of various models used for analysis, the initial and boundary conditions, the number of Eulerian phases, the properties of the materials, the physical and chemical phenomena involved. At last, the set of algebraic equations is solved by iteration process and the cell-center values of the flow variables are calculated.

3.5.11 TWO PHASE MODELING EQUATIONS

A large number of flows encountered in nature and technology are known as a mixture of phases. Physical phases of matter are solid, liquid and gas. But the concept of phase in a multiphase flow system is applied in a wider way. In multiphase flow, a phase can be defined as a particular class of material that has a certain inertial response and interaction with the

flow and the potential field in which it is immersed. Currently there are two approaches for the numerical calculation of multiphase flows: the Euler-Lagrange approach and the Euler-Euler approach.

3.5.12 VOLUME OF FLUID (VOF) MODEL

The VOF formulation in ANSYS FLUENT is generally used to compute a time dependent Solution. An Eulerian variation in which the secondary phase is not dispersed within the primary phase but rather there is an interface between the phases and so the interface must be tracked while also solving a momentum equation for each phase. The volume of fluid (VOF) method is a computational tool for the analysis of free surface flows (Hirt and Nichols 1981). The interface(s) between the phases is accomplished by the solution of a continuity equation for the volume fraction of one (or more) of the phases. For the q^{th} phase, this equation has the following form (Rahimzadeh et al. 2012):

$$\frac{\partial \alpha_q}{\partial t} + \nabla \cdot (\vartheta \cdot \alpha_q) = 0 \qquad \text{Eq.3.23}$$

Where $\propto_q$ is the volume fraction of the q^{th} phase. In each control volume, the volume fractions of all phases sum up to unity. The following three conditions are possible for each cell:

If $\propto_q = 0$, the cell is empty.

If $\propto_q = 1$, the cell is full.

If $0 < \propto_q < 1$, the cell contains the interface between the q^{th} phase and one or more other phases. In each cell the average properties are computed according to the volume fraction of each phase. VOF method was developed to trace the moving free surface of the incompressible viscous flow.

3.5.13 SOLVING FOR TURBULENCE

- For past three decades various numerical turbulence models such as K-ε model, K-ω model, Reynolds stress transport model, Algebric Reynolds stress model Large eddy simulation model etc. have been developed to simulate the complex secondary structure in meandering channel.
- **K-ε** model is the most common model used in CFD to simulate mean flow characteristics for turbulent flow conditions. It is a two equation model which gives a general description of turbulence by means of two transport equation. The first transported variable **(K)** determines the energy in the turbulence and is called turbulence kinetic energy. The second one (ε) is the turbulence dissipation which determines the rate of dissipation of turbulence kinetic energy. This model is given to find an alternative to algebraically prescribing turbulent length scales in moderate to high complexity flows. It focuses on the mechanism that affects the turbulent kinetic energy.It is more expensive in terms of memory.Its accuracy has been reduced for flows containing large adverse pressure gradients.It also performs poorly in variety of important cases such as unconfined flow, curved boundary layer, rotating flows, and flows in non-circular ducts.
- **K-ω** model is a common two equation turbulence model in computational fluid dynamics which is used a closer equation of the Reynolds-averaged Navier-Stokes equation.Where **K** signifies turbulence kinetic energy and **ω** signifies specific rate of dissipation.
- **Large eddy simulation model (LES)** model solves spatially averaged Navier stokes equation. Large eddies are directly resolved but the eddies smaller than mesh are modeled. It solves large spatial as well as smaller scale equations.It operates on the Navier-Stokes equations to reduce the range of the solution reduce the computational

cost. In the present study LES model is used to simulate fluid flow in the meandering channel.

3.5.13.1 USED LARGE EDDY SIMULATION TURBULENCE MODEL

Large eddy simulation model is an intermediate approach to DNS and RANS turbulence model. LES relies on a spatial filter, rather than a time averaging process. Turbulent flows have generally wide range of length and time scales. To distinguish eddies that are going to be calculated from those that are going to be modelled, a filtering function (eg. Gaussian, Box cutoff, Fourier) is used. The large scale motions are generally more energetic than the small ones. Large eddies depend highly on boundary conditions which determine the basic feature of flow. Large scale eddy causes the transfer of momentum and heat. The concept of Large Eddy Simulation (LES) is adopted for accuracy in turbulence nature. The LES model directly resolves the large eddies present in turbulent flows and models the smaller scale eddies. This model captures larger scale motion, as well as it covers the effects of small scales of eddies by using sub-grid scale (SGS) model. In this technique direct calculation is used to resolve the eddies that are larger than the size of the finite volume cell, while a simple model is used to model the more universal nature of the small scale eddies that are smaller than the mesh size. By seeing advantages of the LES method, it is adopted for the simulation.

Generally LES uses a spatial average instead of time-averaging sceam. Here the velocity component is split into a resolved component $\bar{U}$ and an unresolved component u′. The governing equations employed for LES are obtained by filtering the time-dependent Navier-Stokes equations in either Fourier (wave-number) space or configuration (physical) space. The instantaneous velocity variable u can be written as:

$$u = \bar{U} + u' \qquad \text{Eq.3.24}$$

Where u' is the unresolved part and $\bar{U}$ is the large scale part defined through volume averaging as:

$$\bar{U}(x_j,t) = \int_{vol} G(x_i - x_i')u(x_j',t)dx_i' \qquad \text{Eq.3.25}$$

Where $G(x_i - x_i')$ is the Gaussian filter.

The non-filtered Navier-Stokes equation is:

$$\frac{\partial(\rho u_i)}{\partial t} + \frac{\partial(\rho u_i u_j)}{\partial x_j} = -\frac{\partial p}{\partial x_j} + \mu\frac{\partial^2 u_i}{\partial x_i x_j} \qquad \text{Eq.3.26}$$

After performing the volume averaging and neglecting density functions, the filtered Navier-Stokes Equations become

$$\frac{\partial(\rho\overline{U_i})}{\partial t} + \frac{\partial(\rho\overline{u_i u_j})}{\partial x_j} = -\frac{\partial \bar{p}}{\partial x_j} + \mu\frac{\partial^2 \overline{u_i}}{\partial x_i x_j} \qquad \text{Eq.3.27}$$

The Non-linear transport term in equation (15) can be explained as:

$$\overline{U_i U_j} = \overline{(\bar{U}_i + u_i')(\bar{U}_j + u_j')}$$

$$= \overline{\bar{U}_i \bar{U}_j} + \overline{\bar{U}_i u_j'} + \overline{\bar{U}_j u_i'} + \overline{u_i' u_j'} \qquad \text{Eq.3.28}$$

In time averaging the term II &III vanish but not in volume averaging.

Introducing the residual stress or sub grid scale (SGS) stresses defined as τ_{ij} and expressed as

$$\tau_{ij} = \overline{u_i u_j} - \overline{U_i U_j} \qquad \text{Eq.3.29}$$

Now equation (15) can be written as:

$$\frac{\partial(\rho\overline{U_i})}{\partial t} + \frac{\partial(\rho\overline{U_i U_j})}{\partial x_j} = -\frac{\partial \bar{p}}{\partial x_j} + \mu\frac{\partial^2 \overline{U_i}}{\partial x_i x_j} - \frac{\partial(\rho\tau_{ij})}{\partial x_j} \qquad \text{Eq.3.30}$$

Equation (3.27) is the basis of the LES turbulence model.

3.5.14 SETUP PHYSICS

For a given computational domain, boundary conditions are imposed which can sometimes over specify or under-specify the problem. Usually, after imposing boundary conditions in

non-physical domain may lead to failure of the solution to converge. It is therefore important, to understand the meaning of well-posed boundary conditions. The boundary conditions implemented for this study are shown in Fig 3.8 Subsequently these conditions are discussed in the following

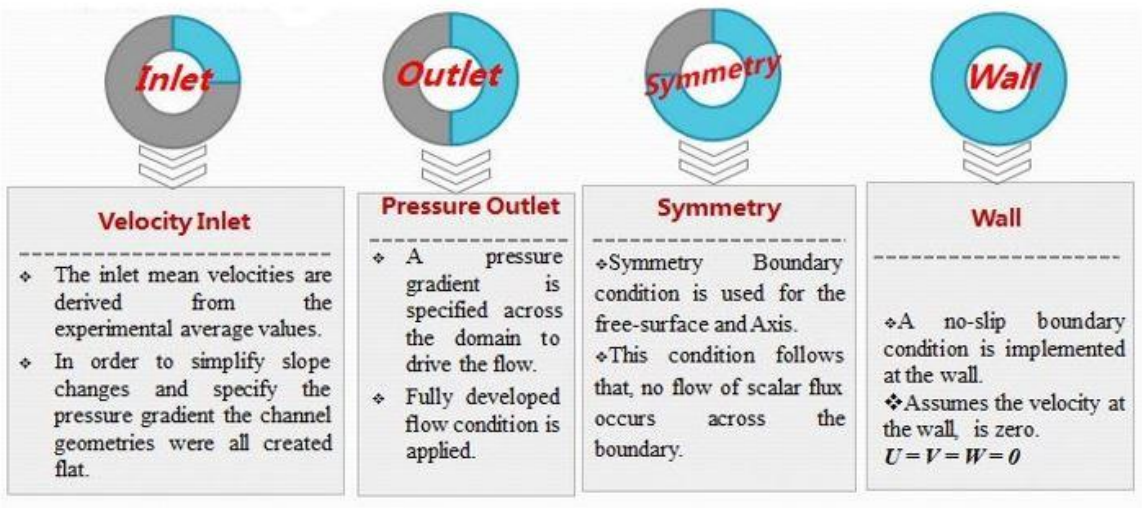

Figure 3.8: Boundary Conditions

3.5.14.1 INLET AND OUTLET BOUNDARY CONDITIONS

All of the channels reported were performed with translational periodic boundaries in the stream wise direction of the flow which allow the values on the inlet and outlet boundaries to coincide. Further the pressure gradient was specified across the domain to drive the flow. To initialize the flow, a mean velocity is specified over the whole inlet plane upon which velocity fluctuations are imposed. The inlet mean velocities are derived from the experimental average values. The mean velocity was specified over the whole inlet plane and is computed by $U_{in} = {}^{Q}/_{A}$, where Q is the flow discharge of the channel and A is the cross sectional area of the inlet. In order to simplify slope changes and specify the pressure gradient the channel geometries were all created flat. The effects of gravity and channel slope implemented via a resolved gravity vector. Here the angle θ represents the angle between the

bed of the channel and the horizontal, the gravity vector is resolved in x, y and z components as : $(0, -\rho g\cos\theta, \rho g\sin\theta)$ Eq.3.31

Where θ = angle between bed surface to horizontal axis and tan θ=slope of the channel. Here, the z component causes the direction responsible for flow of water along the channel and the x component is responsible for creating the hydrostatic pressure upon the channel bed. From the simulation, "y" component of the gravity vector ($-\rho g\cos\theta$) is found to be responsible for the convergence problem of the solver.

CHAPTER 4
RESULT AND DISCUSSION

4.1 OVERVIEW

This Chapter 3 contains the different experimental procedures that have been carried out for conducting series of experiments throughout the meandering path of the meandering channel. In this chapter the results of the tests conducted in form of velocity distributions along the width and depth , boundary shear stress along the wetted perimeter of the channel section ,Numerical results in the form of velocity contour, and boundary shear contour and at last comparison with other researcher's work having same geometrical parameters are presented.

4.2 LONGITUDINAL VELOCITY DISTRIBUTION

The discharge of 6.3 x 10^{-3} m^3/s is to be maintained throughout the experiment and the velocity datas are obtained along the meandering path of the channel at every cross-section. A set of 5 pitot tubes are arranged unequally and are allowed to move across the channel section from the left bank towards the right bank. The velocity datas are recorded at 4cm intervals on either side of the centre of the meandering channel cross section for the bed and depths of 0.2H 0.4H, 0.6H and 0.8H. Where H being the averaged depth of flow of water at the corresponding section. The velocity datas obtained are then analyzed along the width and depth of the channel cross section for better understanding of the characteristics of flow through the meander path of the sinuous channel. The following figures from 4.1.1 to 4.1.13 represent the longitudinal velocity profiles along the meander path.

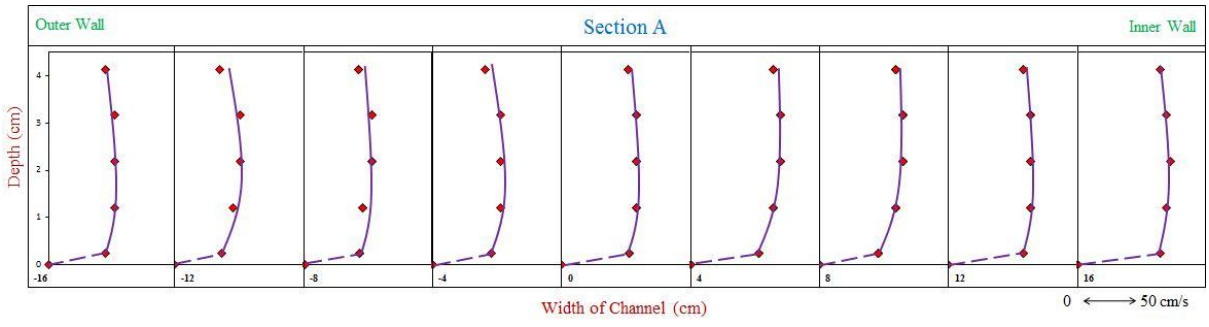

Figure: 4.1.1

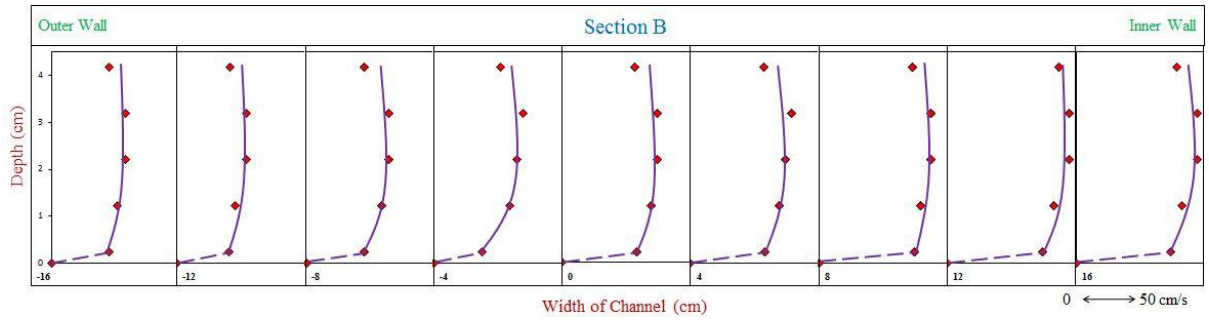

Figure: 4.1 2

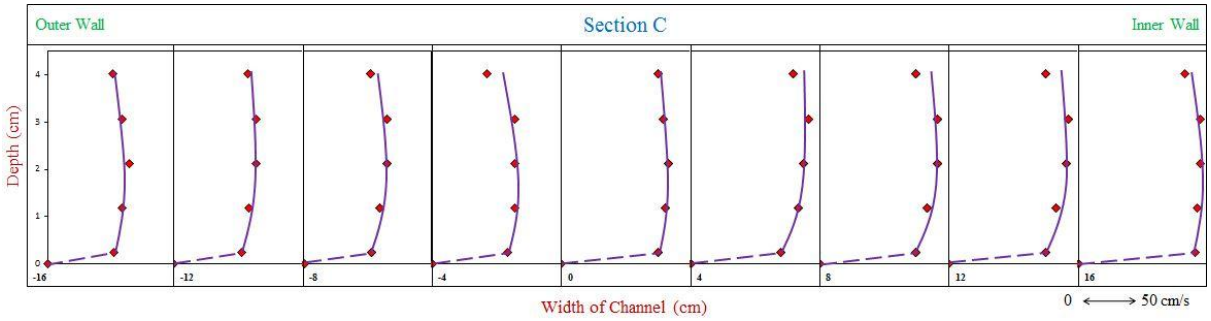

Figure: 4.1.3

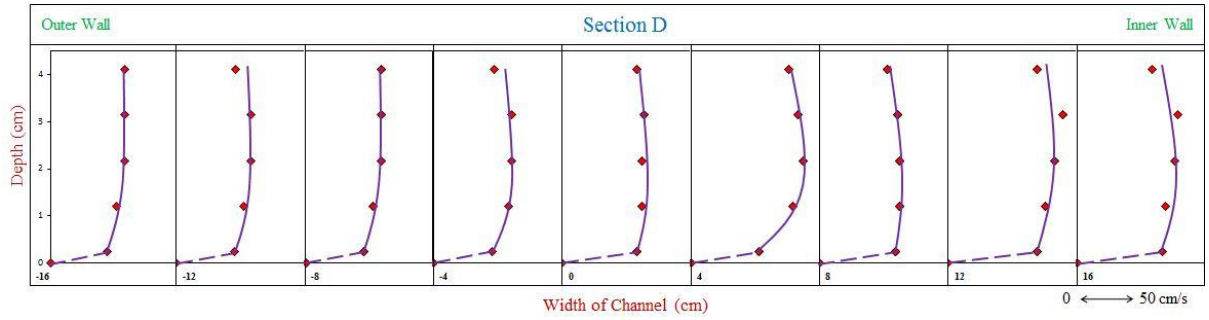

Figure: 4.1.4

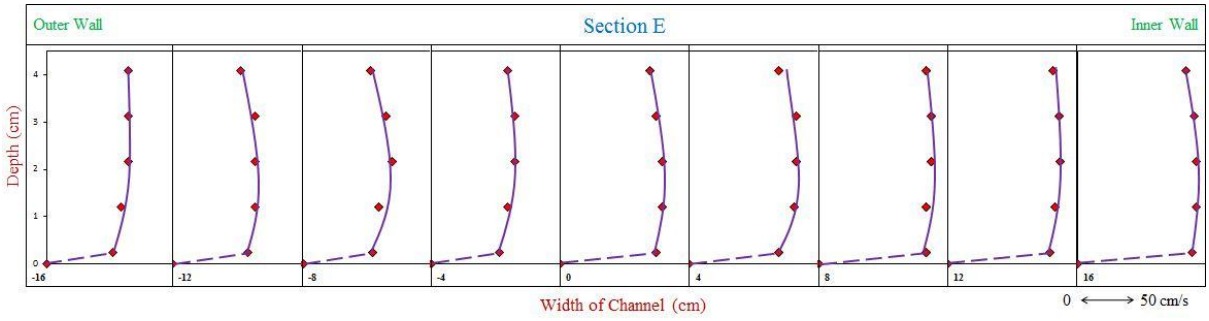

Figure: 4.1.5

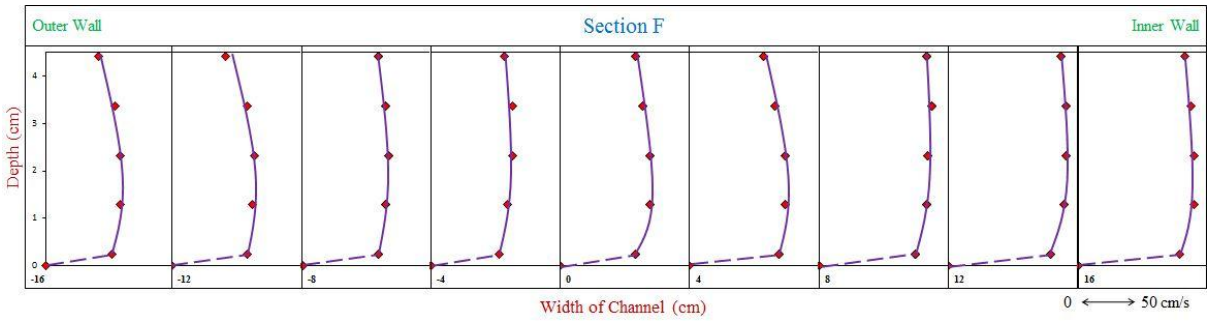

Figure: 4.1.6

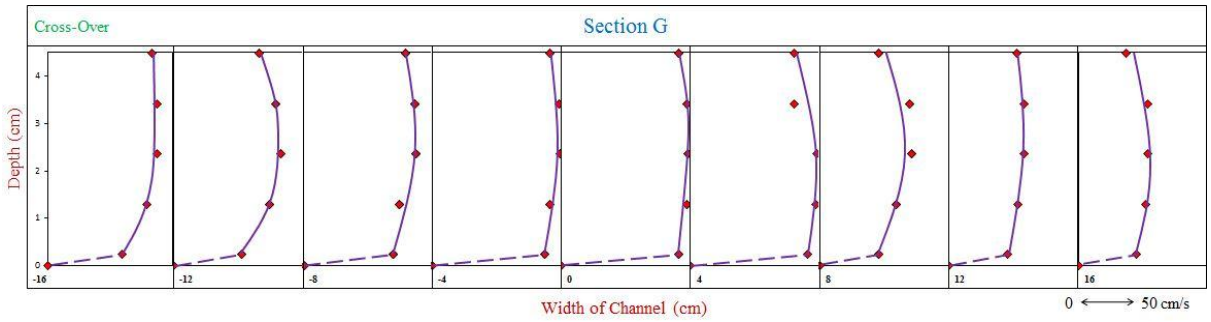

Figure: 4.1.7

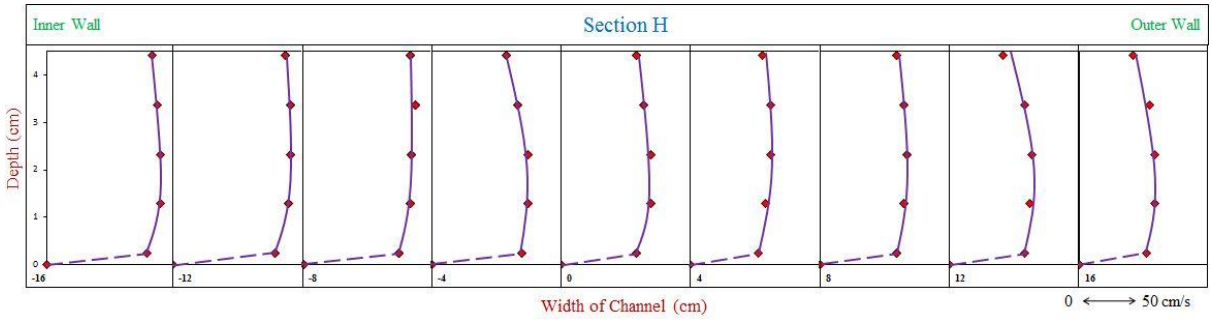

Figure: 4.1.8

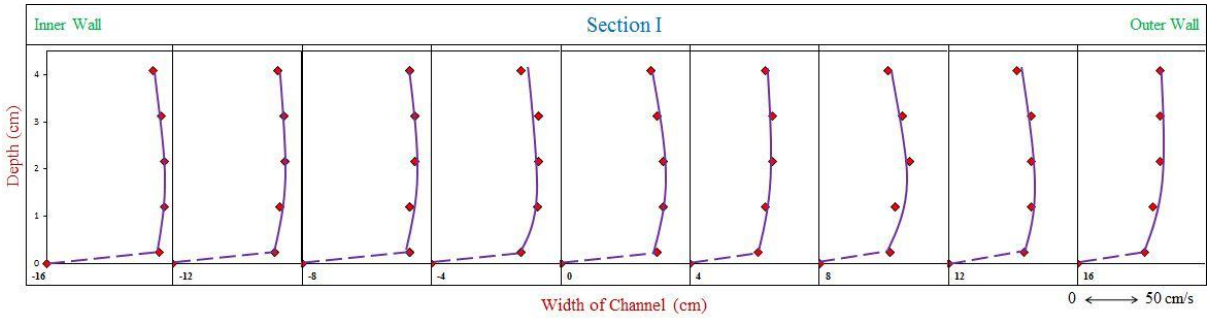

Figure: 4.1.9

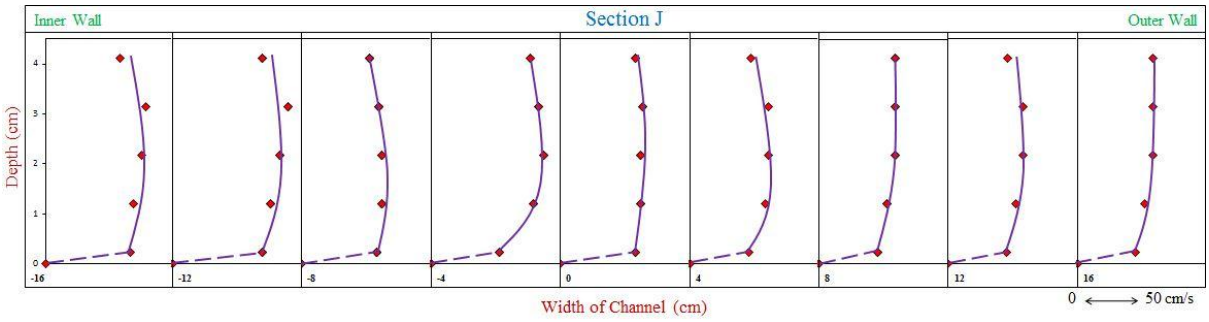

Figure: 4.1.10

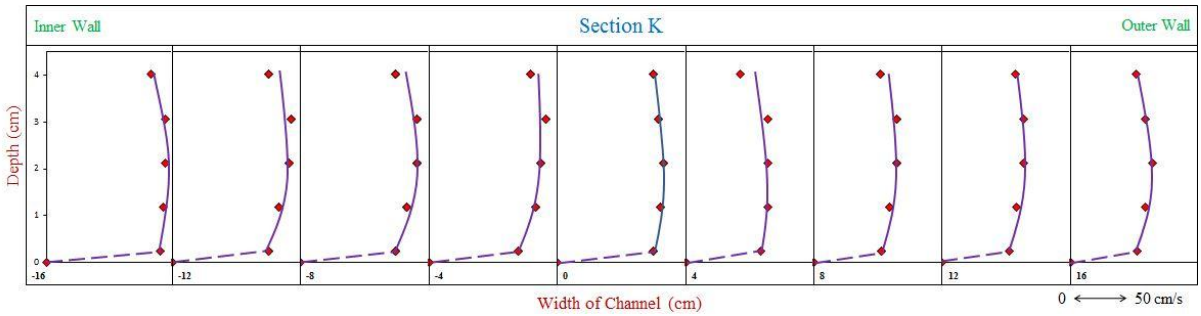

Figure: 4.1.11

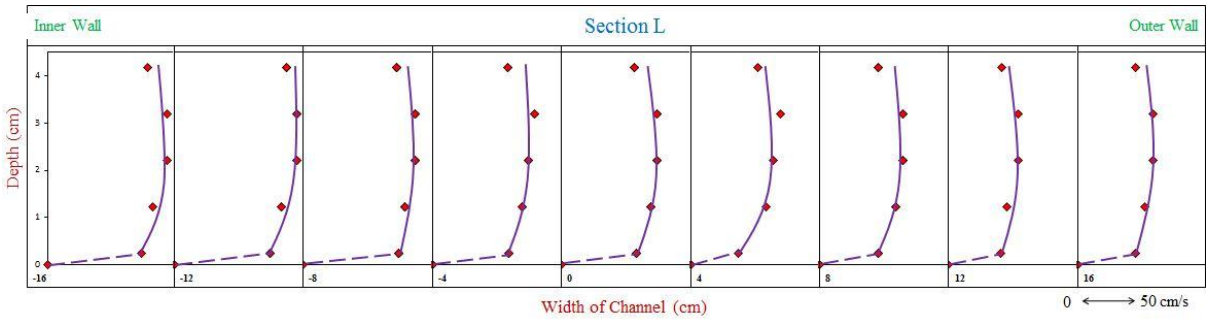

Figure: 4.1.12

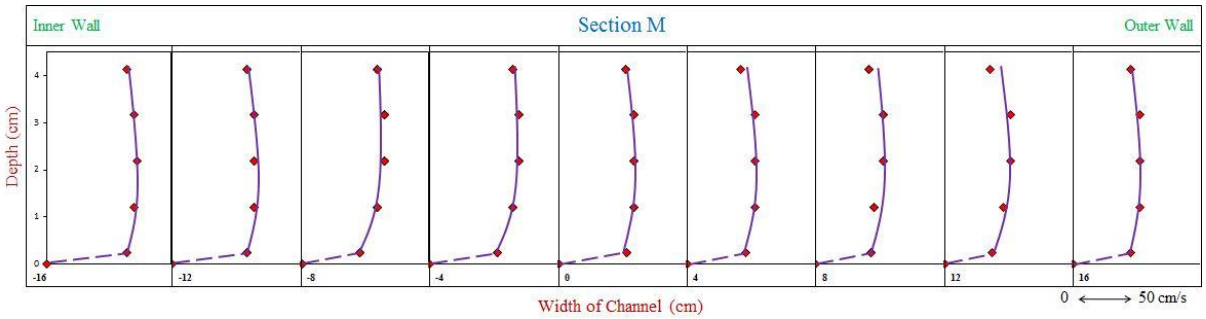

Figure: 4.1.13

Figure 4.1.1 to 4.1.13: Vertical Velocity Profile plots for all 13 Sections along the Meander Path

4.3 LONGITUDINAL VELOCITY CONTOURS AT DIFFERENT SECTIONS ALONG THE MEANDER PATH

The longitudinal velocity distribution in the lateral direction is analyzed along the meander path of the channel. The vertical sections are taken at 4cm intervals from the centreline of the meandering channel. The following figures from 4.2.1 to 4.2.13 represent the contour plots at all the sections along the meander path.

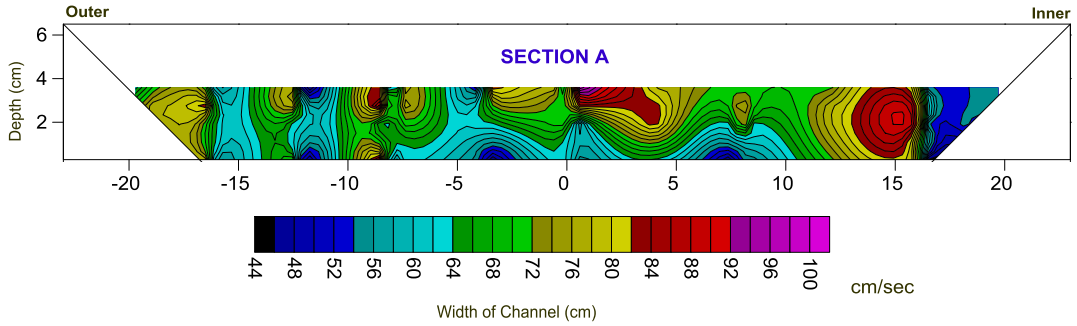

Figure: 4.2.1

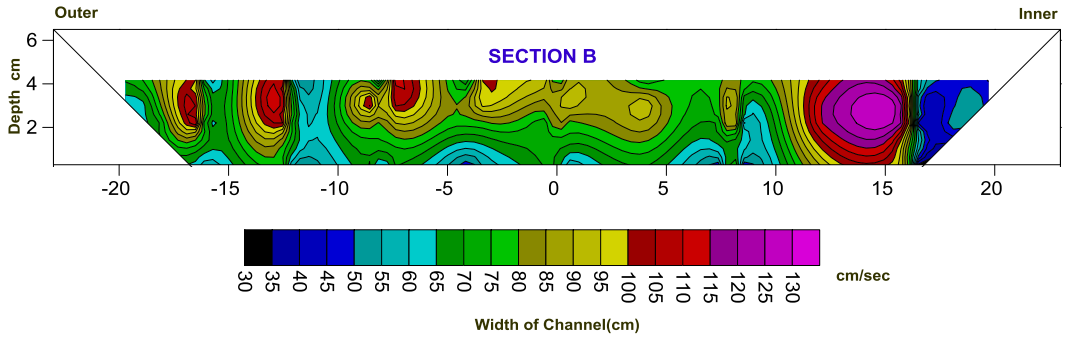

Figure: 4.2.2

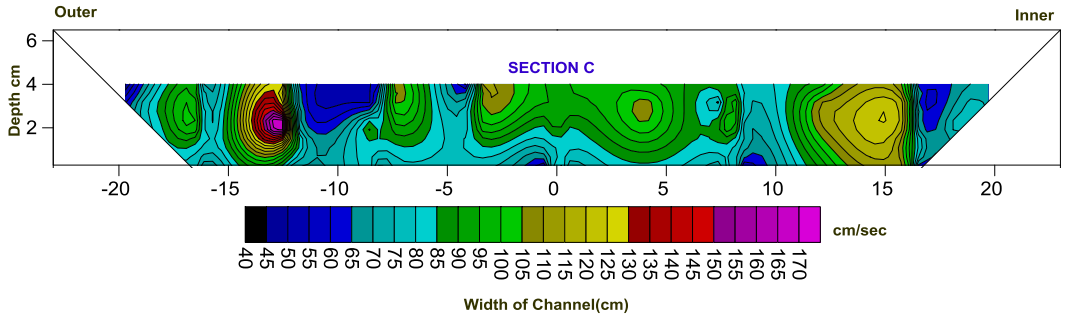

Figure: 4.2.3

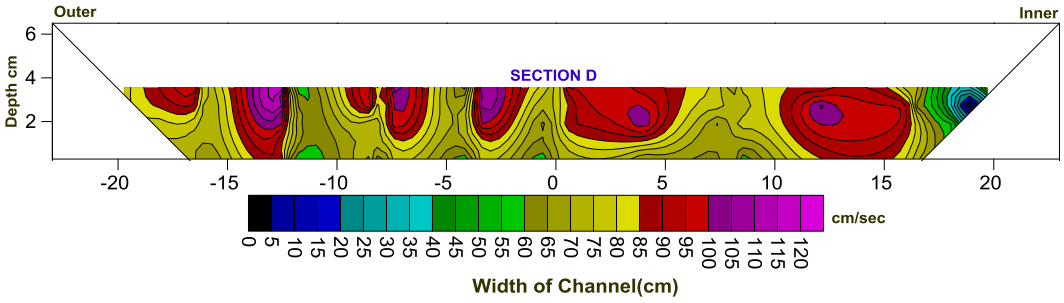

Figure: 4.2.4

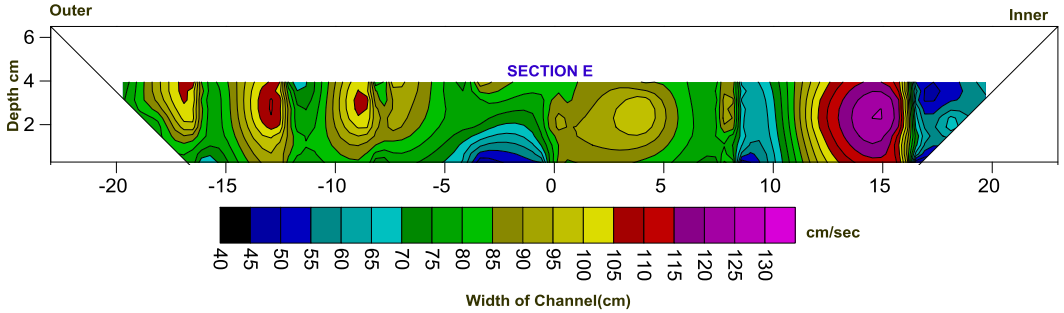

Figure: 4.2.5

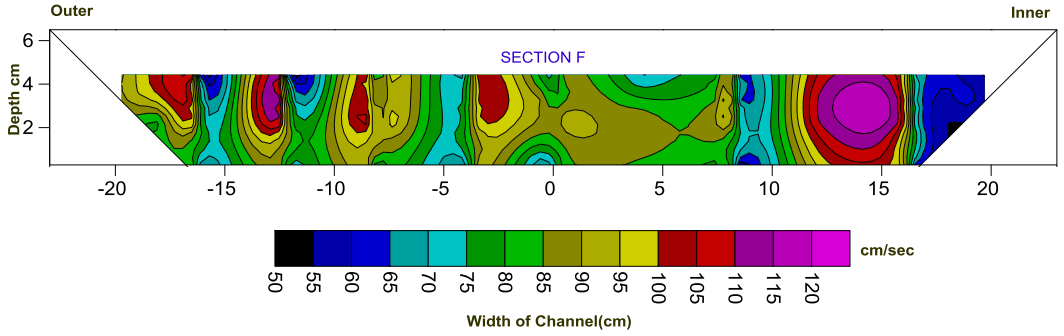

Figure: 4.2.6

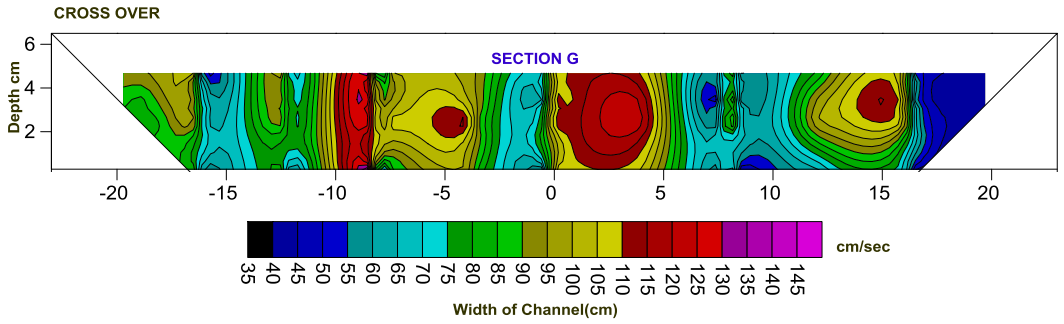

Figure: 4.2.7

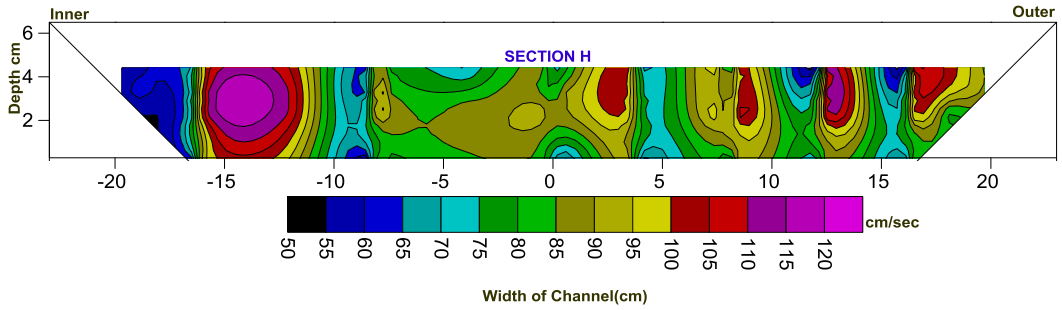

Figure: 4.2.8

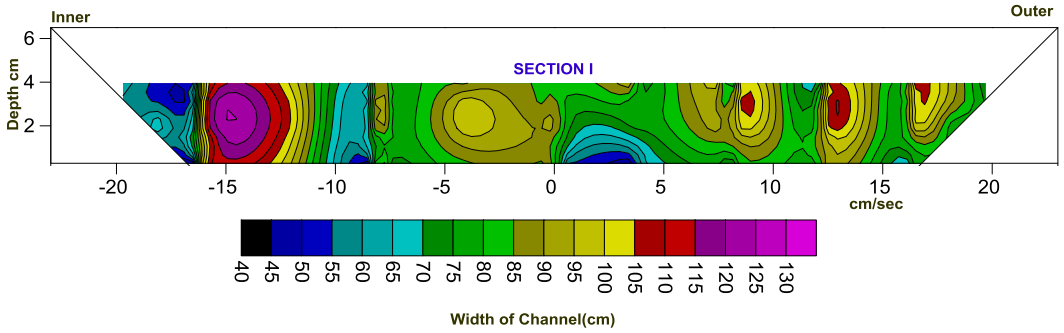

Figure: 4.2.9

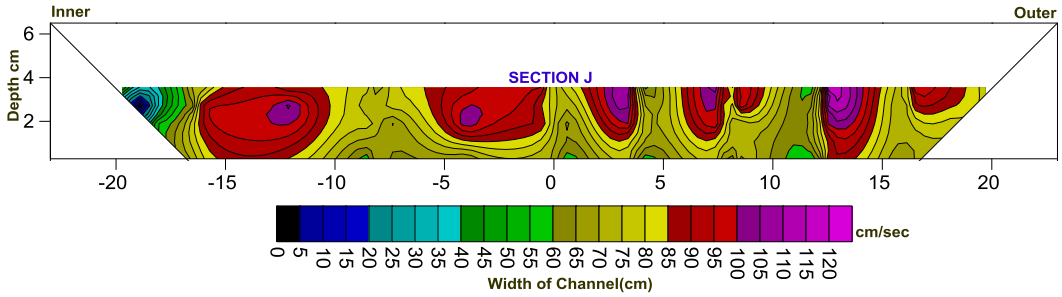

Figure: 4.2.10

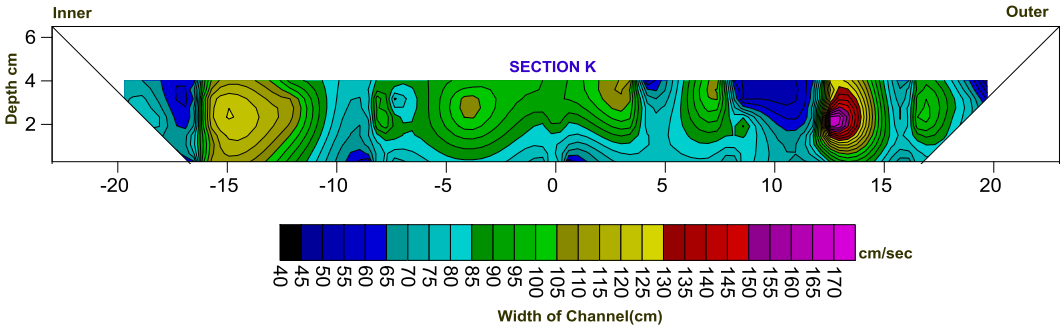

Figure: 4.2.11

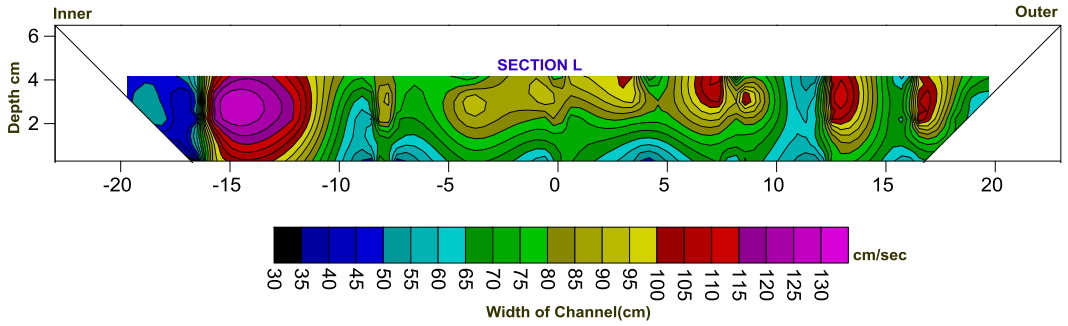

Figure: 4.2.12

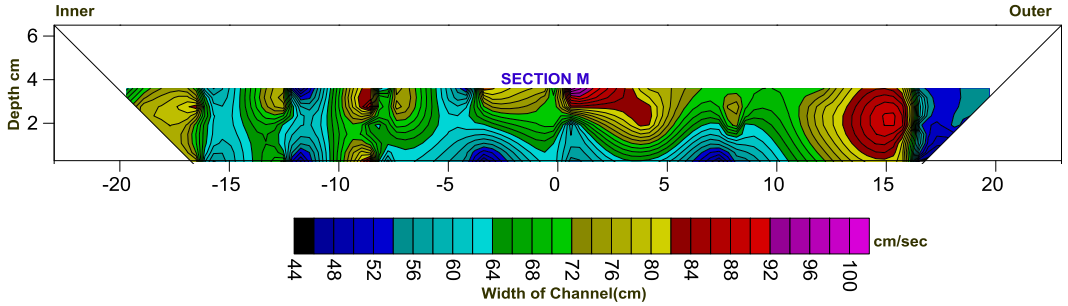

Figure: 4.2.13

Figure 4.2.1 to 4.2.13: longitudinal Velocity contours for all 13 Sections along the Meander Path

The following inferences can be made from the velocity profile plots and contours

1. The velocity contour diagram of section A, shown in Fig. 4.2.1 indicates that higher longitudinal velocity lies towards the right bank i.e. the inner wall of the channel section. The vertical velocity profiles at the same section (Fig. 4.2.1), depicts the similar pattern. The vertical velocity profile sections closer to the inner wall are observed to be bulgier than the outer wall.
2. Longitudinal velocity profile plots given clearly indicate that from sections A and G profiles tend to remain higher towards the inner wall. Contour plots also show the similar pattern and is also observed that velocity goes on increasing as one moves in the lateral direction. The velocity then starts decreasing until the cross-over.

3. At the cross-over it is observed that the velocity profiles are somewhat uniform with its maximum velocity occurring close to the centre of the channel section. This observation is usually seen to be similar in straight channels. Hence the channel follows nearly a steady and uniform flow at the cross-over reach, where the meandering channel changes its sign of curvature and is assumed to behave nearly as a straight channel.
4. Fig. 4.10.8 through 4.1.13 shows that the maximum velocity transfers from the central region of the cross-over section to the left bank i.e. the inner wall of the corresponding anti-clockwise curvature. The maximum velocity initially occures close to the bed and then shifts closer towards the free surface.
5. In the sections following the cross-over, i.e. from sections G to M, the profiles indicate that the local maximum value of velocity at each section starts moving from the central region towards the inner wall of the channel i.e. towards the left hand side.
6. The sections C and K as seen in Fig. 4.1.3 and 4.1.11, have highest maximum velocity throughout the channel, close to 130 cm/s. Such observation is due to the curvature of the meander path, moving towards the cross-over.

4.4 VELOCITY DISTRIBUTION ALONG THE CHANNEL WIDTH THROUGH THE MEANDER PATH

The longitudinal velocity distribution is analyzed along the width of the channel. The measurements are taken at the bed of the channel and the side slopes at by 0.4H, 0.6H, and 0.8H from the bed. H here is the average depth of water at the every corresponding section along the meander path. Depth-averaged velocity is considered to be the average velocity at any vertical section of a channel cross-section. The occurrence of this velocity is generally trusted to be found at 0.4H from the bed of the channel. The depth-averaged velocity is hence considered at 0.4H above the bed from the above experimental investigation. The following

figures from 4.2.1 to 4.2.13 represent the horizontal velocity profile along the channel at a height of 0.4 H along the meander path.

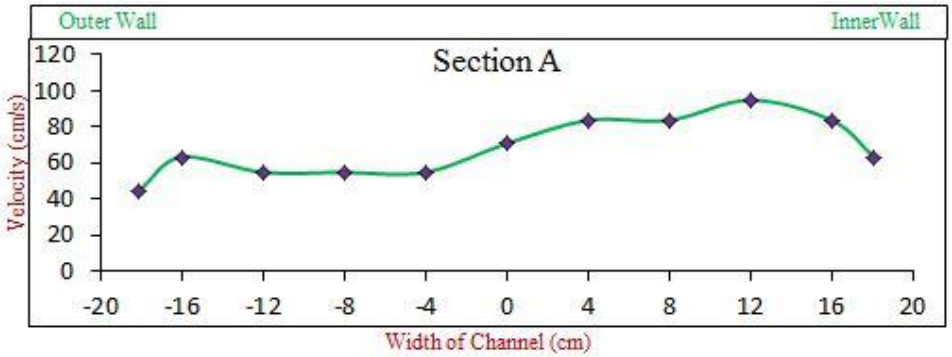

Figure: 4.3.1

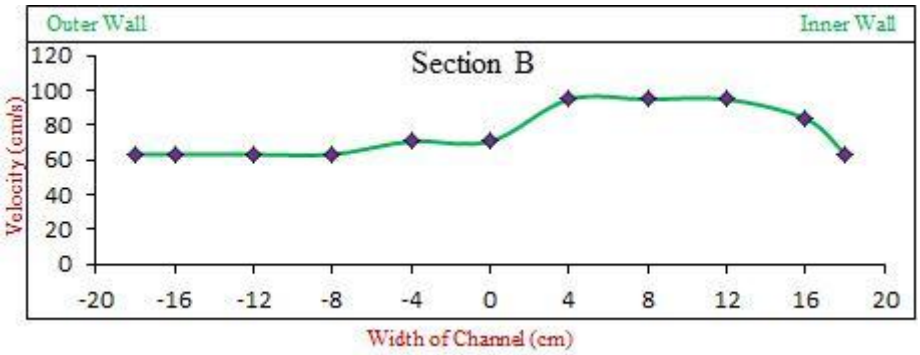

Figure: 4.3.2

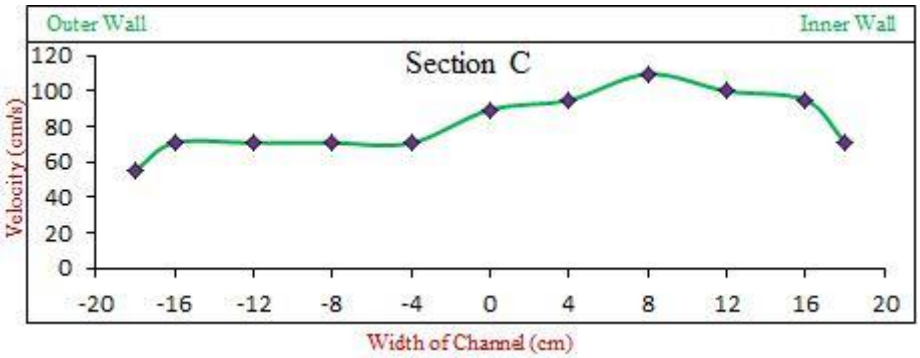

Figure: 4.3.3

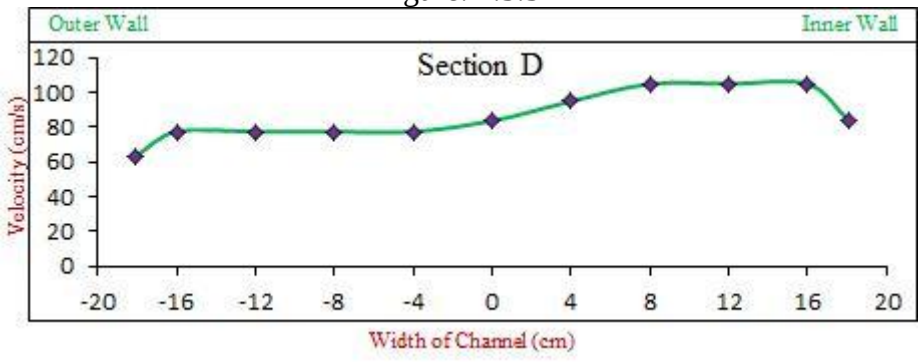

Figure: 4.3.4

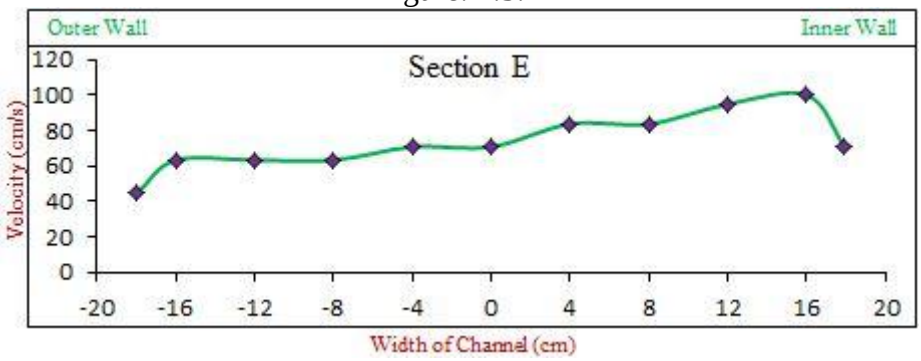

Figure: 4.3.5

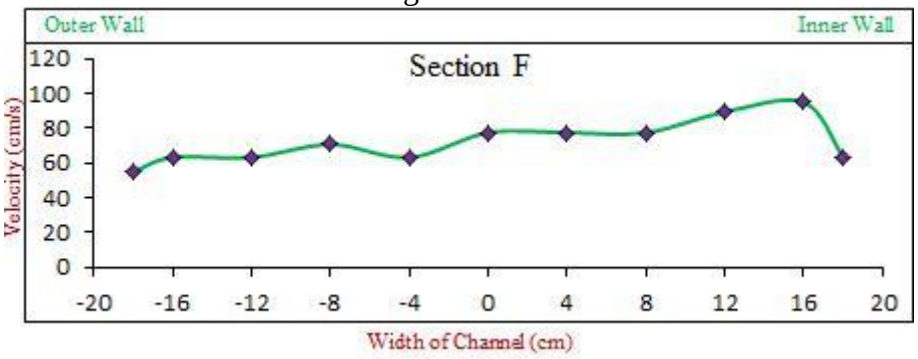

Figure: 4.3.6

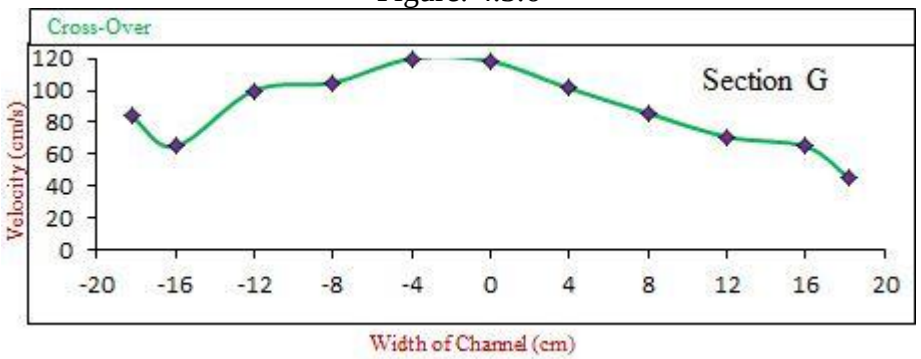

Figure: 4.3.7

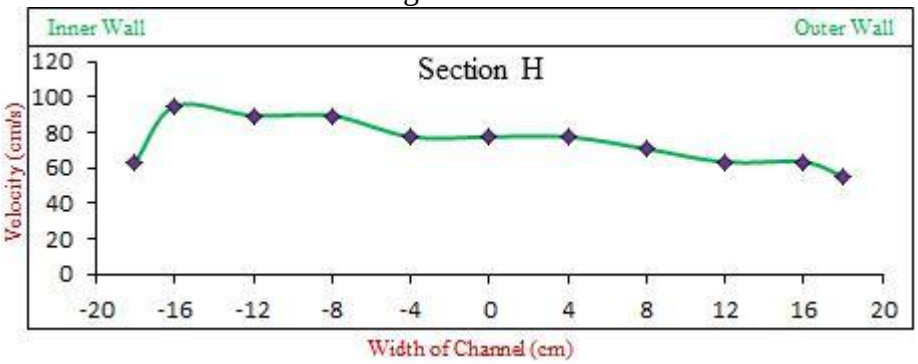

Figure: 4.3.8

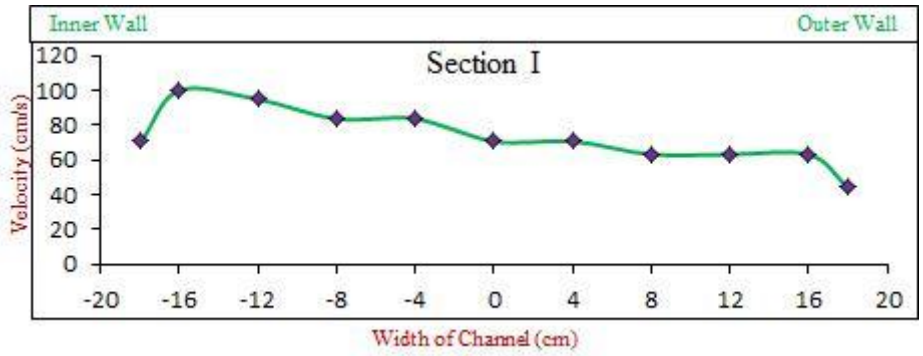

Figure: 4.3.9

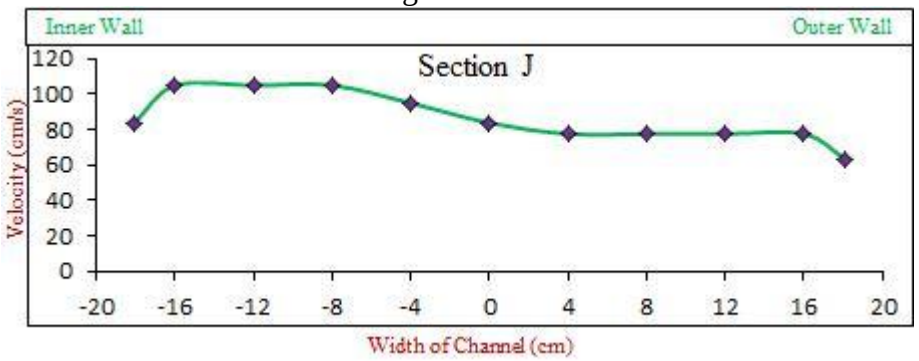

Figure: 4.3.10

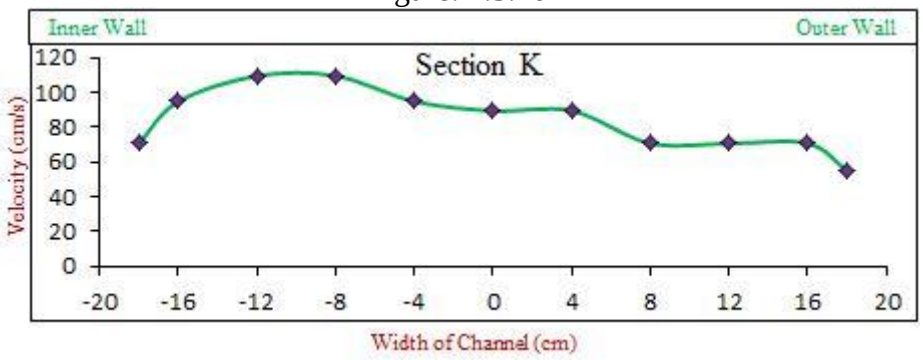

Figure: 4.3.11

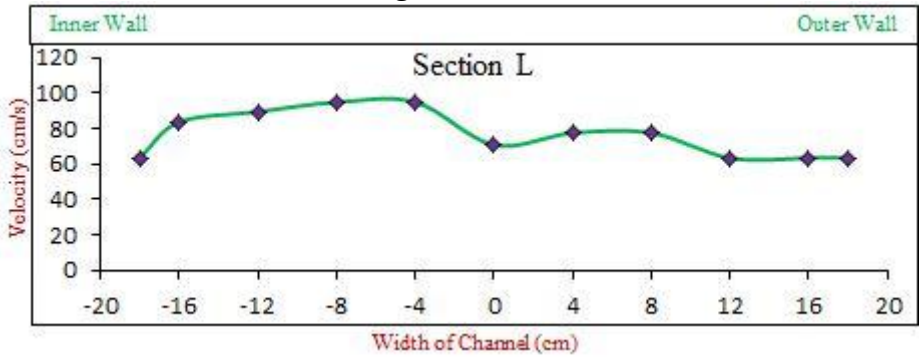

Figure: 4.3.12

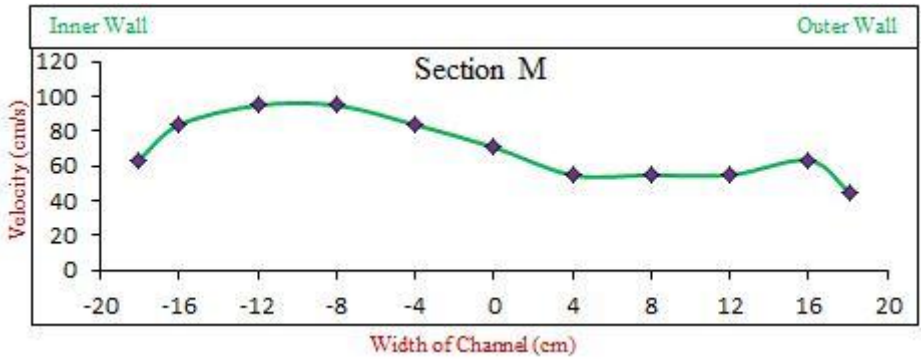

Figure: 4.3.13

Figure 4.3.1 to 4.3.13: Lateral Velocity Profile at 0.4H Depth from bed of the Channel Section along the Meander Path

From the above horizontal profile study at different levels, the following deductions can be made

1. The depth-averaged velocity is usually found to be higher around the centre of the channel section in case of a simple straight channel, but in the present experimental observation higher depth-averaged velocity is found closer towards the inner wall of the simple meandering channel.
2. The horizontal velocity profiles at the bed of the channel at section A i.e. at the bend apex remains higher at the inner wall and there is a drastic difference in velocity between the inner and outer walls as shown in Fig. 4.3.1. The highest velocity remains close to 85 cm/sec.
3. On moving at the bed from the initial bend apex region to the cross-over (Section G) as seen in Fig. 4.3.2 to 4.3.6; there is a gradual variation in the horizontal velocity profile along the width of the channel, with higher velocity at the inner wall.
4. As seen in Fig. 4.3.7, at the bed of the cross-over section G, the maximum velocity moves towards the centre of the channel section, with gradual variation of velocity towards the inner and outer walls. This observation depicts that a meandering channel behaves as a straight channel at around the cross-over section In the following sections,

from Fig. 4.3.8 to Fig. 4.3.12, on moving from cross-over towards the other bend apex, the higher depth-averaged velocity moves towards the left of the channel section, this is now the inner wall for the channel section.

5. Section G shown in fig.4.3.7 indicates the presence of maximum velocity of around 120cm/s close to the middle at a height of 0.4*H* from the bed. Hence, it can be concluded that higher velocity is achieved somewhere at the cross-over.
6. The characteristics shown in Fig.4.3.11 i.e. for section K (anti-clock wise curve)indicates similarity with that of the section C(clock wise curve). Sections remain after the section K i.e. from Fig. 4.3.8 to 4.3.13 show steady variation with highest velocity towards the the inner wall of the channel.

4.5 BOUNDARY SHEAR STRESS DISTRIBUTION AT DIFFERENT SECTIONS ALONG THE MEANDER PATH

Boundary shear stress measurements are carried out at different sections along the meander path through the cross-over. Total 13 reaches of boundary shear stress measurements are carried out.

The figures from 4.4.1 to 4.4.13 illustrate the boundary shear stress distributions across the channel bed and the side walls at the inner and outer walls for all the 13 reaches.

The shear stress profiles along the rigid surface of the channel are presented by showing the stress curves perpendicular to all the three sides of the channel viz. the bed, the inner wall and the outer wall. Hence the figures provide a clear demonstration about the boundary shear stress distribution throughout the channel section along the meander path.

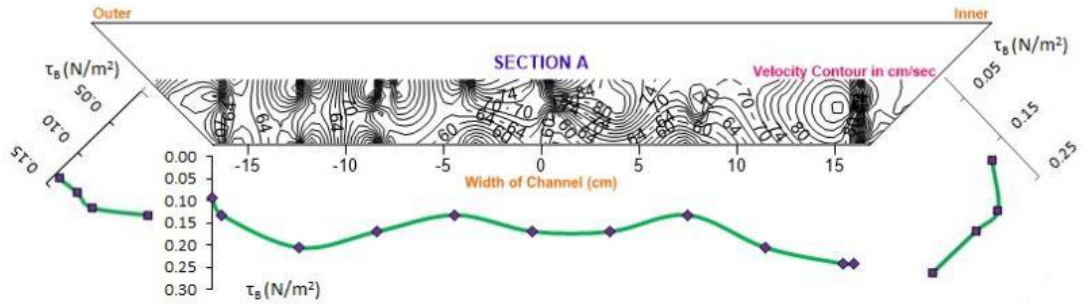

Figure: 4.4.1

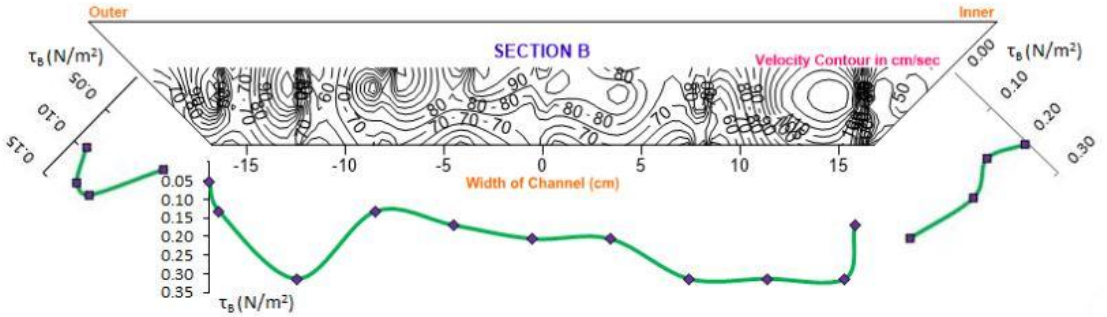

Figure: 4.4.2

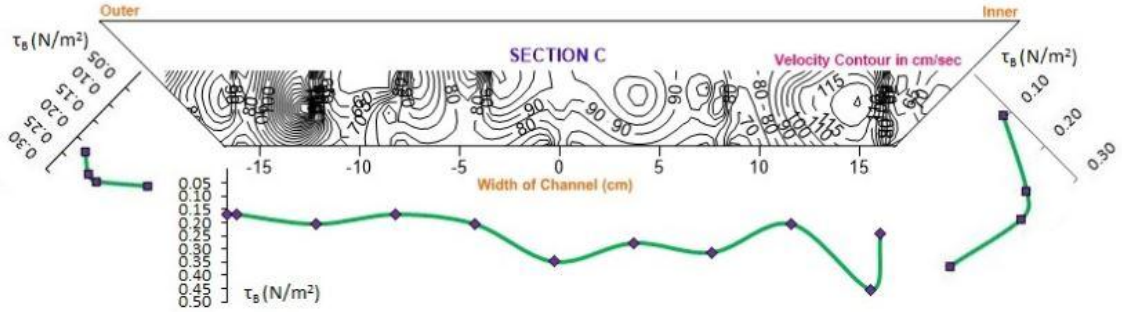

Figure: 4.4.3

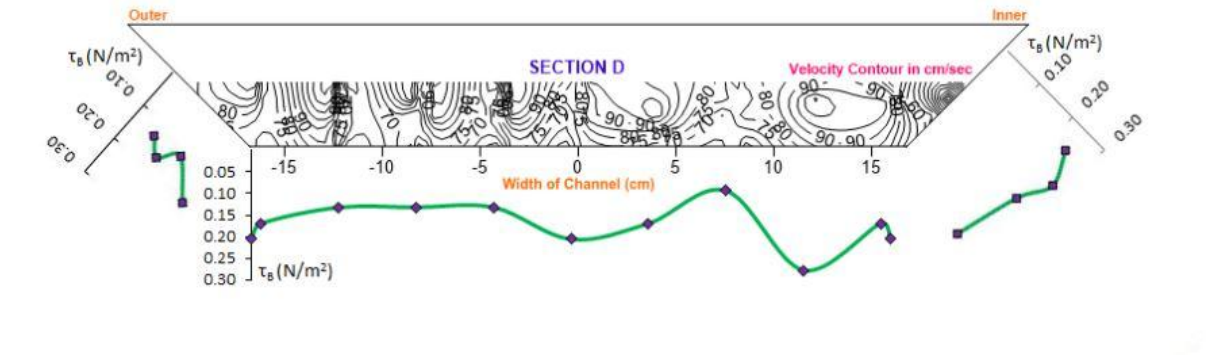

Figure: 4.4.4

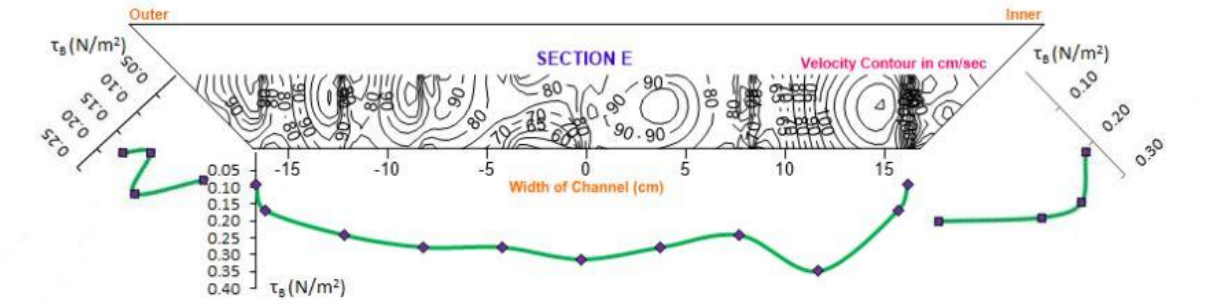

Figure: 4.4.5

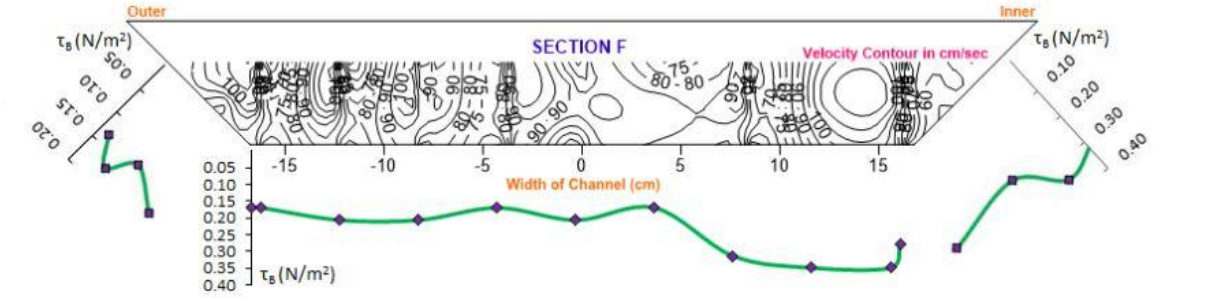

Figure: 4.4.6

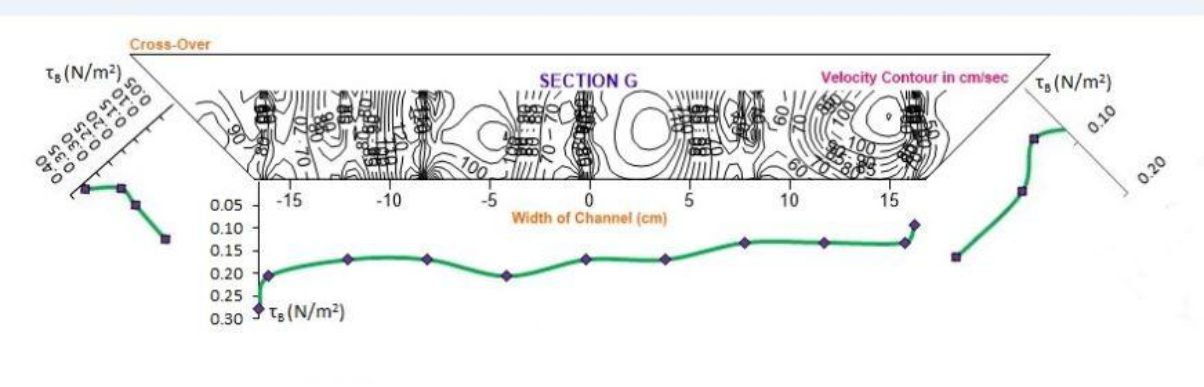

Figure: 4.4.7

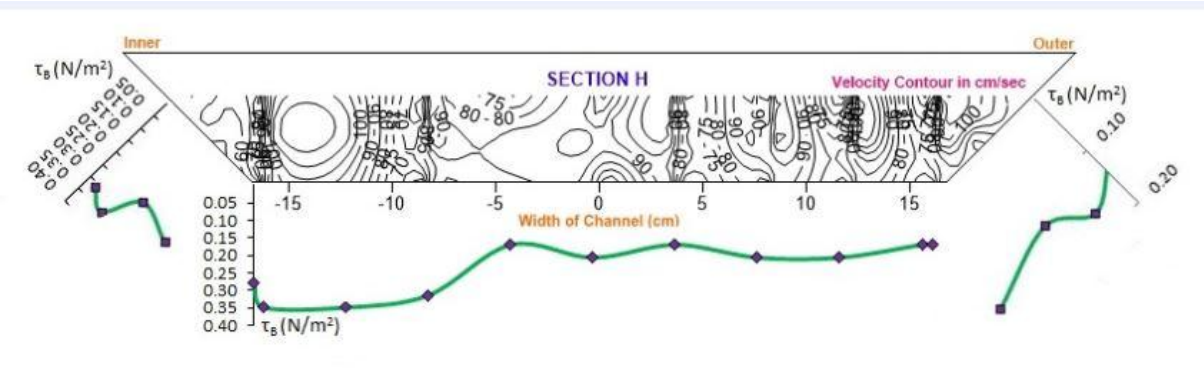

Figure: 4.4.8

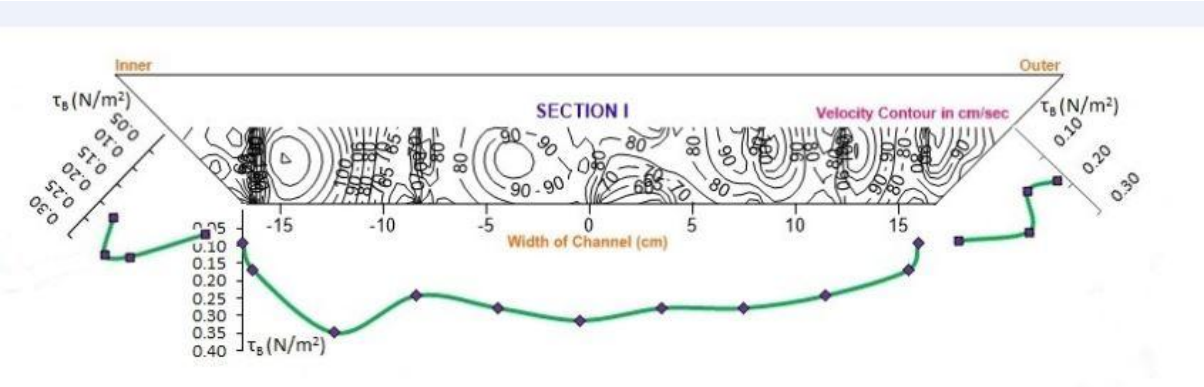

Figure: 4.4.9

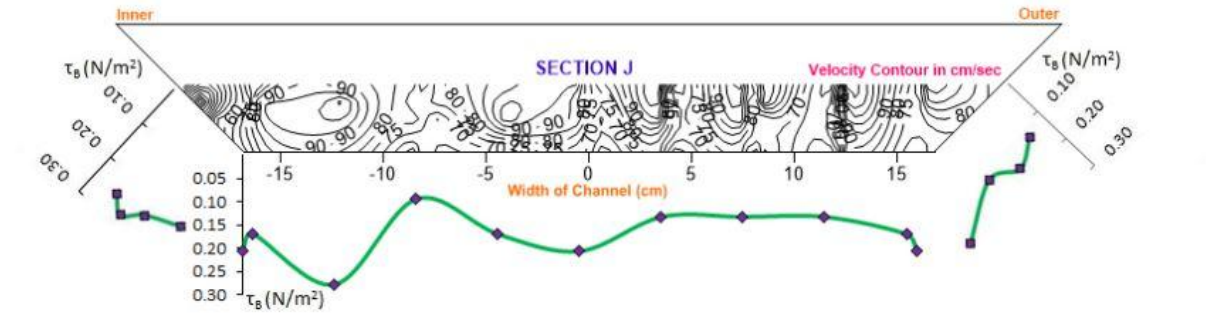

Figure: 4.4.10

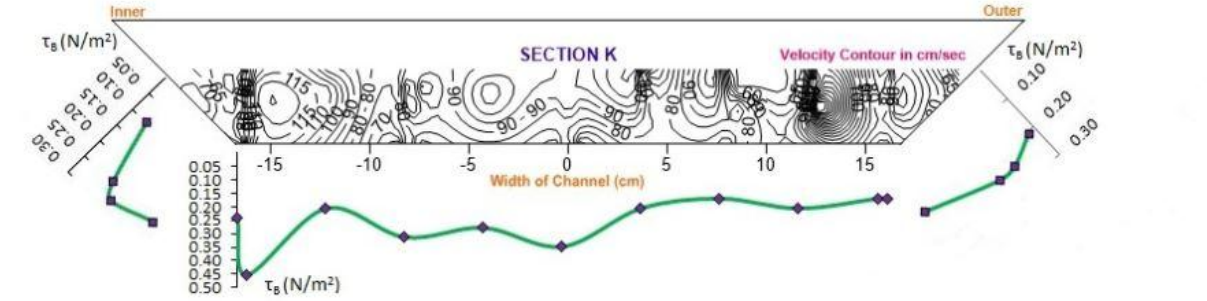

Figure: 4.4.11

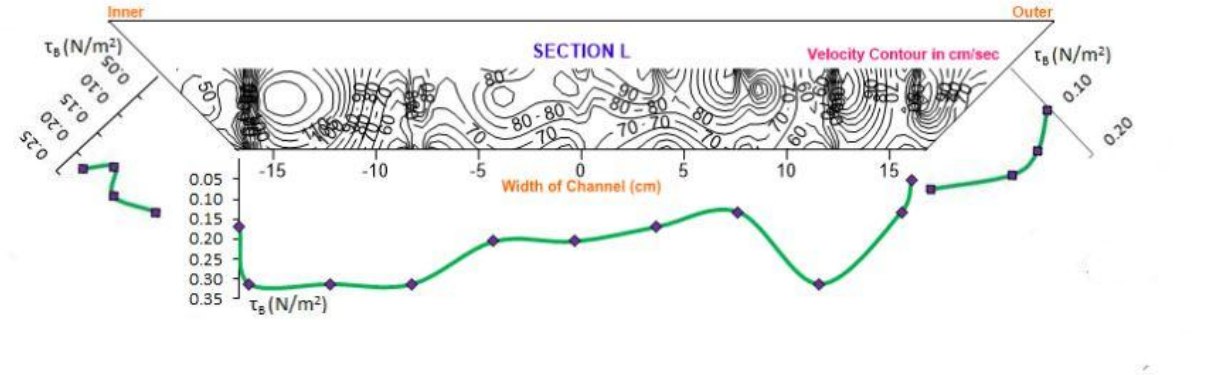

Figure: 4.4.12

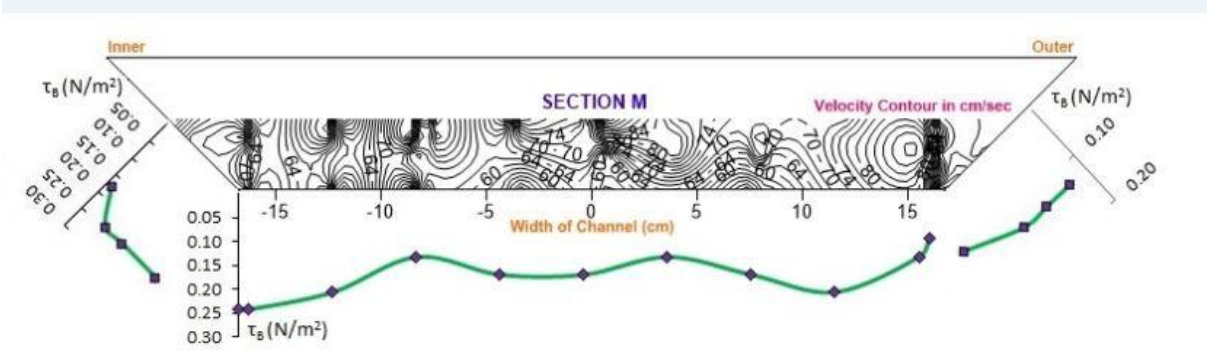

Figure: 4.4.13

Figure 4.4.1 to 4.4.13: Boundary Shear Stress Plots across all 13 Sections along the Meander Path

Following conclusions can be made from the above boundary shear stress plots.

1. At the bend apex section A, given in figure 4.4.1, it can be observed that the shear stress carried by the inner wall is more as compared to the outer wall.
2. The maximum value of shear stress at the inner bank of the section A is found to be around 0.23N/m^2, where as a minimum of 0.10N/m^2 at the outer wall. The variation of shear stress in this section is found to be normal.
3. Fig. 4.4.2 to 4.4.6, which shows section B to F indicate that the shear stress remains higher towards the inner wall. In these sections, the variation of shear stress between the inner and outer walls is observed to be gradual.
4. At section G (cross-over section), the variation of boundary shear stress is found to be more or less uniform throughout the channel section. The shear stress value remains close to 0.28N/m^2.
5. From the Fig. 4.4.1 through 4.4.13, it can be observed that on moving from the initial bend apex section A; the boundary shear stress carried by the inner wall gradually decreases and reaches a minimum at the cross-over and then it increases on the other bank i.e. the inner wall while moving towards the following bend apex section i.e. M.

6. From Fig. 4.4.8 to 4.4.12, it can be seen that there is a gradual variation in boundary shear stress between the inner and outer walls, with higher stress remaining towards the left bank (inner wall).
7. Fig. 4.4.13 describes extreme variation in the boundary shear stress values between the inner and outer walls of the channel section, with higher shear stress lying towards the inner wall.
8. The boundary shear stress at section C Fig.4.4.3 and section K Fig.4.4.11 are having highest value about .44N/m^2 at their inner walls.

9. The variation of boundary shear at section G as per Fig.4.4.7is found to be uniform throughout the width

4.6 COMPARISON WITH OTHER RESEARCHER'S WORK

The longitudinal velocity found experimentally is compared with the work of **Pradhan(2014)**, having the same geometrical parameters with a similar study of longitudinal velocity distribution throughout the meander path. The comparison is done against a single variable, which is the aspect ratio (b/h). Figures 4.5.1 to 4.5.13 show the comparison plot between these two data sets keeping velocity as abscissa and a non-dimensional parameter i.e. inverse aspect ratio (h/b) as the ordinate. The study helps to determine the differences in velocity profiles of the two data sets having different Aspect Ratios.

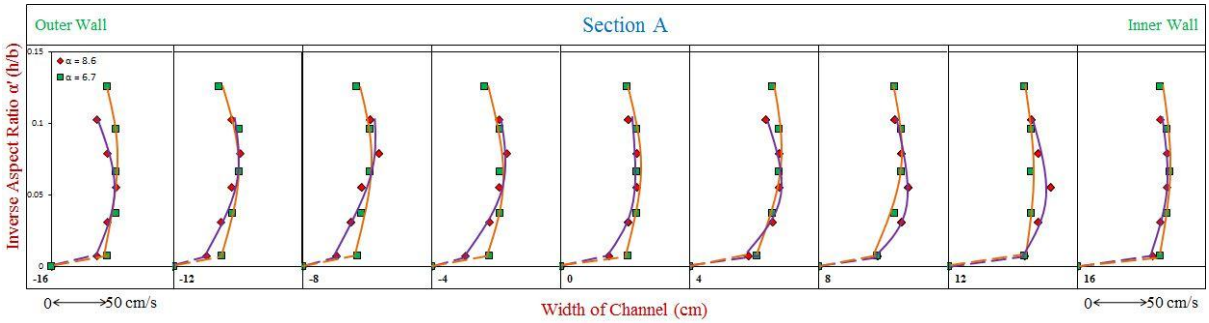

Figure: 4.5.1

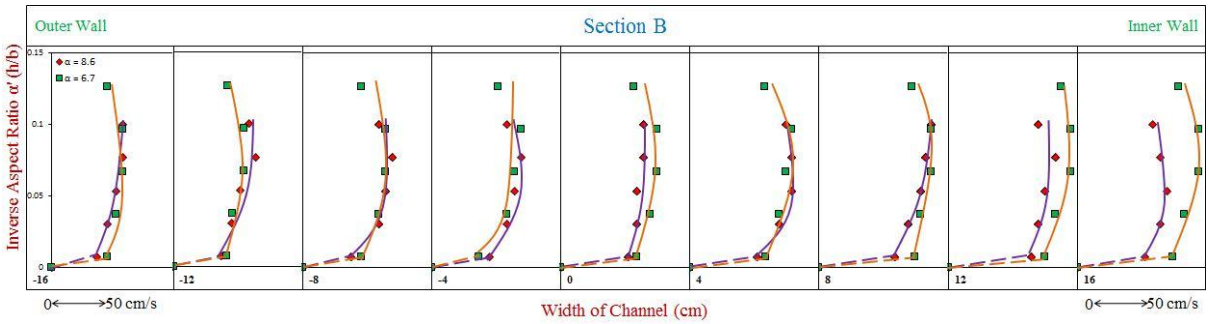

Figure: 4.5.2

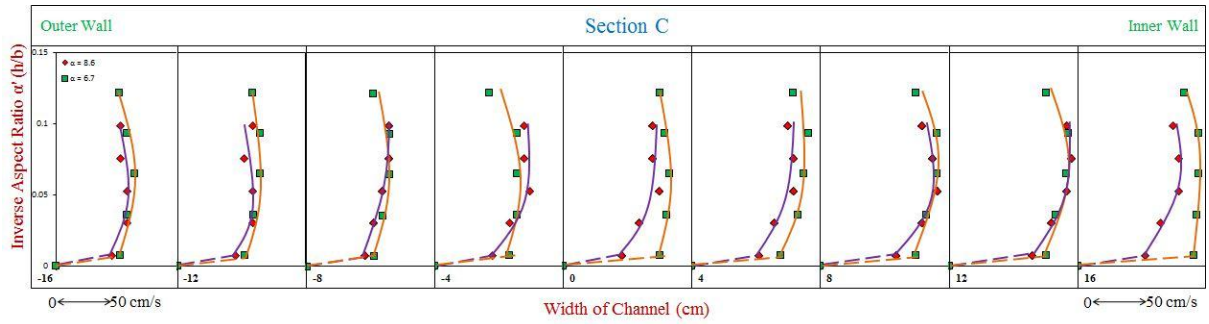

Figure: 4.5.3

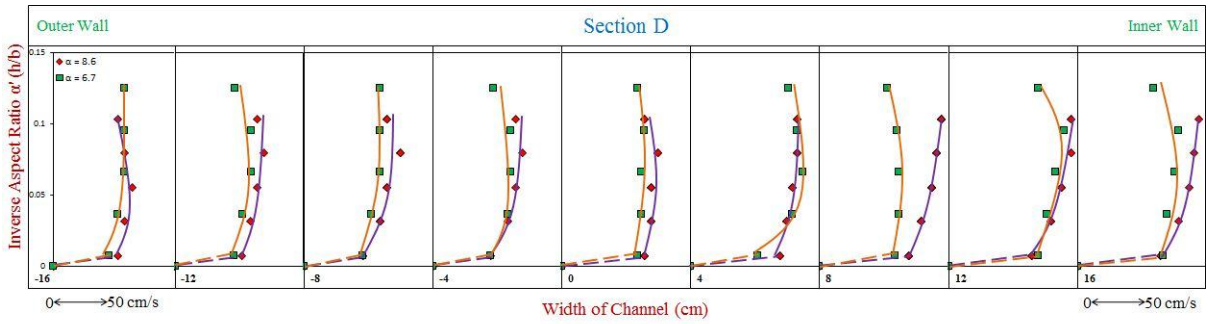

Figure: 4.5.4

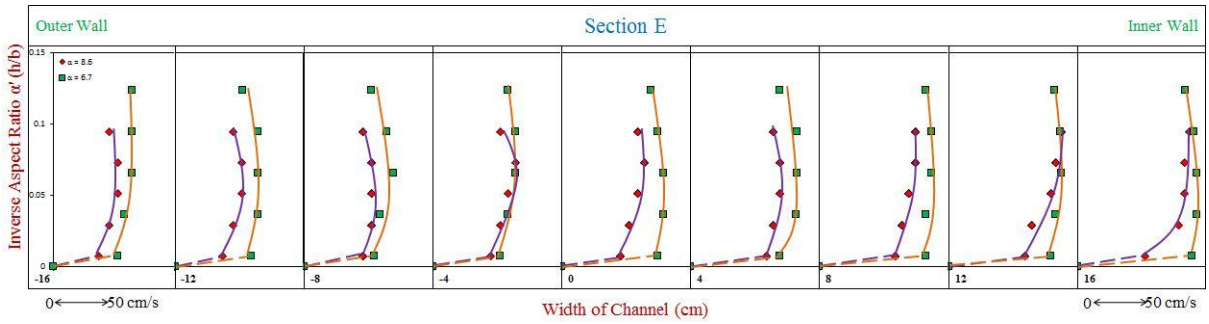

Figure: 4.5.5

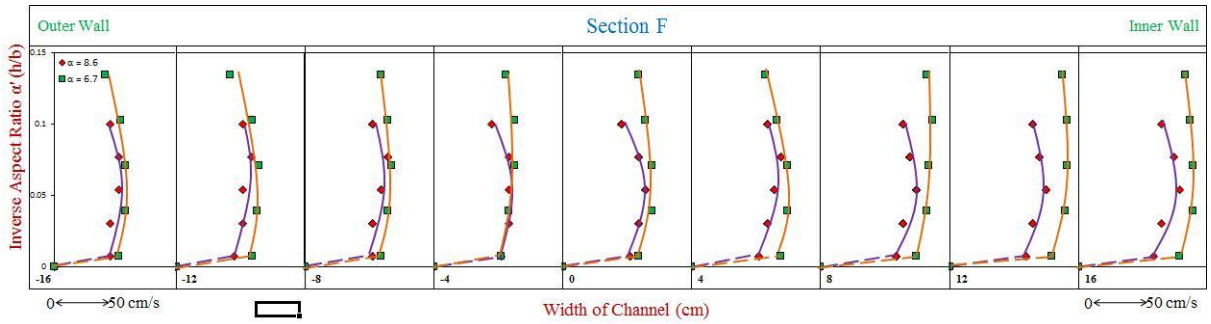

Figure: 4.5.6

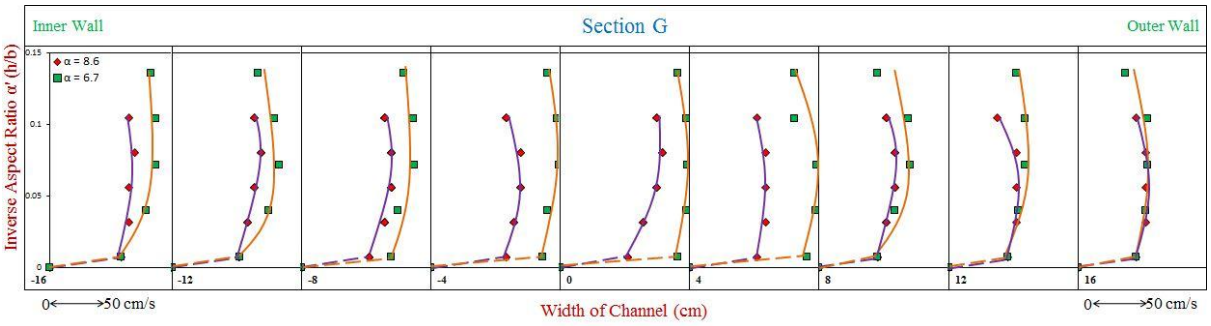

Figure: 4.5.7

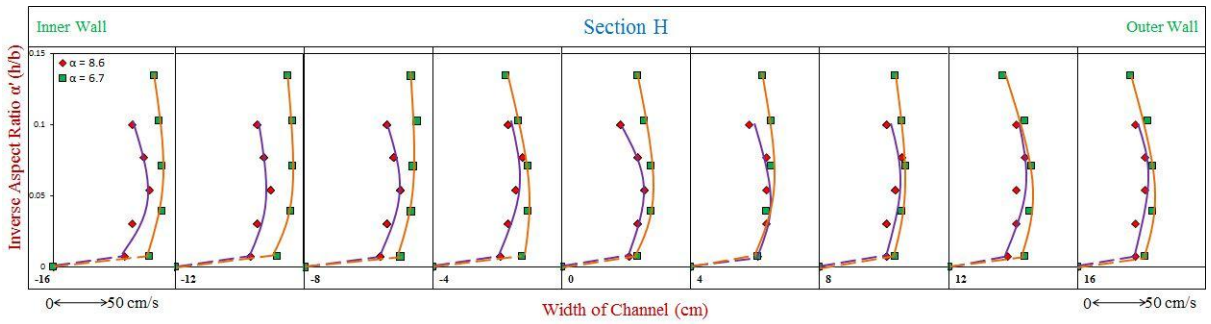

Figure: 4.5.8

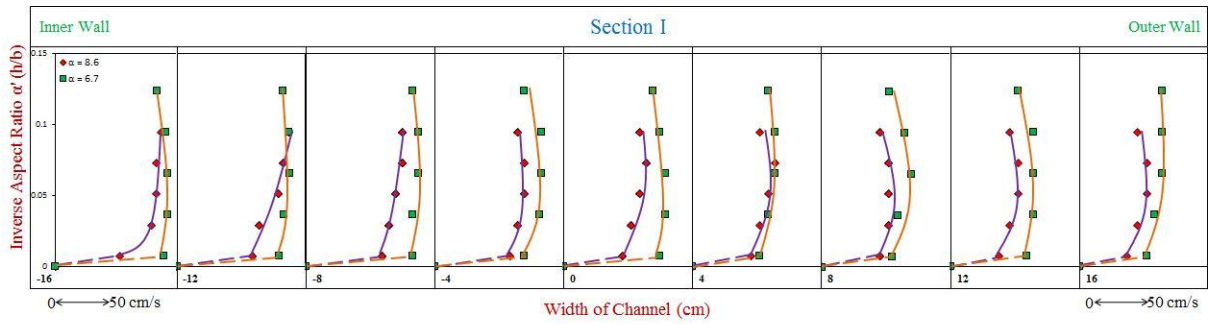

Figure: 4.5.9

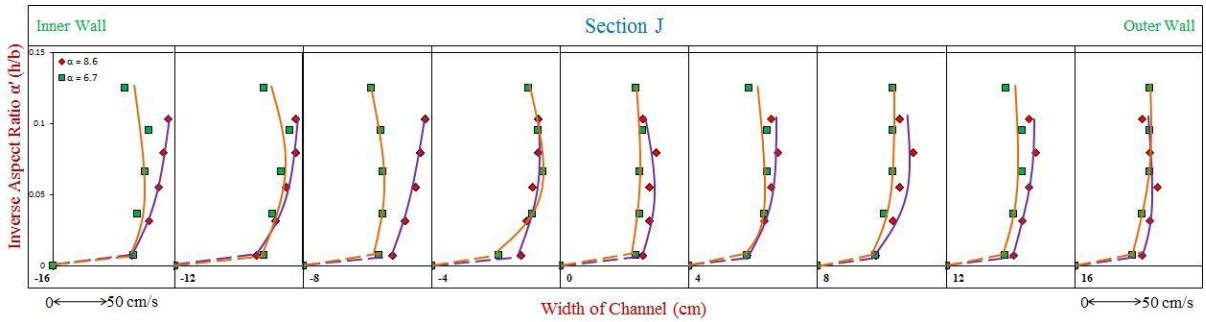

Figure: 4.5.10

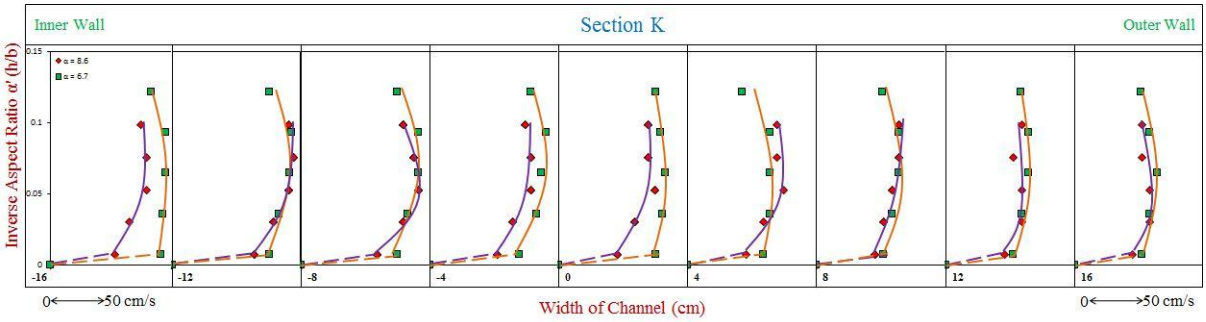

Figure: 4.5.11

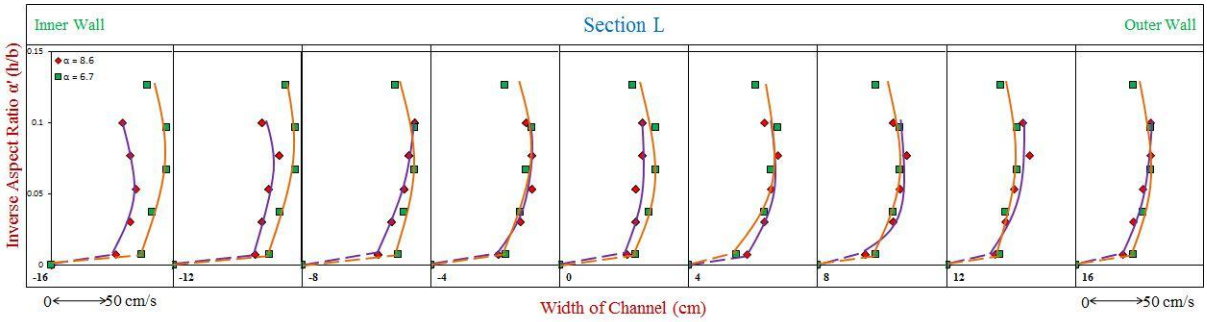

Figure: 4.5.12

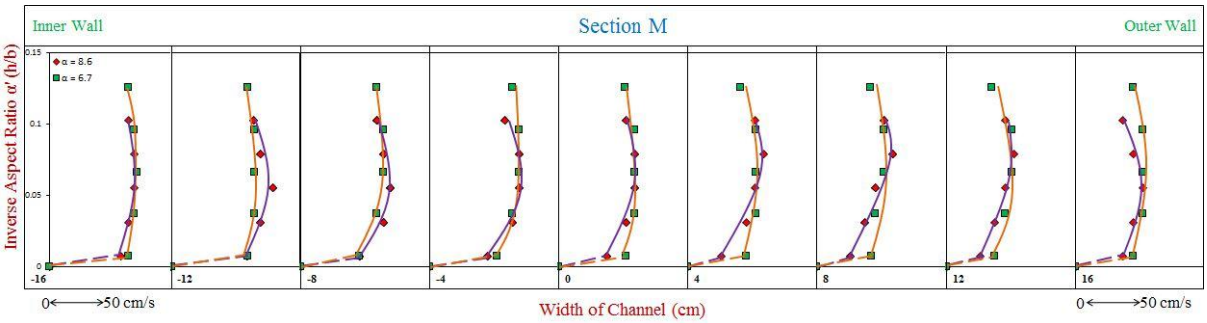

Figure: 4.5.13

Figure 4.5.1 to 4.5.13: Comparison of Velocity Profiles at Different Aspect Ratio

From the above figures we concluded that

- At the bend apex sections A and M the velocity profiles are seen to remain quite close to each other i.e. seem to be similar.
- Moving from bend apex section A towards the cross over G the deviation among them increases towards the inner wall with the velocity profile of the higher aspect ratio value remain higher.
- At the cross over G the deviation among the velocity profiles is observed to be quite high at the central region of the section.
- In the following section the pattern is observed to be similar but towards the left of the channel section,which is now the inner wall.

4.7 NUMERICAL RESULTS

Generally, experimental and theoretical analysis are the main tools for finding out the solution of open channel flow problems to meet the needs of field requirements. In recent times CFD techniques are being used extensively for solving the flow problems. In this study, a few simulations were carried out by using the commercial code namely ANSYS to simulate the present experimental investigation. Simulation was carried out to predict the velocity contour and boundary shear stress distribution along the meanderpath. Here Large Eddy Simulation model is used for turbulence modelling. The LES equations are discretized in both space and time. In this study the algorithms adopted to solve the coupling between pressure and velocity field is PISO which is the pressure implicit splitting operators use in Fluent (Issa 1986). A non-iterative solution method PISO is used to calculate the transient problem as it helps to converge the problems faster

4.7.1 VELOCITY CONTOURS ALONG THE MEANDER PATH

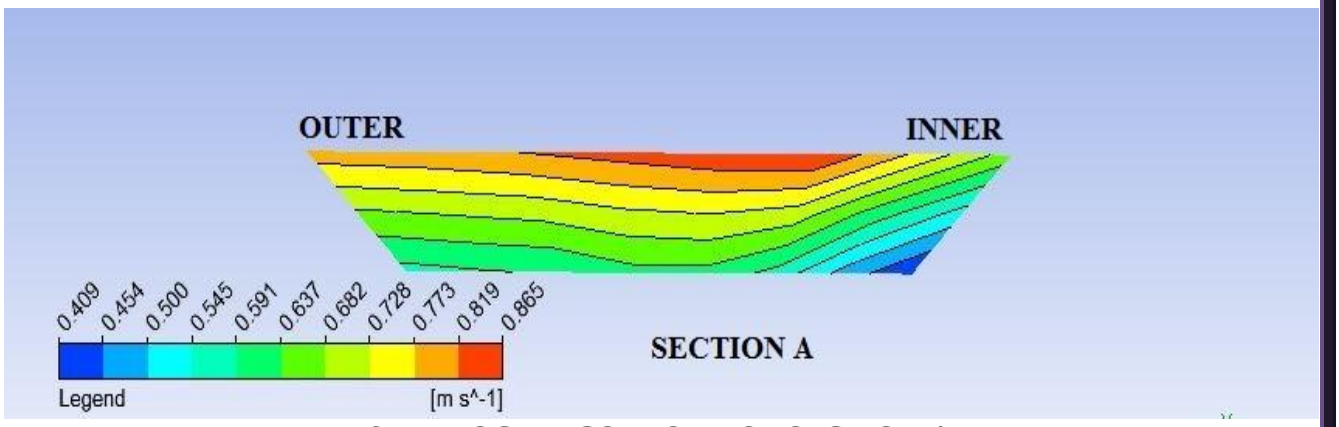

Figure4.6.1VELOCITY CONTOUR OF SECTION A

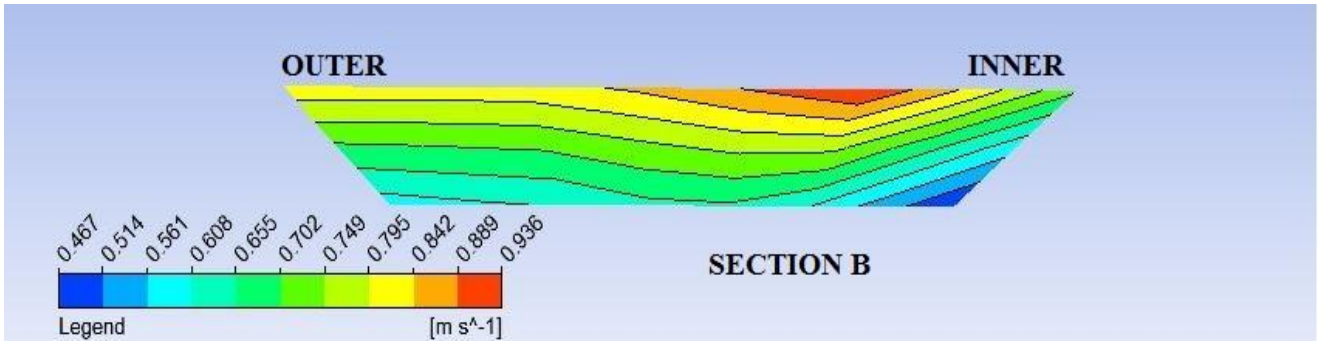

Figure 4.6.2: VELOCITY CONTOUR OF SECTION-B

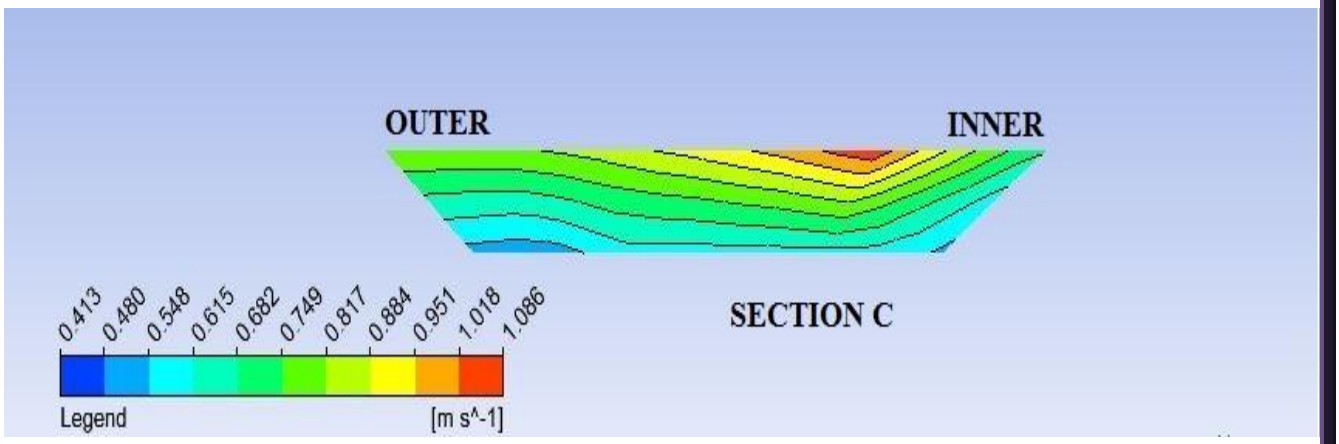

Figure 4.6.3: VELOCITY CONTOUR OF SECTION-C

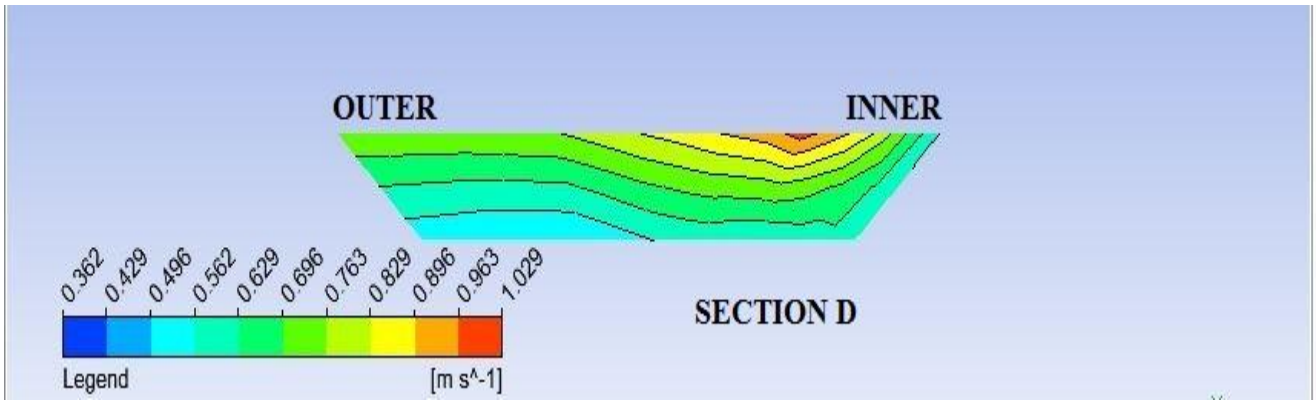

Figure 4.6.4: VELOCITY CONTOUR OF SECTION-D

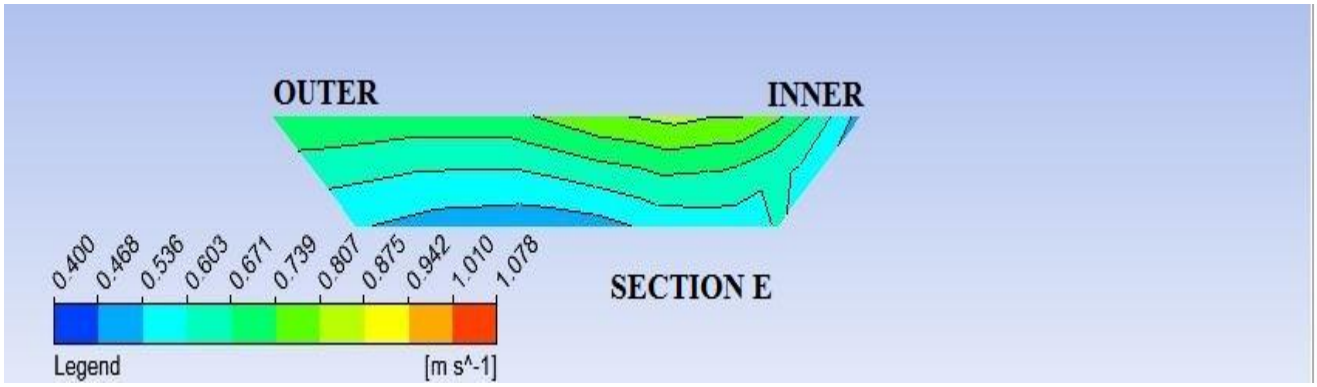

Figure 4.6.5: VELOCITY CONTOUR OF SECTION-E

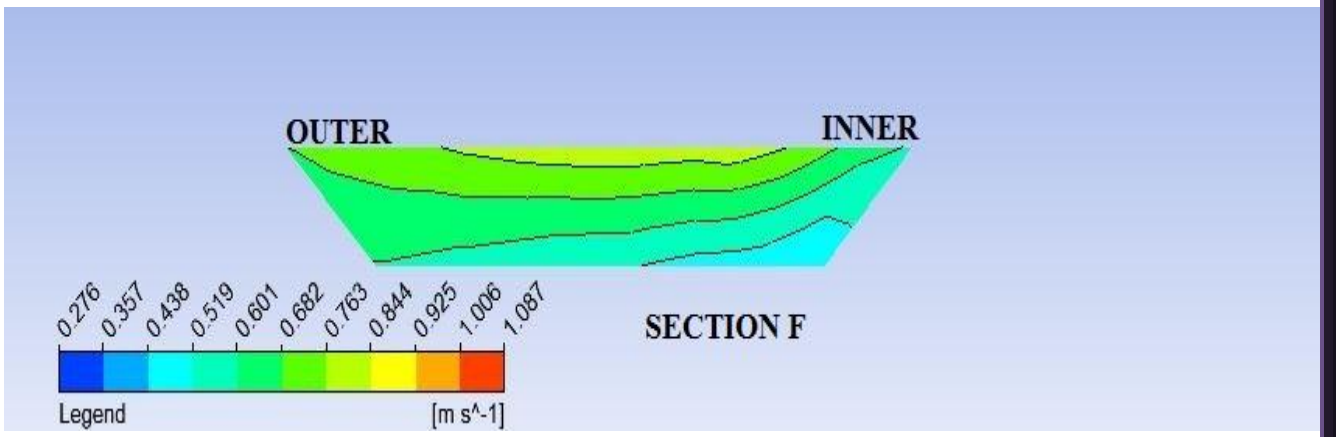

Fig 4.6.6: VELOCITY CONTOUR OF SECTION-F

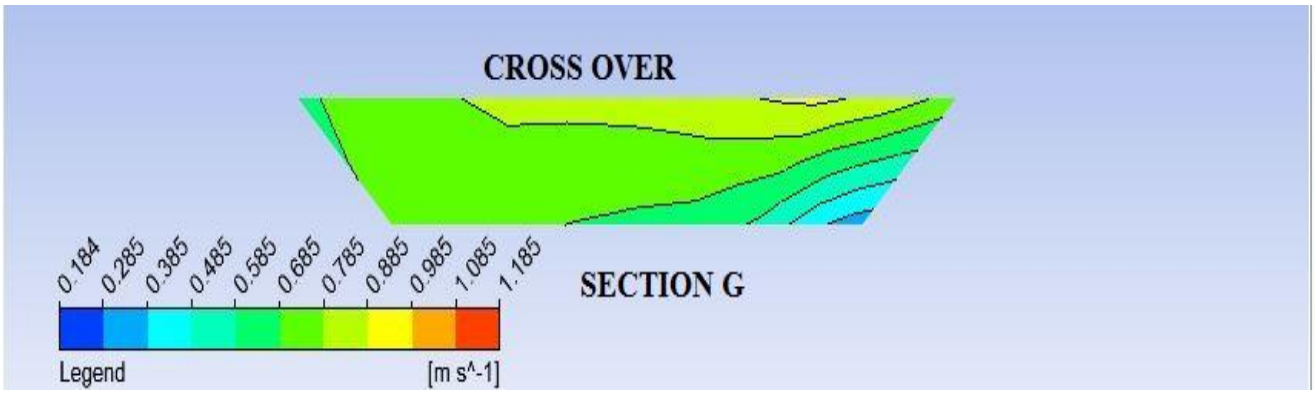

Figure 4.6.7: VELOCITY CONTOUR OF SECTION-G

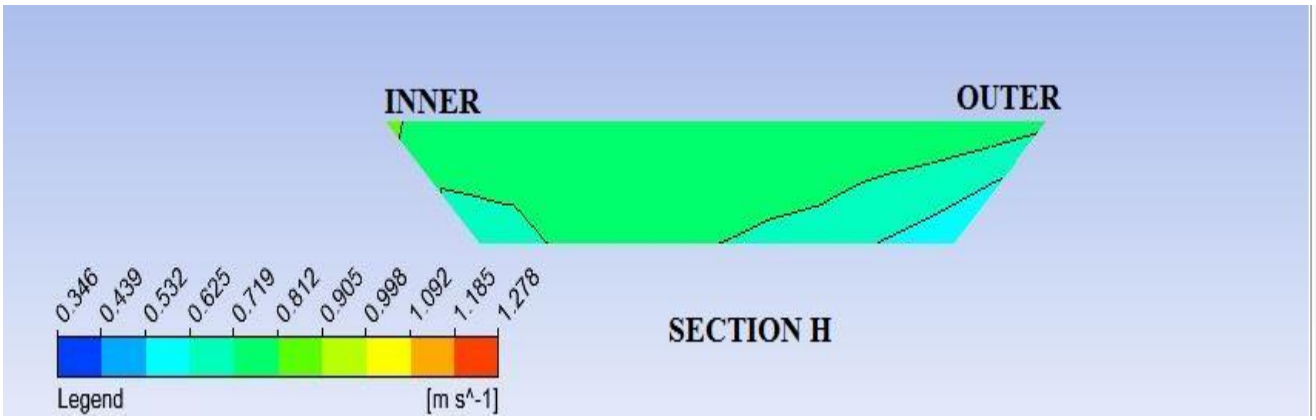

Figure 4.6.8: VELOCITY CONTOUR OF SECTION-H

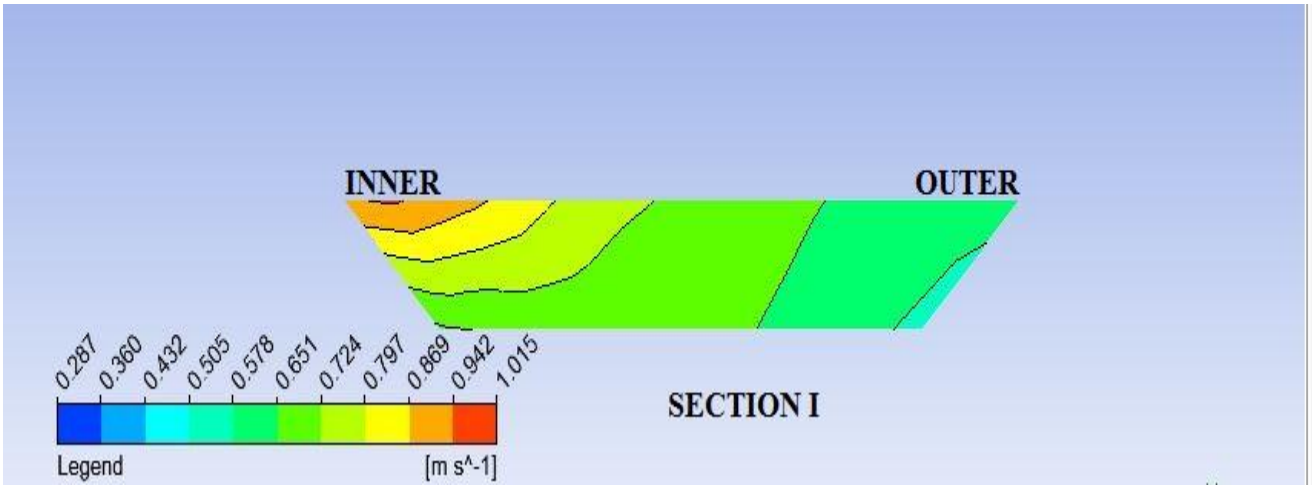

Figure 4.6.9: VELOCITY CONTOUR OF SECTION-I

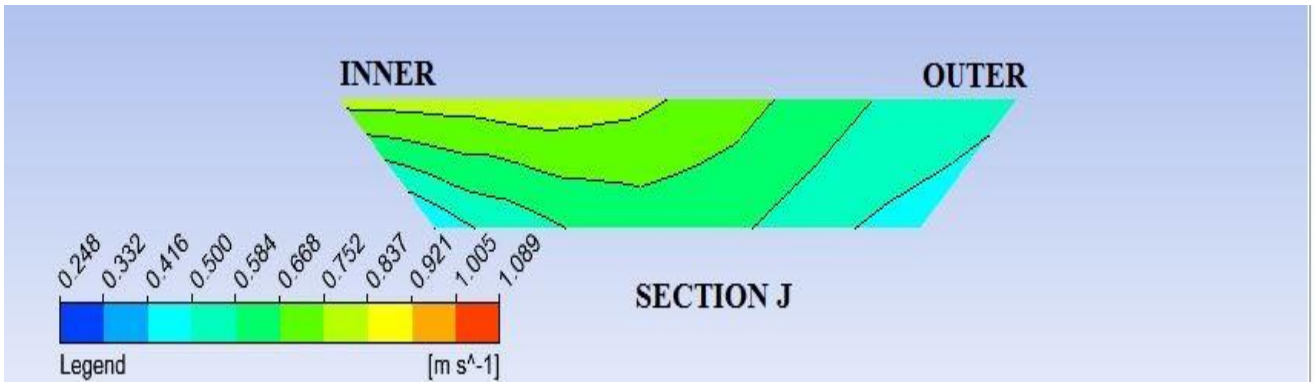

Figure 4.6.10: VELOCITY CONTOUR OF SECTION-J

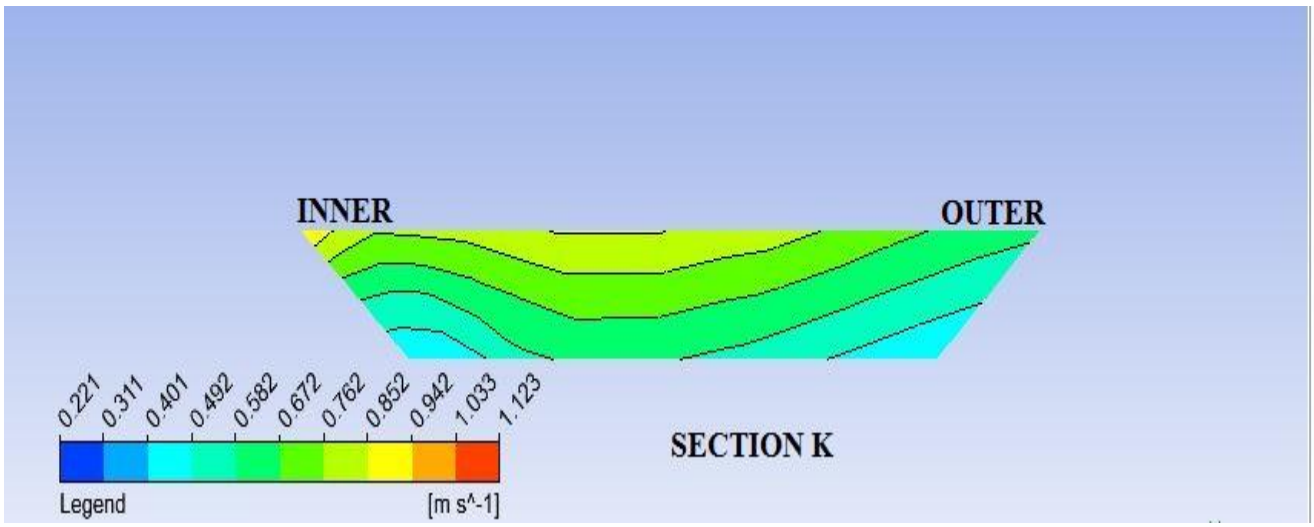

Figure 4.6.11: VELOCITY CONTOUR OF SECTION-K

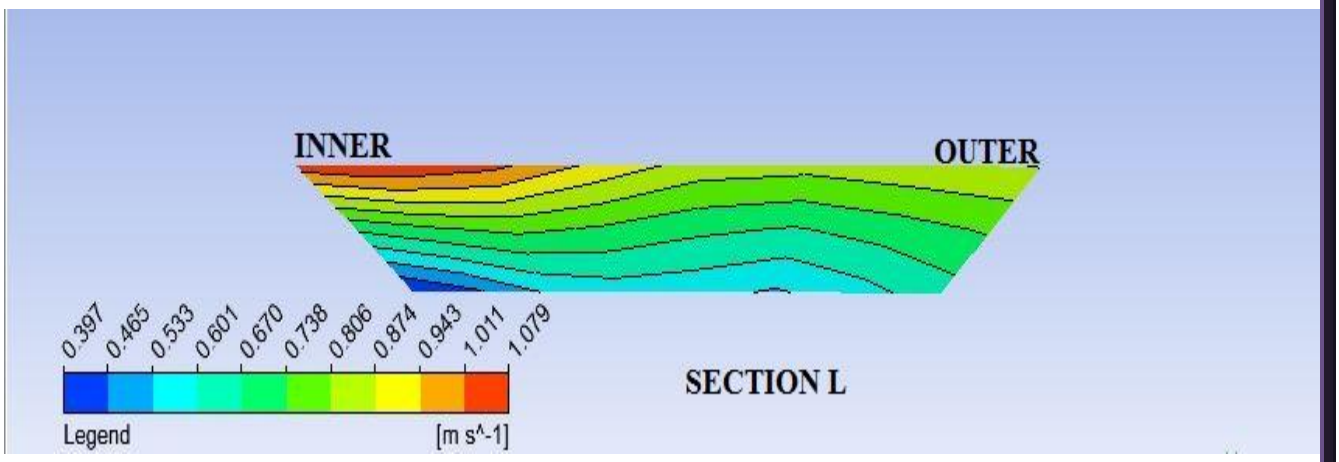

Figure 4.6.12: VELOCITY CONTOUR OF SECTION-L

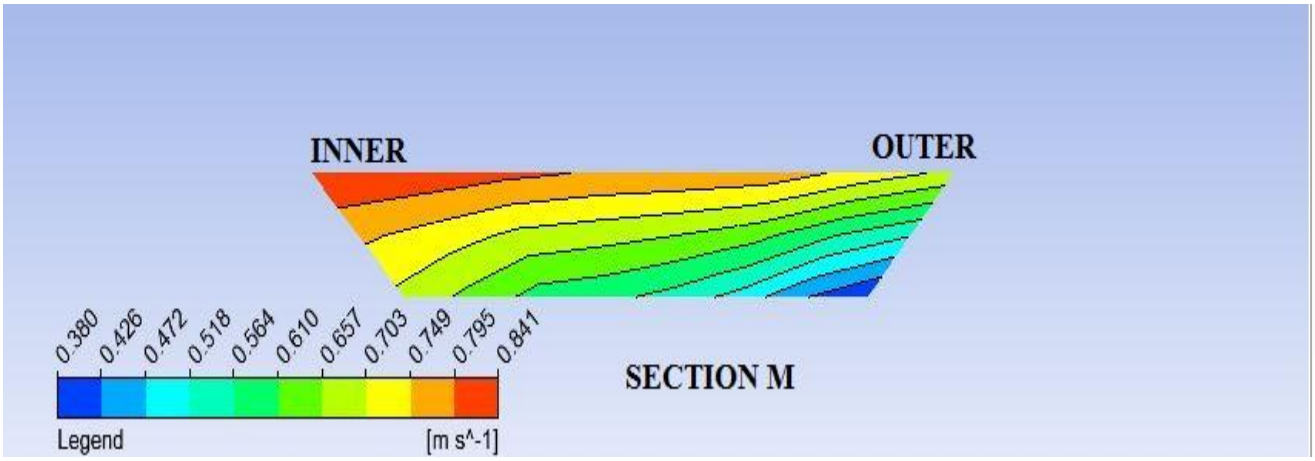

Figure 4.6.13: VELOCITY CONTOUR OF SECTION-M

Figure 4.6.1 to 4.6.13 : Velocity Contours along the meander path of all the 13 sections by Ansys Fluent

4.7.2 VELOCITY CONTOUR FOR TOTAL CHANNEL

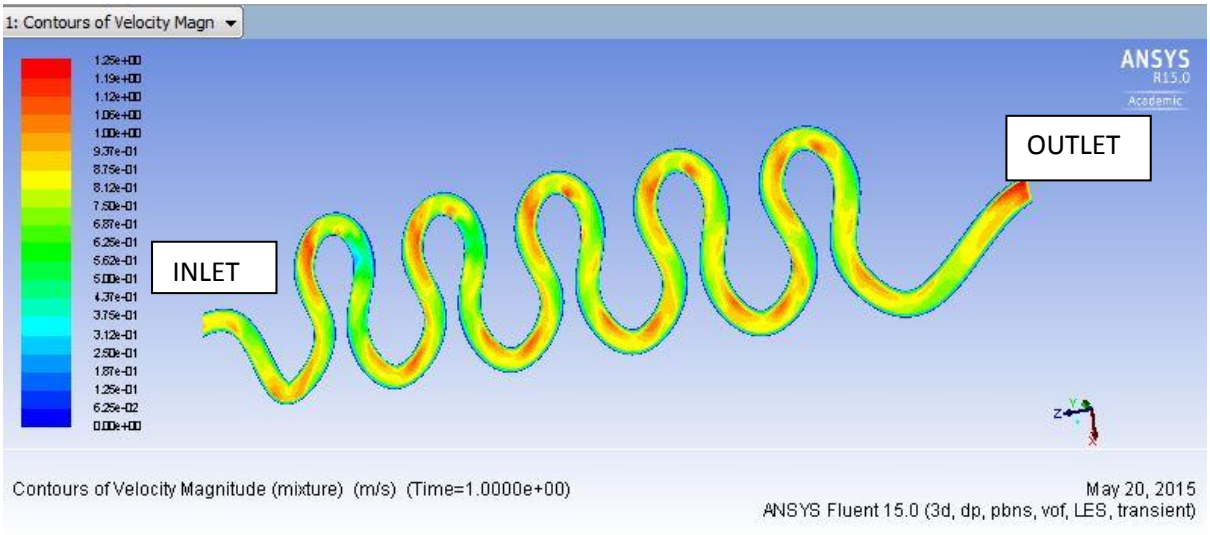

Figure 4.7 Velocity contour for total channel

4.7.3 BOUNDARY SHEAR CONTOUR

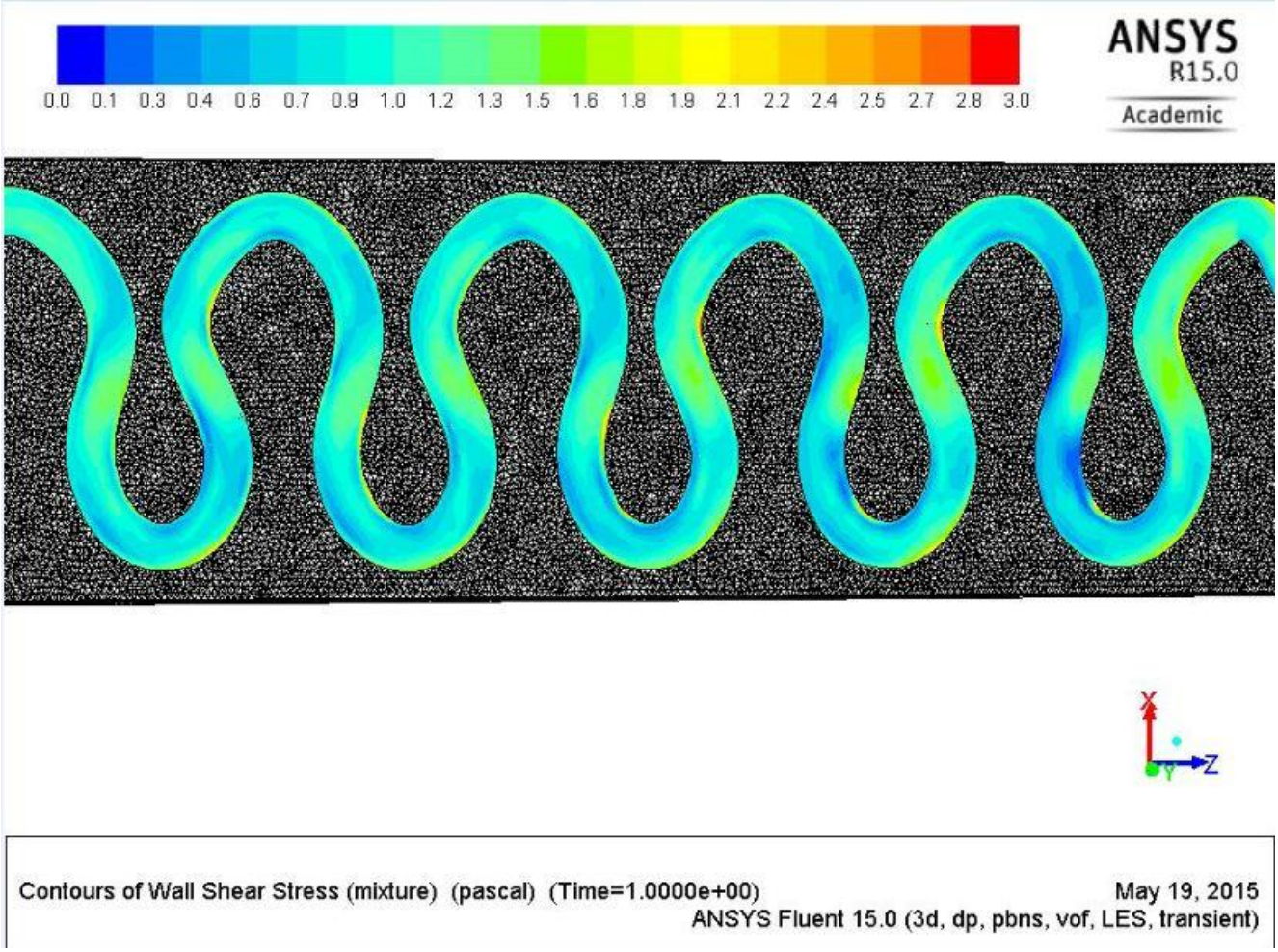

Figure 4.8 Contours of boundary shear

CHAPTER 5
CONCLUSIONS

5.1 CONCLUSIONS

Experimental investigations are carried out on a highly sinuous meander path at different reaches. The different flow characteristics such as velocity distribution, shear stress distribution etc. are investigated Based on the analysis of the experimental investigations, and well validated by numerical results.

- In the sections following the cross-over, i.e. from sections G to M, the profiles indicate that the local maximum value of velocity at each section starts moving from the central region towards the inner wall of the channel i.e. towards the left hand side.
- The depth-averaged velocity is usually found to be higher around the centre of the channel section in case of a simple straight channel, but in the present experimental observation higher depth-averaged velocity is found closer towards the inner wall of the simple meandering channel.
- The horizontal velocity profiles at the bed of the channel at section A (bend apex) remains higher near the inner wall and there is a extreme difference of velocities between the inner and outer walls as shown in Fig. 4.3.1. The highest velocity remains adjacent to 80 cm/sec.
- On moving at the bed from the initial bend apex region towards the cross-over (Section G) as shown in Fig. 4.3.2 to 4.3.6; there is a gradual variation in the horizontal velocity profiles along the width of the channel, with higher velocity occurs near the inner wall.
- As seen in Fig. 4.3.7, at the bed of the cross-over section G, the maximum velocity moves towards the centre of the channel section, with gradual variation of velocity towards the inner and outer walls. This observation depicts that a meandering channel behaves as a straight channel at around the cross-over section In the following sections, from Fig. 4.3.8 to Fig. 4.3.12, on moving from cross-over towards the other

bend apex, the higher depth-averaged velocity moves towards the left of the channel section, this is now the inner wall for the channel section.

- At the bend apex section A, given in figure 4.4.1, it can be observed that the shear stress carried by the inner wall is more as compared to the outer wall.
- The highest shear stress at the inner bank of the section A is found to be around 0.23N/m^2, while a minimum of 0.10N/m^2 at the outer wall. The variation of shear stress in this section is seen to be normal.
- Fig. 4.4.2 to 4.4.6, which shows section B to F indicate that the shear stress remains higher towards the inner wall. In these sections, the variation of shear stress between the inner and outer walls is observed to be gradual.
- At section G (cross-over section), the variation of boundary shear stress is found to be more or less uniform throughout the channel section. The shear stress value remains close to 0.28N/m^2.
- At the bend apex sections A and M the velocity profiles are seen to remain quite close to each other i.e. seem to be similar.
- From the comparison plots we got to know that moving from bend apex section A towards the cross over G the deviation among them increases towards the inner wall with the velocity profile of the higher aspect ratio value remain higher.
- The Numerical results we found are well validated with the experimental results.

5.2 SCOPE FOR FUTURE RESEARCH

The present research gives an extensive scope for future investigators to investigate other aspects of a meandering channel. The present research is limited to a single discharge flow analysis of the meander path. The research can be continued for different discharges to get an

overall depiction about the flow characteristics.The future scope of the present research can be summarized as:

1. This numerical modeling can be done by meandering channel of different sinuosity.
2. Keeping the sinuosity same the bed may be considered as rough by taking different materials of different roughness values as bed material.

REFERENCES

1. Absi, R. (2011). "An ordinary differential equation for velocity distribution and dip-phenomenon in open channel flows" *Journal of Hydraulic Research,* IAHR, Taylor and Francis, Vol. 49, N° 1, pp. 82-89

2. Ansari.K.,Morvan.H.P. andHargreaves.D.M. (2011),"Numerical Investigation into Secondary Currents and Wall Shear in Trapezoidal channels." *Journal of HydraulicEngineering (ASCE)2011*; Vol.137 (4):432-440.

3. ArpanPradhan, Saine S. Dash, K.K.Khatua, "Water Surface Profile along a meander path of a Sinuous Channel", IOSR Journal of Mechanical and Civil Engineering (IOSR-JMCE) e-ISSN: 2278-1684, p-ISSN: 2320-334X, PP 48-52.

4. ArpanPradhan, Kishanjit K. Khatua and Debashish Khuntia, "Study of Variation in Velocity Profile along a 120° Meandering Path" INROADS- An International Journal of Jaipur National University Year: 2014, Volume: 3, Issue: 1s, pp 157-160 Print ISSN : 2277-4904. Online ISSN: 2277-4912.

5. ArpanPradhan, K. K. Khatua, Saine S. Dash, "Boundary Shear Force Distribution along different reaches of a Highly Meandering Channel" International Journal of Scientific Engineering and Technology, Special Issue: HYDRO-2014 International, 19th International Conference on Hydraulics, Water Resources and Environmental Engineering, pp 202-207, ISSN : 2277-1581

6. Arpan Pradhan, Kishanjit. K. Khatua, Saine S. Dash, "Distribution of Depth-Averaged Velocity along a Highly Sinuous Channel", Elsevier Aquatic Procedia, ICWRCOE 2015, Vol 4, pp 805-811.

7. Baghalian, S.,Bonakdari, H., Nazari, F., Fazli, M.(2012), "Closed-Form Solution for Flow Field in Curved Channels in Comparison with Experimental and Numerical

Analyses and Artificial Neural Network". *Engineering Applications of Computational Fluid Mechanics* Vo.6, No.4, pp. 514-526.

8. Bathurst, J. C., Hey, R. D., & Thorne, C. R. (1979). "Secondary flow and shear stress at river bends.", *Journal of the Hydraulics Division*, *105*(10), 1277-1295.
9. Beaman F. Large Eddy Simulation of open channel flows for conveyance estimation, Ph.D. thesis, University of Nottingham, 2010
10. Bhowmik, N. G., and Demissie, M. (1982), "Carrying capacity of flood plains". *Journal of the Hydraulics Division*, *108*(3), 443-452.
11. Bodnar T, Prihoda. Numerical simulation of turbulent free-surface flow in curved channel Flow, turbulence and combustion, 76 (2006):pp. 429-442
12. Bonakdari, H., Baghalian, S., Nazari,F., Fazli, M.(2011), "Numerical Analysis and Prediction of the Velocity Field in Curved Open Channel using Artificial Neural Network and Genetic Algorithm". *Engineering Applications of Computational Fluid Mechanics* Vo.5, No.3, pp. 384-396.
13. Booij R. Measurements and large eddy simulations of the flows in some curved flumes, J. Turbulence, 4 (2003):pp. 1-17
14. Bousmar D, Zech Y. Momentum transfer for practical flow computation in compound channels, Journal of Hydraulic Engineering, 125 (1999):pp. 696-706
15. Bousmar D, Zech Y. Periodical turbulent structures in compound channels, River Flow International Conference on Fluvial Hydraulics, Louvain-la-Neuve, Belgium, 2002:pp. 177-185
16. Boussinesq, J. (1868). Mémoiresurl'influence des frottementsdans les movement reguliers des fluids. J. Math. Pures Appl. (2me sér.), 13, 377-424.
17. Chang, H. H. (1984), "Variation of flow resistance through curved channels", *Journal of Hydr. Engrg.*,ASCE, 110(12), 1772–1782.

18. Cater JE, Williams JJR. Large eddy simulation of a long asymmetric compound open channel, Journal of Hydraulic Research,46 (2008):pp. 445-453

19. Chien K Y. Predictions of Channel and Boundary-Layer Flows with a Low-Reynolds-Number Turbulence Model, AIAA Journal, 20 (1982): pp. 33-38

20. Chow, V. T. (1959), "Open Channel Hydraulics", McGraw-Hill Book Co, New York.

21. Coles, D. (1956). "The law of the wake in the turbulent boundary layer". *Journal of Fluid Mechanics*, *1*(02), 191-226.

22. Cruff R.W. (1965), "Cross Channel Transfer of Linear Momentum in Smooth Rectangular Channels", *U. S. G. S Water Supply*, Paper 1592-B.

23. Dash, S. S. (2013), "Stage-Discharge Modelling of Meandering Channel". Thesis Presented to the National Institute of Technology, Rourkela, in partial fulfilment of the requirements for the Degree of Doctor of philosophy.

24. Dixon AG, Walls G, Stanness H, Nijemeisland M, Stitt EH. Experimental validation of high Reynolds number CFD simulations of heat transfer in a pilot-scale fixed bed tube, J. Chemical Engineering, 200 (2012):pp. 344-356

25. Ervine D. A., Koopaei K.B., and Sellin R. H. J. (2000)." Two-Dimensional Solution for Straight and Meandering Over-bank Flows." *Journal of Hydraulic Engineering*, ASCE, Vol. 126, No. 9, September, paper No.22144, 653-669.

26. Gandhi BK, Verma HK, Abraham B. Investigation of Flow Profile in Open Channels using CFD, 8th Intl Conference on Hydraulic Efficiency Measurement, 2010:pp. 243-251.

27. Ghobadian R, Mohammadi K. Simulation of subcritical flow pattern in 180 uniform and convergent open-channel bends using SSIIM 3-D model, Water Science and Engineering, 4 (2011):pp. 270-283

28. Ghosh, S. N., Jena, S. B.(1971), "Boundary Shear Distribution in open Channel Compound", Proc. I. C. E, Vol. 49, August .

29. "Guide for selecting roughness coefficient "*n*" values for channels". (1963). Soil Conservation Service, *U.S. Dept. of Agric*., Washington

30. Guo, J., and Julien, P. Y. (2005). ''Boundary shear stress in smooth rectangular openchannels.'' Proc., 13th Int. Association of Hydraulic Research, APD Congress, Singapore, Vol. 1, 76–86.

31. Han SS, Biron PM, Ramamurthy AS. Three-dimensional modelling of flow in sharp open-channel bends with vanes, Journal of Hydraulic Research, 49 (2013):pp. 64-72

32. Hartel C, Meiburg E, Necker F. Analysis and direct numerical simulation of the flow at a gravity-current head. Part 1. Flow topology and front speed for slip and no-slip boundaries, Journal of Fluid Mechanics,418 (2000): pp. 3.1

33. Hirt CW, Nichols BD. Volume of fluid (VOF) method for the dynamics of free boundaries, Journal of computational physics, 39 (1981): pp. 201-225

34. "Hydraulic capacity of meandering channels in straight floodway" (1956), Tech.Memorandum No. 2-429, U.S. Army Corps of Engineers, Waterways Experiment Station, Vicksburg, Miss.

35. Inglis, C.C.(1947), "Meander and Their Bering on River Training.", *Proceedings of the Institution of Civil Engineers, Maritime and Waterways Engineering Div., Meeting, 1947.*

36. James, M., and Brown, R. J.(1977), "Geometric parameters that influence flood plain flow", U. S. Army Engineer Waterways Experimental Station, Vicksburg, Miss., June, Research report H-77.

37. Jarrett, R. D. (1984). ''Hydraulics of high gradient streams'', *Journal of Hydr. Engg.,ASCE*, 110, 1519–1539.

38. Javid,S., and Mohammadi,M.(2012). ‘‘Boundary Shear Stress in a Trapezoidal Channel.” IJE TRANSACTIONS A: Basics Vol. 25, No. 4, (October 2012) 365-373.

39. Jin,Y.C.,Zarrati, A. R. andZheng,Y. (2004). “Boundary Shear Distribution in Straight Ducts and Open Channels” *J. Hydraul. Eng.*, ASCE, 130(9), 924-928.

40. Jing H, Guo Y, Li C, Zhang J. Three dimensional numerical simulation of compound meandering open channel flow by the Reynolds stress model, International journal for numerical methods in fluids, 59 (2009):pp. 927-943

41. Johannesson, H., & Parker, G. (1989). “Linear theory of river meanders.”, *Water Resources Monograph, 12,* 181-213.

42. Kang S, Sotiropoulos F. Numerical modeling of 3D turbulent free surface flow in natural waterways, Advances in water resources,40 (2012):pp. 23-36

43. Kassem A, Imran J, Khan JA. Three-dimensional modeling of negatively buoyant flow in diverging channels, Journal of Hydraulic Engineering,129 (2003):pp. 936-947

44. Khatua, K. K. (2008), “Interaction of flow and estimation of discharge in two stage meandering compound channels”. Thesis Presented to the National Institute of Technology, Rourkela, in partial fulfilment of the requirements for the Degree of Doctor of philosophy.

45. Khatua, K.K and Patra, K.C,(2010). Evaluation of boundary shear distribution in a meandering channel.Proceedings of ninth International Conference on Hydro-Scienceand Engineering, IIT Madras, Chennai, India, ICHE 2010, 74.

46. Khatua K.K., Patra K.C., (2013) “stage–discharge prediction for meandering channels”, Int. J. Comp. Meth. and Exp. Meas., Vol. 1, No. 1 80–92

47. Khatua K.K., Patra K.C., Nayak P. (2012), “Meandering effect for evaluation of roughness coefficients in open channel flow” *Sixth* international conf. on river basin

management, WIT Transactions on Ecology and the Environment (ISSN 1743-3541), CMEM, WIT Press., 146(6):213-227.

48. Knight, D. W. (1981). "Boundary shear in smooth and rough channels." *J. Hydraul. Div., Am. Soc. Civ. Eng.,* 107(7), 839–851.
49. Knight D. W. and Demetriou J.D. (1983). "Floodplain and main channel flow interaction." *J. Hydraul. Eng*., ASCE, 109(8), 1073–92.
50. Knight, D. W., and MacDonald, J. A. (1979). "Open-channel flow with varying bed roughness." *J. Hydraul. Div., Am. Soc. Civ. Eng.,* 105(9), 1167–1183.
51. Knight,D.W., and Sterling,M.(2000), "Boundary shear in circular pipes running partially full.", *Journal of Hyd. Engg., ASCE* Vol.126, No.4.
52. Knight,D.W.,Yuan,Y.M.,andFares,Y.R.(1992). "Boundary shear in meandering channels.",*Proceedings of the Institution Symposium on Hydraulic research in nature and laboratory,* Wuhan, China (1992) Paper No.11017, Vol. 118, Sept., pp. 151-159.
53. Langbein, W. B., & Leopold, L. B. (1966). "River meanders--Theory of minimum variance" (pp. 1-15). US Government Printing Office.
54. Leighly, J. B. (1932). "Toward a theory of the morphologic significance of turbulence inthe flow of water in streams." Univ. of Calif. Publ. Geography,6(1), 1–22.
55. Lin B, Shiono K. Numerical modelling of solute transport in compound channel flows, Journal of Hydraulic Research, 33 (1995):pp. 773-788
56. Lien H, Hsieh T, Yang J, Yeh K. Bend-Flow Simulation Using 2D Depth-Averaged Model, Journal of Hydraulic Engineering, 125 (1999):pp. 1097-1108
57. Lu WZ, Zhang WS, Cui CZ, Leung AYT. A numerical analysis of free-surface flow in curved open channel with velocity-pressure-free-surface correction, Computational Mechanics, 33 (2004):pp. 215-224

58. Mellor GL, Herring HJ. "A survey of mean turbulent field closure.", AIAA Journal 1973; 11:590 – 599.
59. Mohanta.A(2014)" Flow Modelling of Non Prismatic compound channel By UsingC.F.D"Thesis Presented to the National Institute of Technology, Rourkela, in partial fulfilment of the requirements for the Master of technology.
60. Mohanty, L.(2013), "Velocity Distribution in Trapezoidal Meandering Channel". Thesis Presented to the National Institute of Technology, Rourkela, in partial fulfilment of the requirements for the Degree of Doctor of philosophy.
61. Mohanty, P.K., Dash,S.S. and Khatua,K.K. (2012). "Flow Investigations in a Wide Meandering Compound Channel." International Journal of Hydraulic Engineering 2012, 1(6) : 83-94
62. Myers, W. R. C. (1978). "Momentum transfer in a compound channel." *J. Hydraul. Res.,16(2),* 139–150.
63. Nicholas AP. Computational fluid dynamics modelling of boundary roughness in gravel-bed rivers: an investigation of the effects of random variability in bed elevation, Earth Surface Processes and Landforms,26 (2001):pp. 345-362
64. Patel, V. C. (1965). "Calibration of the Preston tube and limitations on its use in pressure gradients.", *Journal of Fluid Mechanics*, *23*(01), 185-208.
65. Patnaik, M. (2013), "Boundary Shear Stress Distribution in Meandering Channels". Thesis Presented to the National Institute of Technology, Rourkela, in partial fulfilment of the requirements for the Degree of Doctor of philosophy.
66. Patra, K.C, and Kar, S. K. (2000), "Flow Interaction of Meandering River with Floodplains". *Journal of Hydr. Engrg., ASCE,* 126(8), 593–604.

67. Patra, K.C., and Kar, S.K., Bhattacharya, A.K. (2004). "Flow and Velocity Distribution in Meandering Compound Channels.", *Journal of Hydraulic Engineering, ASCE*, Vol. 130, No. 5. 398-411.

68. Pradhan .A(2014)" analysis of flow along the meander path of a highly sinuous rigid channel" Thesis Presented to the National Institute of Technology, Rourkela, in partial fulfilment of the requirements for the Master of technology.

69. Preston, J. (1954). "The determination of turbulent skin friction by means of Pitot tubes.", *Journal of the Royal Aeronautical Society*, *58*(518), 109-121.

70. Rajaratnam, N., and Ahmadi, R.M. (1979). "Interaction between Main Channel and Flood Plain Flows." *Journal of Hydraulic Division, ASCE,*Vol..105, No. HY5, pp. 573-588.

71. Ramamurthy AS, Han SS, Biron PM. Three-Dimensional Simulation Parameters for 90° Open Channel Bend Flows, Journal of Computing in Civil Engineering, 27 (2013):pp. 282-291

72. Channel flows, Journal of Hydraulic Engineering, 129 (2003):pp. 645-652

73. Rhodes, D. G., and Knight, D. W. (1994). "Distribution of Shear Force on Boundary of Smooth Rectangular Duct.",*Journal of HydralicEngg.*, 120-7, 787– 807.

74. Saine S. Dash, K.K.Khatua, P.KMohanty(2013), "Energy loss for a highly Meandering open Channel Flow", *Res. J. Engineering Sci.*, Vol. 2(4), 22-27, April (2013).

75. Saine S. Dash, K.K.Khatua, P.K. Mohanty(2013), "Factors influencing the prediction of resistance in a meandering channel", *International Journal of Scientific & Engineering Research* ,Volume 4, Issue 5, May-2013.

76. Salvetti M.V., Zang Y., Street R.L. and Banerjee S. Large-eddy simulation of free surface decaying turbulence with dynamic subgrid -scale models, Physics of Fluids, 9 (1997): pp.2405.

77. Sellin R. H. J. (1961.), “A Study of the Interaction between Flow in the Channel of a River and that over its Floodplain”, Ph. D Thesis, University of Bristol, Bristol, England

78. Sellin, R. H. J. (1964), “A Laboratory Investigation into the Interaction between the Flow in the Channel of a River and that over its Floodplain”, La. Houille Blanche.

79. Seyedashraf O, Akhtari AA, Shahidi MK. Numerical Study of Channel Convergence Effects on Flow Pattern in 90 Degree Bends, 9th International Congress, IUT, 2012

80. Shiono K., Al-Romaih I. S., and Knight D. W., (1999), “Stage-discharge assessment in compound meandering channels”, *Journal of Hydraulic Engineering*, ASCE, 125 (1), 66-77, Mar., 45-54, and discussion in 1993, 101, Dec., 251-252.

81. Shiono, K., Muto, Y., Knight, D.W. & Hyde, A.F.L.(1999), “Energy Losses due to Secondary Flow and Turbulence in Meandering Channels with Overbank Flow.”, *Journal of Hydraulic Research*, IAHR, Vol. 37, No. 5, pp. 641-664.

82. Shukry A.(1950), “Flow around Bends in an Open Flume”, Transactions ASCE, Vol. 115, pp 75L788.

83. Song CG, Seo IW, Kim YD. Analysis of secondary current effect in the modeling of shallow flow in open channels, Advances in water resources, 41 (2012): pp. 29-48.

84. Sovan Sankalp, Kishanjit. K. Khatua, Arpan Pradhan, "Boundary Shear Stress Analysis in Meandering Channels at the Bend Apex", Elsevier Aquatic Procedia, ICWRCOE 2015, Vol 4, pp 812-818

85. Sugiyama H, Hitomi D, Saito T. Numerical analysis of turbulent structure in compound meandering open channel by algebraic Reynolds stress model, International journal for numerical methods in fluids, 51 (2006): pp. 791-818.

86. Sumit K. Jena, Kishanjit. K. Khatua, Arpan Pradhan, "Longitudinal Velocity Distribution Modeling of a Highly Sinuous Meandering Channel using CFD", IOSR

Journal of Mechanical and Civil Engineering (IOSR-JMCE) e-ISSN: 2278-1684, p-ISSN: 2320-334X, PP 01-06.

87. Thomas TG, Williams JJR. Large eddy simulation of turbulent flow in an asymmetric compound open channel, Journal of Hydraulic Research,33 (1995): pp. 27-41
88. Thomson J. (1876), "On the origins of windings of rivers in alluvial plains, with remarks on the flow of water round bends in pipes", Proc. Royal Society of London,Vol. 25, 5-8.
89. Thomas TG. and Williams J.(1999). Large eddy simulation of flow in a rectangular open channel. *J. Hydraul Res.* 37(3), pp. 345-361.
90. Toebes, G.H., and Sooky, A.A. (1967),"Hydraulics of Meandering Rivers with Floodplains." *Journal of the waterways and Harbor Division, Proceedings of ASCE*, Vol.93, No.WW2, May, pp. 213-236.
91. Van Balen W, Uijttewaal WSJ, Blanckaert K. Large-eddy simulation of a curved open-channel flow over topography, Physics of Fluids,22 (2010): pp. 075108
92. Willetts B.B. and Hard Wick R.I. (1993), "Stage dependency for overbank flow in meandering channels", *Proc. Instn Civ. Engrs, Wat., Marit. & Energy*, 101.
93. Wormleaton, P.R., Allen, J.,andHadjipanos, P.(1982). "Discharge Assessment in Compound Channel Flow." *Journal of Hydraulic Engineering, ASCE*, Vol.108, No.HY9, pp. 975-994.
94. Yang, S. Q. and McCorquodale, John A. (2004) "Determination of Boundary Shear Stress and Reynolds Shear Stress in Smooth Rectangular Channel Flows." *Journal of Hydr. Engrg.*, Volume 130, Issue 5, pp. 458-462.